INTERNATIONAL SOCIETY ON
OXYGEN TRANSPORT TO TISSUE

ISOTT 2019
ALBUQUERQUE

www.isott.org
www.isott2019.com
info@isott2019.com

VirTech Bio

27 Strathmore Road
Natick, MA

Table of Contents

ISOTT 2019

is being generously sponsored by

The Journal of Physiology

ISOTT 2019 Planning Committee

Edwin Nemoto

Edwin Nemoto is a Research Professor in the Department of Neurosurgery and has served for the past ten years as Director of Research in Neurosurgery. He was a founding member of ISOTT in 1973 and hosted the ISOTT meeting at the University of Pittsburgh in 1995. Edwin is the current President of ISOTT.

Sally Pias

Sally Pias is an Associate Professor and Associate Chair of the Department of Chemistry at the New Mexico Institute of Mining and Technology (New Mexico Tech) in Socorro, NM, USA. She is a biochemist with a research focus on oxygen transport modeling. Sally was given ISOTT's Melvin H. Knisely Award in 2016, and she currently serves on the Executive Committee.

Denis Bragin

Denis Bragin, PhD, FAHA, is a Research Associate Professor in the Department of Neurosurgery of the University of New Mexico School of Medicine. His research focuses on the circulation, oxygen supply and metabolism of the brain under various pathological conditions.

We deeply appreciate the efforts of Joyce Fang (Conference Manager); CCS, LLC Meeting Managers; and Marty Herrera (Audio-Visual Coordinator) in helping plan and execute the meeting. Thanks also to Peter Keipert, whose assistance with planning was invaluable.

ISOTT 2019 General Information

47th Annual Meeting
July 27 – 31, 2019

Hotel Albuquerque at Old Town
800 Rio Grande Blvd. NW
Albuquerque, New Mexico 87104
+1-505-843-6300

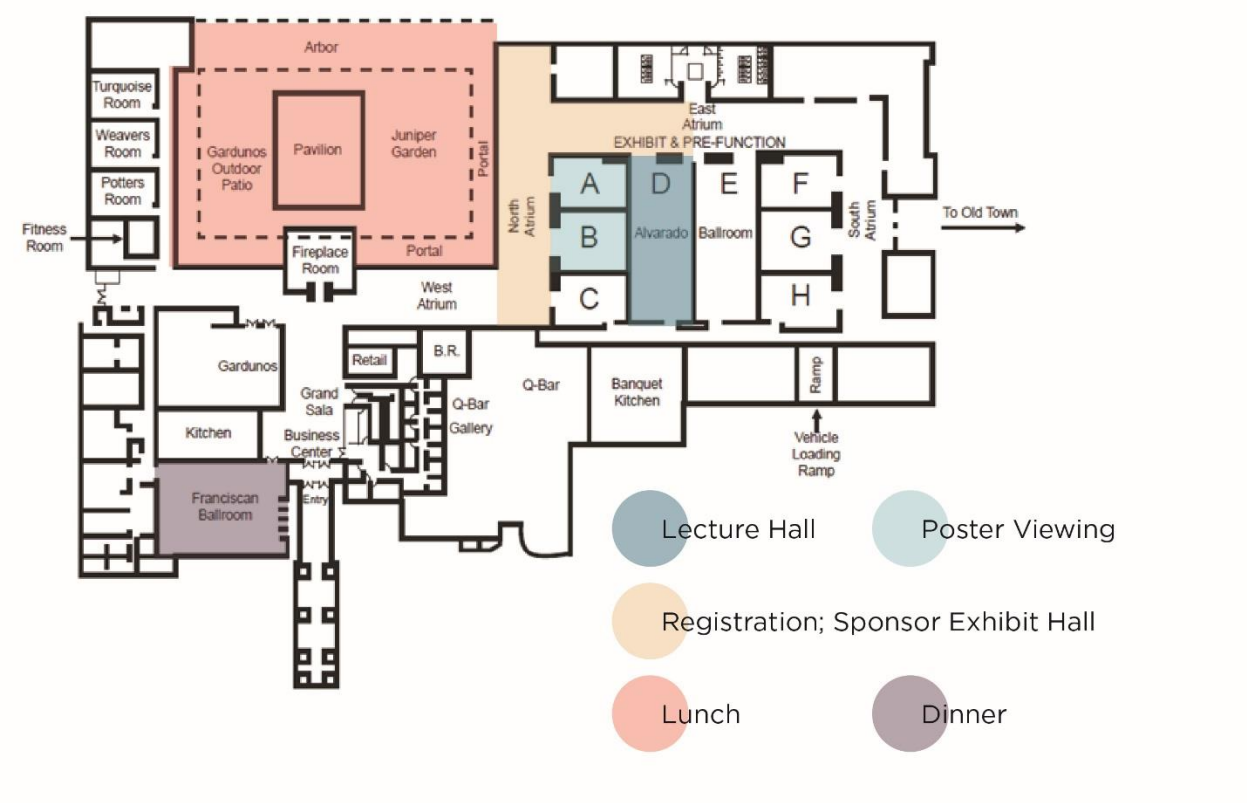

All lectures will take place in Alvarado D.
All posters will be displayed, and poster sessions take place, in Alvarado AB.

Breakfast is not included though the ISOTT Planning Committee will be having breakfast at Garduno's Restaurant at the hotel. Everyone is welcome.
All lunches will be in the outdoor pavilion. In the case of rain, lunches will be in Franciscan Ballroom.
Sunday and Monday's dinners will be in the Franciscan Ballroom.

Wednesday's Annual Banquet will be off-site, at the Indian Pueblo Cultural Center located at:
2401 12th Street NW
Albuquerque, New Mexico 87104

ISOTT 2019 Program at a Glance

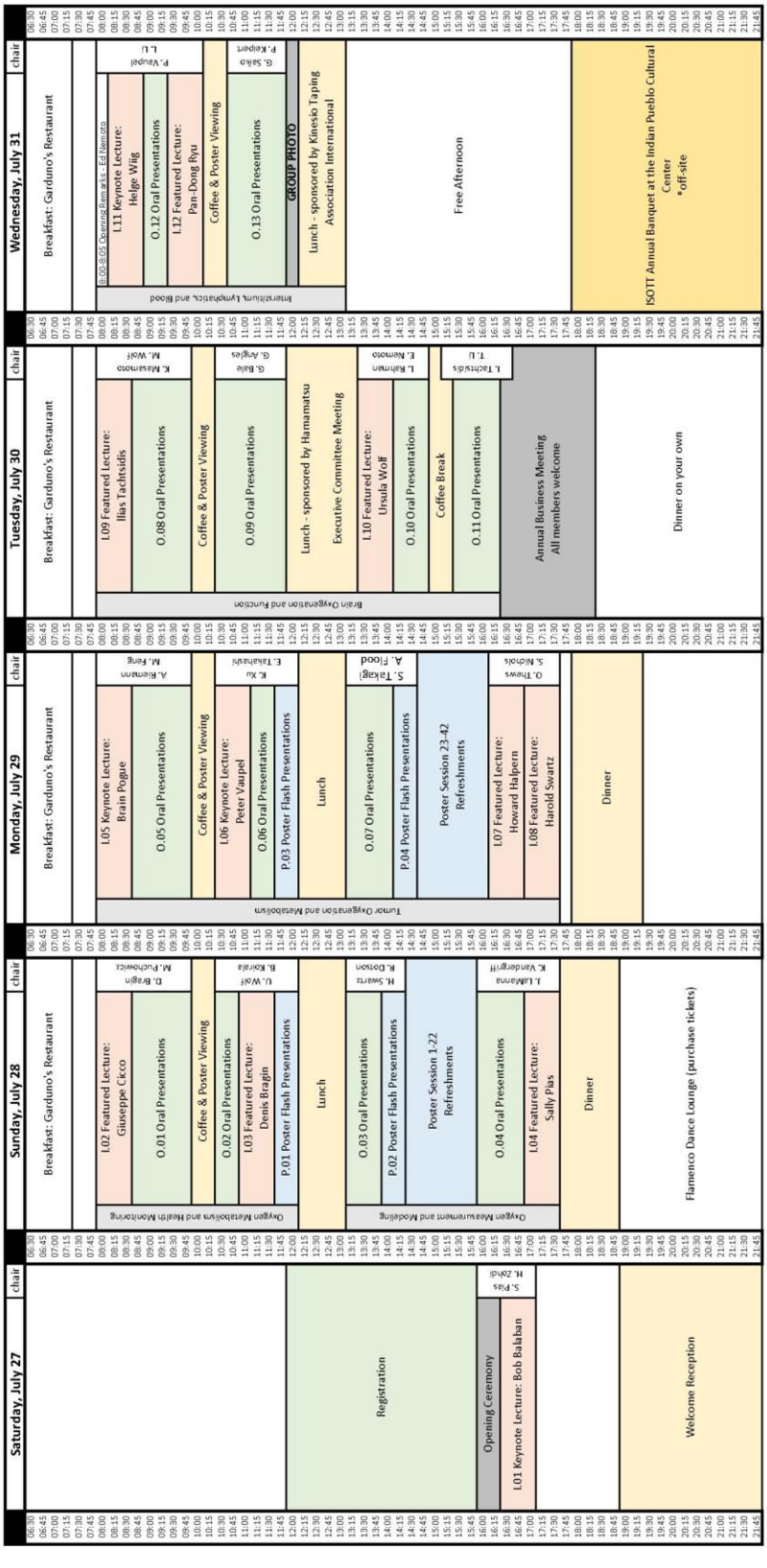

ISOTT 2019 Meeting Details

Registration Desk

The registration desk is located in the North Atrium of Hotel Albuquerque.

It will be open Saturday, July 27th from 12:00 – 16:00.

Conference Badges

Please wear your conference badge at all times. Your badge is required for access to all lectures, meals and social events.

Poster Presentations

Poster sessions are a core component of the ISOTT 2019 meeting. Posters should be designed to spark interest and start conversations among the broad ISOTT membership.

Posters should fit within a space of 42 in x 42 in, or 107 cm x 107 cm. Posters can be smaller than this, but not larger.

All posters will be displayed for the entirety of the conference.

Please mount your poster, according to number, on Saturday, July 27th, from 13:00 to 15:45. If you are not present on July 27th, please mount your poster prior to 8am on July 28th or July 29th.

Each poster presenter will be scheduled to give a **1- or 2-slide** "flash presentation" during a plenary session. The flash presentation should very briefly introduce your work and invite participants to learn more during a Poster Viewing session. The time allotted for each flash presentation is **2 minutes**.

The flash presentation slide(s) must be provided on-site to the audio-visual coordinator on July 27th, at the registration desk at Hotel Albuquerque. The slides should be provided as a PowerPoint or PDF file, and MUST have the surname of the author in the file name.

Presenters are requested to stand by their posters during the afternoon Poster Session on the same day as their flash presentation.

Oral Presentations

Each speaker should prepare a **10-minute** presentation.

Oral presentation slides must be provided on-site to the audio-visual coordinator on July 27th, at the registration desk at Hotel Albuquerque. The slides should be provided as a PowerPoint or PDF file, and MUST have the surname of the author in the file name.

Keynote and Featured Lectures
Each speaker should prepare a **30-minute** presentation.

Slides must be provided on-site to the audio-visual coordinator on July 27th, at the registration desk at Hotel Albuquerque. The slides should be provided as a PowerPoint or PDF file, and MUST have the title of the author in the file name.

Chairperson Guidelines

Chairpersons should ensure that all presentations are uploaded ahead of the start of their session. Chairpersons will introduce the session and each speaker. All chairpersons are asked to remind speakers to adhere to the time limits and assist in compliance. Chairpersons should also facilitate the discussion sessions and direct the use of the mobile microphone for questions. We remind speakers and questioners that overly long discussions can and should be extended into the next break, rather than into the next speaker's allotted time.

On days that we have a lunch sponsor, chairpersons are expected to introduce our lunch sponsor for that day. Please reference the agenda to see who your lunch sponsor is.

Manuscript Submission

Peer-reviewed proceedings of the annual meeting of ISOTT are published in the Advances in Experimental Medicine and Biology series published by Springer Nature. Presenters are eligible to submit a full-length manuscript based on their presentation (poster or oral) given at the conference.

All files mentioned below can be found on our website: https://www.isott2019.com.

We strongly recommend that you read the instructions ("Instructions for ISOTT Authors 2019") before starting to prepare your manuscript.

Manuscripts should be submitted as MS Word files. The electronic version of the manuscript must be prepared using the template provided by Springer ("T1-Book Template").

Accompanying this on a separate page should be 5 keywords, the e-mail address of the corresponding author and a copyright release form ("Consent to Publish Form"). If copyrighted material has been used in the manuscript, a permission form should be included from the original publisher. Figures should be submitted as individual .tif graphic files having a resolution of 300 dpi.

The maximum number of pages (including abstract, main text, figures, tables, and references) is **6.**

The deadline for the submission of manuscripts is **September 9, 2019.**

Please send your manuscript, together with the copyright form, a title page with the name and address of the corresponding author and a list of keywords, to **info@isott2019.com** and to Editor David Harrison at **harrison.david.k@gmail.com**.

Sponsors

We are fortunate to have generous sponsors supporting our conference. We hope you get to know them throughout the meeting.

- Clin-EPR, LLC
- Kinesio Taping Association International
- The Journal of Physiology
- Hamamatsu Photonics, KK
- Scintica Instrumentation/ Oxford Optronix
- FujiFilm VisualSonics, Inc.
- VirTech Bio

Sponsored Exhibits

The following sponsors will have exhibits in the Exhibit Hall, located in the North Atrium. We encourage you to visit their exhibits and get to know their companies.

- Kinesio Taping Association International
- Scintica Instrumentation/ Oxford Optronix
- FujiFilm VisualSonics, Inc.

Wi-Fi in Meeting Rooms

Wireless internet access is available in the meeting rooms, through the "Hotel Albuquerque" network. This network does not require a password.

Disclaimer

The organizers cannot accept any liability for personal injuries sustained or for loss or damage to property belonging to conference attendees (or their accompanying persons) either during or as a result of the conference. Registration fees do not include insurance.

ISOTT Awards

ISOTT offers a variety of awards to honor junior scientists working in the field of oxygen transport and to support participation in the ISOTT meeting.

1. Melvin H. Knisely Award (age: 40 or younger)

The Melvin H Knisely Award was established in 1983 to honor Dr. Knisely's accomplishments in the field of the transport of oxygen and other metabolites and anabolites in the human body. Over the years, he has inspired many young investigators and this award is to honor his enthusiasm for assisting and encouraging young scientists and engineers in various disciplines. The award includes a Melvin H. Knisely plaque and a cash prize.

2. Dietrich W. Lübbers Award (age: 35 or younger)

The Dietrich W. Lübbers Award was established in honor of Professor Lübbers's long-standing commitment, interest, and contributions to the problems of oxygen transport to tissue and to the society. The award includes a plaque and a cash prize.

3. Britton Chance Award (age: 30 or younger)

The Britton Chance Award was established in honor of Professor Chance's long-standing commitment, interest and contributions to the science and engineering aspects of oxygen transport to tissue and to the society. The award includes a plaque and a cash prize.

4. Duane F. Bruley Travel Awards (no age limit)

The Duane F. Bruley Travel Awards were created to provide travel funds for student researchers in all aspects of oxygen transport to tissue. As a co-founder of ISOTT in 1973, Dr. Bruley emphasizes cross-disciplinary research among basic scientists, engineers, medical scientists, and clinicians. It is hoped that receiving the Duane F. Bruley Travel Award will inspire students to excel in their research and will assist in securing future leadership for ISOTT.

Clin EPR, LLC
Lyme, N.H.

Services for In Vivo EPR

- Development, deployment, maintenance, and upgrades of systems and devices purchased from Clin-EPR
- Development of application specific data acquisition and processing software
- Consultation on issues involving applications in human subjects
- Instrumental developments such as magnets, resonators, coils, etc.
- Paramagnetic materials for clinical and preclinical oximetry

Clin-EPR, LCC is the world's first and only provider of in vivo clinical EPR systems, equipment, methods, and support to the medical research and scientific community.

CLINICAL:
- Whole Body with various ergonomic interfaces (gurney, chair, etc.)
- Head system for in vivo tooth dosimetry for emergency triage
- Partial body (e.g. for limb)
- Automated systems for emergency dosimetry for large events (radiation triage)

PRECLINICAL RESEARCH:
- Small animal systems
- Large animal systems

Components for Applications in Humans and Animals (L-Band)

CLINICAL:
- Surface probes for measurements of oxygen or free radicals
- Flexible resonators to minimize effects of pressure and motion artifacts
- Implantable resonators (Developmental for clinical use – currently preclinical only)
- Intraoral (for tooth dosimetry)

PRECLINICAL RESEARCH:
- Surface probes
- Implantable resonators

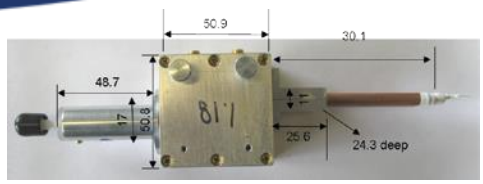

Clin-EPR, LLC
278 River Road, Lyme, NH 03768
1-603-795-4919

President, Ann Flood, Ph.D
clin.EPR_abf@yahoo.com

For scientific information, please contact
Harold Swartz
clin.EPR_hms@yahoo.com

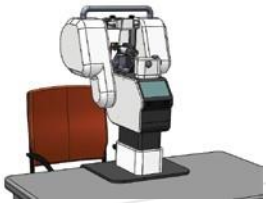

Table-top In Vivo Tooth Dosimeter

20-cm gap Tooth Dosimeter Magnet

Prototype Stand-alone In vivo Tooth Dosimeter

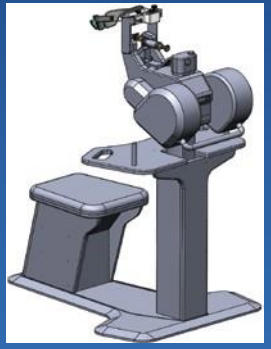

Clin-EPR is a company that has been developed to facilitate the development of in vivo EPR by enabling technology developed at Dartmouth (and elsewhere) to become available for purchase for investigational use. Clin-EPR, LCC is the world's first and only provider of clinical EPR systems, equipment, methods, and support to the medical research and scientific community.

Founded and directed by Harold Swartz, it now includes EPR experts from engineering, Medicine and Biology. Clin-EPR is chiefly responsible for delivering functional investigation devices and deploying practical procedures to aspiring researchers in clinical settings looking to advance their developments using this novel technique to establish applications that can impact the effectiveness of clinical medicine. Existing in vivo applications include: tooth and nail dosimetry for unexpected radiation exposures, and oximetry to improve treatment and outcomes for cancer, wound healing, and peripheral vascular disease.

Clinical Oximeter

ISOTT 2019 Conference Program
Saturday, July 27th

12:00 – 16:00 Registration

Session Chairs: Sally Pias, Hamoon Zohdi

16:00 – 16:30 Opening Ceremony
Edwin Nemoto, *ISOTT 2019 President*
Richard Larson, *University of New Mexico Vice Chancellor of Research*
Duane Bruley, *ISOTT Co-Founder*

16:30 – 17:15 Keynote Lecture
Bob Balaban, *National Heart, Lung, and Blood Institute (NHLBI), National Institutes of Health (NIH), USA*
I.01 Mitochondrial Function in the Intact Heart

19:00 – 22:00 Welcome Reception – *Alvarado ABCD*

Sunday, July 28th

Session: Oxygen Metabolism and Health Monitoring

Session Chairs: Denis Bragin, Michelle Puchowicz

08:00 – 08:45 Featured Lecture

Giuseppe Cicco, *University Aldo Moro Bari, Italy*
I.02 Microcirculation and Diabetes Mellitus

08:45 – 10:00 O.01 Oral Presentations

Aarti Sethuraman, *University of Tennessee, USA*
O.01-1 Chronic Ketosis Modulates Metabolite Profile and HIF1α Mediated Inflammatory Response in Rat Brain

Eiji Takahashi, *Saga University, Japan*
O.01-2 Mitochondrial Membrane Potential can be Sustained Without Functioning Complex IV

Guiseppe Cicco, *University Aldo Moro Bari, Italy*
O.01-3 The Computerized Nailfold Video-Capillaroscopy as a New Technique for Microvascular Monitoring in Diabetes Type 2

Monica Lozano, *Profusa, Inc, USA*
O.01-4 Continuous Monitoring of Healthy Volunteers Using Profusa's Lumee™ Tissue-Integrating O_2 Sensor and a Clinical Non-Invasive, Wearable Device

10:00 – 10:30 Coffee Break & Poster Viewing

Session Chairs: Ursula Wolf, Bhabuk Koirala

10:30 – 11:00 0.02 Oral Presentations

Labiblais Rahman, *Nihon University, Japan*
O.02-1 Event-Related NIRS and EEG Analysis for Mental Stress Monitoring

Scott Nichols, *Profusa, Inc, USA*
O.02-2 Characterizing Tissue Oxygen Kinetics During Continuous Real-Time Monitoring in Healthy Subjects

11:00 – 11:45 Featured Lecture

Denis Bragin, *University of New Mexico, USA*
I.03 Pathophysiology of Microcirculation and Oxygen Supply in Traumatic Brain Injury

11:45 – 12:15 P.01 Poster Flash Presentations

Eiji Takahashi, *Saga University, Japan*
P.01-1 Extracellular Gradients of pH Direct Migration of MDA-MB-231 Cells

Simin Yan, *University of New Mexico, USA*
P.01-2 Mitochondria-Derived Reactive Oxygen Species Mediate Enhanced Basal Pulmonary Arterial Tone Following Chronic Hypoxia

Qi Wang, *New Mexico Institute of Mining and Technology, USA*
P.01-3 Simulation Study of Breast Cancer Lipid Changes Affecting Membrane Oxygen Permeability

Rachel Dotson, *New Mexico Institute of Mining and Technology, USA*
P.01-4 Protein Influence on Membrane Oxygen Permeability

Joshua Russell-Buckland, *University College London, UK*
P.01-5 Application to the Piglet Model of a Systems Biology Model of Cerebral Oxygen Delivery and Metabolism During Therapeutic Hypothermia

Kaoru Sakatani, *The University of Tokyo, Waseda University, Japan*
P.01-6 Long-Term Monitoring of Physical and Mental Health Conditions using IoT Monitoring System

Yu Okuma, *Feinstein Institute for Medical Research, USA*
P.01-7 NIRS Might Contribute to Detect the Harmful Effect of Adrenaline

Dominik Wyser, *ETH Zurich, University of Zurich, Switzerland*
P.01-8 Scalp Hemodynamics Over Brain Motor Regions: A Homogeneous or Inhomogeneous Phenomenon?

Eileen Thiessen, *Synthesizer, Inc, USA*
P.01-9 Two Consecutive Invasive Surgeries Utilizing Zymogen Protein C (ZPC) That Enhanced Patient Safety and Reduced Costs

Shai Ashkenazi, *University of Minnesota, A-Scan LLC, USA*
P.01-10 A New Needle Mounted Optical Scanner for Measuring Spatio-Temporal Distributions of Tissue Oxygen in Cancer Tumors

Oxana Semyachkina-Glushkovskaya, *Saratov State University, Russia*
P.01-11 Transcranial Photobiomodulation of Clearance of Beta-Amyloid from the Mouse Brain: The Effects on Meningeal Lymphatic Drainage and Blood Oxygen Saturation of the Brain

Yiming Shen, *Seoul National University, Republic of Korea*
P.01-12 Gene Expression Pattern of the Primo Vascular System is Similar to that of the Spleen

12:15 – 13:15 Lunch

Session: Oxygen Measurement and Modeling

Session Chairs: Harold Swartz, Rachel Dotson

13:15 – 14:00 O.03 Oral Presentations

Hiroshi Hirata, *Hokkaido University, Japan*
O.03-1 Simultaneous Measurement of pH and Partial Pressure of Oxygen in Solutions Using Electron Paramagnetic Resonance (EPR) Spectroscopy: A Feasibility Study By 750 MHz EPR

He Nucleus Xu, *University of Pennsylvania, USA*
O.03-2 Developing Quantitative Optical Redox Imaging Techniques to Identify Potential Alzheimer's Disease Biomarkers

Chenyang Gao, *Chinese Academy of Medical Sciences & Peking Union Medical College, China*
O.03-3 Online Assessment of Hemodynamics in Suctioned Volume of Biological Tissue by the Embedded Near-Infrared Spectroscopy Sensor

14:00 – 14:30 P.02 Poster Flash Presentations

Shun Takagi, *Doshisha University, Japan*
P.02-13 Skeletal Muscle Deoxygenation and Its Relationship to Aerobic Capacity During Early and Late Stages of Aging

Edwin Nemoto, *University of New Mexico, USA*
P.02-14 Near-Infrared Spectroscopy (NIRS) of Muscle Oxygenation During Exercise

Shinichiro Morishita, *Niigata University of Health and Welfare, Hyogo College of Medicine, Japan*
P.02-15 Relationship Between Corticosteroid Dose and Muscle Oxygen Consumption in Recipients of Hematopoietic Stem-Cell Transplantation

Shinichiro Morishita, *Niigata University of Health and Welfare, Japan*
P.02-16 Relationship Between the Borg Scale Rating of Perceived Exertion and Leg Muscle Deoxygenation During Incremental Exercise in Healthy Adults

Tsubasa Watanabe, *Tokyo Medical University, Japan*
P.02-17 Effects of Exercise Training on Cardiac and Skeletal Muscle Function in Chronic Heart Failure Patients

Tatsuki Endo, *Tokyo Medical University, Japan*
P.02-18 Reduced Scattering Coefficient During Incremental Exercise is Constant Without Being Affected by Changes in Muscle Oxygenation or Hemodynamics

Atsuhiro Tsubaki, *Niigata University of Health and Welfare, Japan*
P.02-19 The Influence of Posture on Lower Limb Muscle Oxygenation During Incremental- Cycle Bicycle Ergometer Exercise

Sho Kojima, *Niigata University of Health and Welfare, Japan*
P.02-20 Relationship Between the Decrease of Oxygenation During Incremental Exercise, Partial Pressure End-Tidal Carbon Dioxide: Near-Infrared Spectroscopy Vector Analysis

Ryotaro Kime, *Tokyo Medical University, Japan*
P.02-21 Exercise-Induced Blood Volume Expansion Measured by NIRS is Derived from Muscle Tissue, Not from Skin

Kazuya Hashimoto, *Niigata University of Health and Welfare, Japan*
P.02-22 Cerebral Oxygenation is Enhanced During Arm Cranking Incremental Exercise Compared to Cycling in Healthy Male Adults

14:30 – 16:00 Poster Session with Refreshments (Posters 1- 22)

Session Chairs: Joseph LaManna, Kim Vandergriff

16:00 – 17:00 O.04 Oral Presentations

Jingjing Jiang, *University Hospital Zurich, Switzerland*
O.04-1 Localization of Deep Ischemia and Hemorrhage in Preterm Infants' Head with Near Infrared Optical Tomography: A Numerical Case Study

Jon Nguyen, *Arizona State University, USA*
O.04-2 Molecular Origins of ROS Formation Revealed by Hybrid Modeling of CIII-CIV Supercomplexes

Gary Angles, *New Mexico Institute of Mining and Technology, USA*
O.04-3 Discerning Membrane Steady-State Oxygen Flux by Monte Carlo Markov Chain Modeling

17:00 – 17:45 Featured Lecture

Sally Pias, *New Mexico Institute of Mining and Technology, USA*

I.04 Computer Modeling of Oxygen Transport in Cells and Tissues

17:45 – 18:45 Dinner

19:00 – 22:00 Flamenco Dance Lounge (purchase tickets)

Monday, July 29th

Session: Tumor Oxygenation and Metabolism

Session Chairs: Anne Riemann, Min Feng

08:00 – 08:45 Keynote Lecture

Brian Pogue, *Dartmouth College, USA*
I.05 Cherenkov Excited Luminescence Imaging of pO_2 in Tumors During Radiation Therapy

08:45 – 10:00 0.05 Oral Presentations

Lin Li, *University of Pennsylvania, USA*
O.05-1 An Observation on Enhanced Extracellular Acidification Induced by Inhibition of the Warburg Effect

Luisa Lange, *University of Halle, Germany*
O.05-2 Role of MicroRNA Expression for Proliferation and Apoptosis of Tumor Cells: Impact of Hypoxia-Related Acidosis

Thea Hüsing, *Julius-Bernstein-Institute of Physiology, Martin-Luther-University Halle-Wittenberg, Germany*
O.05-3 Functional Impact of Acidosis-Regulated MicroRNAs on Migration and Invasiveness of Tumor Cells

Mandy Rauschner, *Julius-Bernstein-Institute of Physiology, Martin-Luther-University Halle-Wittenberg, Germany*
O.05-4 Impact of Acidosis-Regulated MicroRNAs on the Expression of Their Target Genes in Experimental Tumors In Vivo

10:00 – 10:30 Coffee Break & Poster Viewing

Session Chairs: Kui Xu, Eiji Takahashi

10:30 – 11:15 Keynote Lecture

Peter Vaupel, *University Medical Center, Germany*
I.06 The Warburg Effect: Historical Dogma vs. Current Rationale

11:15 – 11:45 O.06 Oral Presentations

Anne Riemann, *Julius-Bernstein-Institute of Physiology, Martin-Luther-University Halle-Wittenberg, Germany*
O.06-1 The Acidic Tumor Microenvironment Affects Epithelial-Mesenchymal Transition Markers as well as Adhesion of NCI-H358 Lung Cancer Cells

Ana Ureba, *Karolinska Institutet, Skandionkliniken, Sweden*
O.06-2 Assessment of the Probability of Tumor Control for Prescribed Doses Based on Imaging of Oxygen Partial Pressure

11:45 – 12:15 P.03 Poster Flash Presentations

Stephanie Blair, *Washington State University, USA*
P.03-23 Oxidative Stress and Oxygen Transport Impairment in Coho Salmon (Oncorhynchus Kisutch) Exposed to Urban Runoff

Scott Nichols, *Profusa, Inc, USA*
P.03-24 Real-Time Tissue Oxygen Monitoring Reveal Hind Limb Hypoxia Following REBOA Treatment in a Swine Model

Gennadi Saiko, *Swift Medical Inc, Canada*
P.03-25 On Feasibility of Pulse Wave Velocity Imaging for Remote Assessment of Physiological Functions

Oxana Semyachkina-Glushkovskaya, *Saratov State University, Russia*
P.03-26 Mechanisms of Sound-Induced Opening of the Blood-Brain Barrier

Gemma Bale, *University College London, UK*
P.03-27 Multimodal Measurements of Brain Tissue Metabolism and Perfusion in a Neonatal Model of Hypoxic-Ischaemic Injury

Kaoru Sakatani, *The University of Tokyo, Waseda University, Japan*
P.03-28 Effects of Aging, Cognitive Dysfunction, Brain Atrophy on Cerebra; Blood Oxygenation and Optical Characteristics in the Prefrontal Cortex: A Time-Resolved Spectroscopy Study

Tongsheng Zhang, *University of New Mexico, USA*
P.03-29 Disruption of Cross Frequency Coupling (CFC) by Cortical Spreading Depression (CSD)

Hamoon Zohdi, *University of Bern, Switzerland*
P.03-30 Effects of Long-Term Blue-Colored Light Exposure on Frontal and Occipital Cerebral Hemodynamics: A Subgroup Analysis of fNIRS Data

Masamichi Moriya, *Teikyo Heisei University, Jikei University Graduate School of Medicine, Japan*
P.03-31 Cerebral Blood Flow Changes in the Prefrontal Cortex Induced by Standing Up Measured by NIRS -Comparison Between Healthy Adults and Post-Stroke Patients-

Kentaro Taniguchi, *Kyoto University, Chubu University, Nagahama Institute of Bio-Science and Technology, Japan*
P.03-32 Parasympathetic Nervous Activity Associated with Dis-coordination Between Physical Acceleration and Heart Rate Variability in Patients with Sleep Apnea

Alex Trofimov, *Privolzhsky Research Medical University, Russia*
P.03-33 The Changes in Brain Oxygenation During tACS at Consequences of TBI: A Near-Infrared Spectroscopy Study

Hiroki Suzuki, *Graduate School of Informatics and Engineering, Japan*
P.03-34 Cerebral Capillary Dilation and Constriction in the Somatosensory Cortex of Awake Mouse: in vivo Two-Photon Microscopic Studies

12:15 – 13:15 Lunch

Session Chairs: Shun Takagi, Ann Flood

13:15 – 14:45 O.07 Oral Presentations

Min Feng, *University of Pennsylvania, USA*
O.07-1 Potential Biomarker for Triple Negative Breast Cancer Invasiveness by Optical Redox Imaging

Jinxia Jiang, *University of Pennsylvania, USA*
O.07-2 Optical Redox Imaging Differentiates Triple-Negative Breast Cancer Subtypes

Maciej Kmiec, *Dartmouth College, USA*
O.07-3 An Implantable MicroChip for Clinical EPR Oximetry

Yu Okuma, *Feinstein Institute for Medical Research, USA*
O.07-4 Oxyhemoglobin Might Evaluate the Quality of Chest Compression

14:45 – 15:20 P.04 Poster Flash Presentations

Lei Ma, *Nantong University, China*
P.04-35 Physical Stress Attenuates Cognitive inhibition: An fNIRS Examination

Denis Bragin, *University of New Mexico, USA*
P.04-36 Drag Reducing Polymer Addition to Colloid Resuscitation Fluid Enhances Cerebral Microcirculation and Tissue Oxygenation After Traumatic Brain Injury Complicated by Hemorrhagic Shock

Sang-Suk Lee, *Sangji University, Republic of Korea*
P.04-37 Magnetoresistance Properties of Several RBCs Combined with Magnetic Nano-Particles and Magnetic Beads Passing Channel Above the GMR-SV Device

Sang-Suk Lee, *Sangji University, Republic of Korea*
P.04-38 Prox-1 and Hif1-a Genes Expression of Primo Vessel in Rabbit's Lymphatic Vessel

Yiming Shen, *Seoul National University, Republic of Korea*
P.04-39 Sympathetic Activity Mediates Extra-Medullary Erythropoiesis in the Primo Vascular System of Heart Failure Rats

Atsuhiro Tsubaki, *Niigata University of Health and Welfare, Japan*
P.04-40 Changes of Prefrontal Cortex and Premotor Area Oxygenation Laterality During 20 min of Moderate-Intensity Cycling Exercise

Weixiang Qin, *Niigata University of Health and Welfare, Japan*
P.04-41 Effects of 20-Minute Intensive Exercise on Subjects with Different Working Memory Bases

Daichi Sato, *Niigata University of Health and Welfare, Japan*
P.04-42 Supine Cycling Exercise Enhances Cerebral Oxygenation of Motor-Related Areas in Healthy Male Volunteers

15:20 – 16:15 Poster Session with refreshments (Posters 23-42)

Session Chairs: Oliver Thews, Scott Nichols

16:15 – 17:00 Featured Lecture
Howard Halpern, *University of Chicago, USA*
I.07 Biologic Validation of Spin Lattice Relaxation Based 3D Patterns of Tumor Hypoxia: Clinical Importance in Preclinical Models

17:00 – 17:45 Featured Lecture
Harold Swartz, *Dartmouth College, USA*
I.08 “Oxygen Level in a Tissue” – What Do We Really Mean When We Report This? – Part 3

18:00 – 19:30 Dinner

Tuesday, July 30th

Session: Brain Oxygenation and Function

Session Chairs: Kazuto Masamoto, Martin Wolf

08:00 – 08:45 Featured Lecture

Ilias Tachtsidis, *University College London, UK*
I.09 Monitoring with Near-Infrared Spectroscopy Brain Oxygenation and Beyond

08:45 – 10:00 O.08 Oral Presentations

Tsukasa Yagi, *Feinstein Institute for Medical Research, USA*
O.08-1 Assessment of Cerebral Blood Oxygenation by NIRS During Asphyxia Cardiac Arrest and Resuscitation in Rats

Timothy R. Darlington, *Case Western Reserve University, USA*
O.08-2 Effects of 3-day and 21-day Hypoxic Conditioning on Recovery Following Cerebral Ischemia in Rats

Carleton J.C. Hsia, *AntiRadical Therapeutics LLC, USA*
O.08-3 Triple-Stroke-Therapy to Eliminate Acute Ischemic Stroke as an Unmet Medical Need

Takuma Sugashi, *Graduate School of Informatics and Engineering, Japan*
O.08-4 Quantitative Volumetric Analysis and Time Scope Tracking of Cerebral Microvascular Networks Imaged with in vivo Two-Photon Microscopy

10:00 – 10:30 Coffee Break & Poster Viewing

Session Chairs: Gemma Bale, Gary Angles

10:30 – 11:45 O.09 Oral Presentations

Lei Ma, *Nantong University, China*
O.09-1 Altered Behavioral Performance in the Neuron-Specific HIF-1 and HIF-2 Deficient Mice Following Chronic Hypoxic Exposure

Ting Li, *Chinese Academy of Medical Sciences & Peking Union Medical College, China*
O.09-2 Online Noninvasive Assessment of Human Brain Death by Near-Infrared Spectroscopy with Protocol at Varied Fraction of Inspired O_2

Edwin Nemoto, *University of New Mexico, USA*
O.09-3 Microvascular Shunts in the Pathogenesis of Cerebral Ischemia of Cerebral Small Vessel Disease to Leukoaraiosis, MS, SLE, MCI, VaD, AD White Matter Hyperintensities

Dmitriy Atochin, *Harvard Medical School, USA* ***Unable to attend.***
O.09-4 Effects of Normobaric and Hyperbaric Hyperoxia on Cerebral Blood Flow and Oxygenation in Traumatic Brain Injury

Kui Xu, *Case Western Reserve University, USA*
O.09-5 Environmental Enrichment Improved Cognitive Performance in Mice Under Normoxia and Hypoxia

11:45 – 13:30 Lunch – *sponsored by Hamamatsu*
Executive Committee Meeting – *Alvarado C*

Session Chairs: Labiblais Rahman, Edwin Nemoto

13:30 – 14:15 Featured Lecture
Ursula Wolf, *University of Bern, Switzerland*
I.10 The Whole Picture: Why a Holistic View of Brain and Body is Desirable in fNIRS

14:15 – 15:00 O.10 Oral Presentations

Mathias Hansen, *University of Copenhagen, Denmark*
O.10-1 The Effect of Not Removing the Glossy White Cover on Adhesive INVOS Neonatal Sensors on Measured Values in the Blood-Lipid Phantom

Helene Isler, *University of Zurich, Switzerland*
O.10-2 Influence of Melanin-like Absorption on Near-Infrared Spectroscopy (NIRS) Oximetry

15:00 – 15:30 Coffee Break

Session Chairs: Ilias Tachtsidis, Ting Li

15:30 – 16:30 O.11 Oral Presentations

Alexander Kalyanov, *University of Zurich, Switzerland*
O.11-1 In-phantom Validation of Time-Resolved Near-Infrared Optical Tomograph Pioneer for Imaging Brain Hypoxia and Hemorrhage

Jianting Wang, *U.S. Food and Drug Administration, USA*
O.11-2 Phantom-Based Testing for Evaluation of Confounding Factors in NIRS Tissue Oximetry

Aldo Di Costanzo-Mata, *University of Zurich, Switzerland*
O.11-3 Time-resolved NIROT 'Pioneer' System for Imaging the Oxygenation of the Preterm Brain: 'Pioneer' Probe Design Optimization

Yu Okuma, *Feinstein Institute for Medical Research, USA, Hiroshima Citizens Hospital, Japan*
O.11-4 Treatment Options for High-Risk Hyperperfusion Patients After Carotid Artery Stenting

16:30 – 18:30 Annual Business Meeting
*All members welcome

18: 30 – Dinner on your own

Wednesday, July 31st

Session: Interstitium, Lymphatics, and Blood

08:00 – 08:05 Opening Remarks
Edwin Nemoto

Session Chairs: Peter Vaupel, Lin Li

08:05 – 08:50 Keynote Lecture
Helge Wiig, *University of Bergen, Norway*
I.11 The Interstitium and Lymphatics – Role in Fluid Volume and Blood Pressure Regulation

08:50 – 09:30 O.12 Oral Presentations

Luca Pollonini, *University of Houston, USA*
O.12-1 Effect of Prolonged Pressure on Sacral Tissues Hemodynamics Assessed by Diffuse Optical Imaging: A Pilot Study

Gennadi Saiko, *Swift Medical Inc, Canada*
O.12-2 Gelatin-Based Phantoms for Oximetry Imaging in the Presence of Edema

09:30 – 10:15 Featured Lecture
Pan-Dong Ryu, *Seoul National University, Republic of Korea*
I.12 Progress in Characterizing Structure and Function of Primo Vascular System

10:15 – 10:45 Coffee Break & Poster Viewing

Session Chairs: Gennadi Saiko, Peter Keipert

10:45 – 12:00 O.13 Oral Presentations

Kim Vandergriff, *VirTech Bio, Inc, USA*
O.13-1 VIR-HBOC: A Novel Highly Polymerized Oxygen Carrier

Paul Buehler, *Food and Drug Administration, USA*
O.13-2 Oxygen Homeostasis and Red Blood Cell Transfusion Quality

Kazuki Hotta, *Niigata University of Health and Welfare, Japan*
O.13-3 Skeletal Muscle Stretching Prolongs Time Constant of Reactive Hyperemia Detected by a Multi-Channel Near-Infrared Spectroscopy in Healthy Male Volunteers

Bhabuk Koirala, *Old Dominion University, USA*
O.13-4 Effect of Blood Flow on Hemoglobin and Myoglobin Oxygenation in Contracting Muscle Using Near Infrared Spectroscopy

12:00 – 12:15 Group Photo

12:15 – 13:15 Lunch – *sponsored by Kinesio Taping Association International (KTAI)*
*Brief (15-min.) talk by **Kenzo Kase** on the Kinesio Taping® rehabilitative taping technique*

13:15 – 18:00 Free Afternoon

18:00 – 22:00 ISOTT Annual Banquet – *Indian Pueblo Cultural Center*
*off-site

KINESIO®

The Original from Dr. Kenzo Kase Since 1979

Taping the World for Health

Certified Kinesio Taping™ and the Kinesio® Taping Method are fast becoming a preferred alternative to opiods.

When properly applied, Kinesio® Tape can be quite effective on helping facilitate movement of interstitial fluid through lymphatic pathways.

Whether you're taping for circulation, lymphatic drainage or bruising, Kinesio® Tape has you covered.

www.kinesiotape.com

/KinesioTapeOfficial

@KinesioTape

Presentations

Presentations are sorted according to the conference agenda

I.01

Mitochondrial function in the intact heart

R. S. Balaban[a]

[a]*National Heart, Lung, and Blood Institute (NHLBI), National Institutes of Health (NIH), USA*

Balaban, Robert S: balabanr@nhlbi.nih.gov

Abstract: Over the last several years several new technologies have revealed important new aspects of cardiac mitochondrial function/structure in the intact heart. Using FIBSEM, the structure of mitochondria on the 10 nm scale of the mouse and shrew heart have revealed a complex mitochondria reticulum supporting the distribution of potential energy for ATP production via electrical conduction rather than relatively slow metabolite diffusion. This system has several “fail-safe” mechanisms to protect this highly coupled system. Using an optical catheter system, coupled to an integrating sphere, transmural near real-time spectroscopic measures of the metabolically active chromophores of the mitochondria within a beating hearts from murine to rabbit models. These measures provide information on cytosolic oxygenation (Myoglobin), mitochondria oxygen tension (COX at 605nm), mitochondrial membrane potential (cyto bL and bH) as well as the redox status of most ofthe respiratory chain in an intact beating heart. The mitochondrial membrane potential using the intrinsic signals from cyto bL and bH of complex III has been validated in isolated heart mitochondria and the intact beating heart. The different redox states of COX including the 2- electron state (607nm), 3 electron state (580nm) and the fully reduced state (605nm) can be detected under physiological conditions in the intact heart, and isolated mitochondria, revealing internal regulatory process within COX with membrane potential and reducing equivalent flux. Using this approach, we have demonstrated that the saline perfused heart is hypoxic under normal perfusion conditions that is actually an active process that can be reversed with exogenous vasodilators, suggesting that the heart is not using its vascular reserve to eliminate hypoxia, so called paradoxical arterial contraction. We have also investigated mitochondrial effects of vascular nitric oxide and ischemia reperfusion in the intact heart.

I.02

Microcirculation and diabetes mellitus

Giuseppe Cicco

Department of Emergency and Organ Transplantation, Section of Internal Medicine, Endocrinology, Andrology and Metabolic Diseases, University of Bari Aldo Moro, Italy

Abstract: *Background* – Hyperglycaemia leads to the development of microcirculation alterations through different mechanisms: a) oxidative stress with excessive production of Reactive Oxygen Species (ROS) and b) endothelial dysfunction. These alterations, together with many biochemical pathways, induce several vasculature complications in diabetics, leading to blindness, end stage renal failure, amputation, acute myocardial infarction (AMI), ictus, transient ischaemic attack (TIA), and stroke. *Materials and Methods* – In this talk it is considered the influence of ROS overproduction diabetes induced with the decrease of superoxide dismutase (SOD) and of glutathione reductase, the value of higher activation of the polyol pathway on the vessels, the action of AGE (Advanced Glycosylation End Products), Protein Kinase C (PKC) activation on microcirculation. To study the alterations in diabetes on eyes, kidneys, brain, hearth and vessels it could be useful to evaluate the red blood cells (RBC) deformability and aggregability using the LORCA (Laser assisted Optical Rotational Red Cells Analyzer), to study vascular morphology the computerized videocapillarioscopy, to evaluate blood flow the laser Doppler and for tissue oxygenation the transcutaneous oxymeters. *Conclusions* – These methodologies and techniques could help physicians to obtain high-quality and rapid diagnosis in diabetic patients and therapies able to restore hyperglycaemia as well as endothelial homeostasis in several organs affected by diabetic complications.

O.01-1

Chronic ketosis modulates metabolite profile and HIF1α mediated inflammatory response in rat brain

Aarti Sethuraman[a], Prahlad Rao[a], B. Atul Pranay[a], Joseph C LaManna[b], Kui Xu[b], and Michelle Puchowicz[a,c]

[a] *Department of Pediatrics, University of Tennessee Health Science Center, USA*
[b] *Department of Physiology and Biophysics, and* [c] *Department of Nutrition, Case Western Reserve University, USA*

Corresponding author e-mail address: mpuchowi@uthsc.edu

Abstract: Hypoxia inducible factor alpha (HIF1α) is associated with neuroprotection conferred by diet-induced ketosis but the underlying mechanism remains unclear (1). In this study we use a ketogenic (high fat, carbohydrate restricted; KG) diet in rodents to induce a metabolic state of chronic ketosis. Ketone bodies are known to be used efficiently by the brain, especially under glucose sparing conditions. Metabolism of ketone bodies is associated with increased cytosolic succinate levels that inhibits prolyl hydroxylases thereby abrogating the ubiquitination of HIF1α, allowing HIF1α to accumulate (1, 2). We have consistently shown that ketosis induced by KG diet correlates with neuroprotection in the aged and following focal cerebral ischemia and reperfusion (via middle cerebral artery occlusion, MCAO); in mouse and rat models (1,2). Studies have also implicated ketosis in modulating metabolic profiles and inflammatory pathways (2, 3), as well as show that HIF1α is necessary for gene expression of IL10 (4). Therefore we hypothesized that ketosis-stabilized HIF1α modulates the expression of inflammatory cytokines orchestrating neuroprotection. To test changes in cytokine levels in rodent brain, eight week old rats were fed either the standard chow diet (SD) or the KG diet for four weeks before ischemia experiments (MCAO) were performed and the brain tissues were collected. Immunoblotting was used to quantify the levels of pro- inflammatory cytokines – IL6 and TNFα and anti-inflammatory cytokine IL10 in the cortical tissues. Consistent with our hypothesis, IL10 levels were significantly higher in KG diet rat brain compared to SD, whereas the TNFα and IL6 levels were significantly lower in the KG group. Further studies are required to confirm if the reduction in IL6 and TNFα levels is due to attenuation of the NLRP3 Inflammasome (5) or via the JAK1-STAT3 pathway (6).

References:

1. Puchowicz M.A., et al. (2008) Neuroprotection in diet-induced ketotic rat brain after focal ischemia. Journal of Cerebral Blood Flow Metabolism. 28(12):1907-16.
2. Puchowicz M.A., et al. (2017). Diet-Induced Ketosis Protects Against Focal Cerebral Ischemia in Mouse. Adv Exp Med Biol.;977:205-213
3. Businaro R., et al. (2018) Anti-Oxidant and Anti-Inflammatory Activity of Ketogenic Diet: New Perspectives for Neuroprotection in Alzheimer's disease. Antioxidants (Basel) 7(5): 63.
4. Semenza G.L., et al. (2013). Hypoxia-inducible factor 1 is required for remote ischemic preconditioning of the heart. PNAS 110 (43) 17462-1746
5. Kanneganti T.D., (2015). Chronic TLR Stimulation Controls NLRP3 Inflammasome Activation through IL-10 Mediated Regulation of NLRP3 Expression and Caspase-8 Activation. Scientific Reports; 5: 14488.
6. S Shankar (2015). A network map of Interleukin-10 signaling pathway. J Cell Commun Signal 10(1): 61–67.

O.01-2

Mitochondrial membrane potential can be sustained without functioning complex IV

E. Takahashi and Y. Yamaoka

Graduate School of Advanced Health Sciences, Saga University, Japan

ejji@cc.saga-u.ac.jp

Abstract: Inhibition of prolyl 4-hydroxylase by a cell permeable α-ketoglutarate analog dimethyloxalylglycine (DMOG) induces HIF-1α in cultured cells. In these cells, glycolysis is stimulated while mitochondrial respiration is significantly suppressed; a phenotype similar to that found in solid tumor tissues *in vivo*. We demonstrated in DMOG treated COS-7 cells that mitochondrial membrane potential (MMP) as assessed by tetramethylrhodamine methyl ester (TMRM) fluorescence did not change despite the considerable reductions in mitochondrial respiration. Theoretically, MMP can be sustained with decreased electron transports if the forward proton translocations in the complex V is simultaneously suppressed. However, the rate of fall of the TMRM fluorescence following electron transport inhibition by antimycin A was unchanged in the DMOG treated cells, indicating that the forward complex V activity was comparable to the untreated cell. These results have led us to a hypothesis that in some cell lines MMP can be maintained without electron transport to the respiratory complex IV. Here, we demonstrate that inhibition of the complex IV by 2 mM KCN did not decrease MMP in COS- 7 cells in which mitochondrial respiration was almost completely abolished. Oligomycin added to KCN-treated COS-7 cells did not affect the MMP, thus excluding the possibility that the reversal of the complex V maintained the MMP. We also demonstrated that complex II inhibition by thenoyltrifluoroacetone (TTFA) significantly decreased the TMRM fluorescence in KCN-treated COS-7 cells. Based on these results, the possibility of electron transport without functioning complex IV will be discussed.

O.01-3

The computerized nailfold video-capillaroscopy as a new technique for microvascular monitoring in Diabetes Type 2

Cicco G., Lisco G., Modugno L., Paparella M.T., Giorgino F***.***

Section of Internal Medicine, Endocrinology, Andrology and Metabolic Diseases – Department of Emergency and Organ Transplantation University Aldo Moro Bari – Bari Italy

Corresponding author e-mail address: gcicco.emo@tiscali.it

Abstract. Patients with type 2 diabetes (T2D) display chronic hyperglycemia, insulin- resistance and relevant diabetes-related comorbidities, such as hypertension, hypercholesterolemia, overweight/obesity with both microvascular and macrovascular complications. Endothelial dysfunction and microvascular damage are involved and should be considered as a target in the prevention of diabetes-related chronic complications. The computerized nailfold video-capillaroscopy (CNVC) is a useful tool to analyze capillaries at the level of the fingers and can provide information on the microvasculature in T2D. Relevant nailfold microvascular alterations can be related to the level of glucose control in patients with T2D. We carried-out a CNVC examination at the level of the IV and V fingers of the non-dominant hand on 102 consecutive and unselected T2D patients (68 males, median age 64y, [26; 83]y). Qualitative and quantitative CNVC parameters were considered. Patients with worse glycemic control (HbA1c >7%) displayed thicker [42.8 (9.8) vs. 38.2 (9.4) µm; p 0.019] and longer capillaries [216.4 (103.8) vs. 174.8 (73.4); p 0.021] compared to those with better glucose control (HbA1c < 7.0%). *Ectasiae* (62.5% vs. 37.7%; p 0.017) and *microaneurysm* (64.6% vs. 43.4%; p 0.045) were also observed to be more prevalent in patients with HbA1c >7.0% than in those with HbA1c < 7.0%. Additionally, patients at high risk of erectile dysfunction (IIEF-5 questionnaire <17 points) compared to those at low risk displayed a lower frequency of capillary with bizarre shape (35% vs. 68.9%, p=0.02). Finally, a higher frequency of *microaneurysm* was noted in patients with carotid stenosis >20% compared to those without stenosis (63.3% vs. 39%, p=0.02). ***Conclusions.*** In T2D, CNVC is an inexpensive tool to better analyze microvascular damage of the hand fingers and identify patients with greater microvascular damage requiring further interventions. Additionally, CNVC could be used as a novel technique to improve microvasculature monitoring during patient follow-up.

O.01-4

Continuous monitoring of healthy volunteers using Profusa's Lumee™ tissue-integrating O_2 sensor and a clinical non-invasive, wearable device

Monica M. Lozano, Jaime Heiss, Dylan Li, Scott Nichols and Natalie Wisniewski

Profusa, Inc, 345 Allerton Ave, South San Francisco, CA 94080 USA

monica.lozano@profusa.com

Abstract: Profusa's Lumee™ oxygen sensors have been functioning in healthy volunteers for up to 4.5 years to date. These novel tissue-integrating sensors are useful indicators of local tissue ischemia (e.g. tourniquet, REBOA), as well as a measure of systemic hypoxia (e.g. altitude, exercise physiology). In this presentation, we will discuss the predictive value of Profusa's sensing platform during real-time, continuous monitoring in an effort to apply it in the early detection of diseases before symptoms present (e.g. influenza).

The Wireless Lumee™ Oxygen Platform is intended for mobile and continuous monitoring of tissue O_2. The Lumee Oxygen Sensor is a soft, biocompatible, and injectable hydrogel designed to sense and report oxygen levels in the subcutaneous tissue. The Lumee Pen is a single-use injector device designed to place a sensor in the subcutaneous tissue. The Lumee Patch is a wireless electronic device used to collect and report tissue oxygen from the sensor. The Lumee Patch App is an iOS application designed to receive, view and transfer information from the Patch via Bluetooth. The App pushes data streams to Profusa's cloud server via WiFi.

In this presentation, we will discuss a clinical feasibility study in which 10 subjects received 2 to 4 Lumee Oxygen sensors in different body location (e.g. abdomen, chest, arm, and/or leg). Subjects were monitored continuously for 7 days during 3 collection periods starting at 0, 1 and 3 months after sensor injection. Subjects were also monitored with a non-invasive wearable device that can collect multiple clinically-relevant, physiological metrics. Subjects were required to perform specific tasks to characterize and predict sensor performance, including: 1) *pressure cuff modulations* to test arm sensors; 2) *leg lift* to test leg sensors; and, 3) *postural change* to test chest/abdomen sensors. Additionally, sensor response to putative sleep, awake, exercise, and health status was characterized.

O.02-1

Event-related NIRS and EEG analysis for mental stress monitoring

L. Rahman [a], K. Oyama [a], A. Tsubaki [b], K. Sakatani [c]

[a] *Nihon University, Japan*
[b] *Niigata University of Health and Welfare, Japan*
[c] *The University of Tokyo, Japan*

Corresponding author e-mail address: oyama.katsunori@nihon-u.ac.jp

Abstract: Mental disorder caused by chronic stress is difficult to be aware of, and your colleagues in the work environment can suddenly report the symptoms. There are social barriers including the financial cost of medical service and lack of perceived need for treatment even if the potential patients have the desire to receive mental healthcare. On the other hand, self-report inventories such as the Beck Depression Inventory (BDI-II) and State-Trait Anxiety Inventory (STAI) can tell the emotional valence for the mental health assessment, which may require medical expertise in the interpretation of their results. Contingency plans for clinical supervision and referral sources are necessary for sufficient mental healthcare. Laterality Index at Rest (LIR) was originally proposed for evaluation of mental stress level from NIRS data in the prefrontal cortex at the resting state, however, potentials in long-term monitoring has not been investigated with sufficient evaluation results. In this study, we use LIR for mental health assessment through long-term monitoring of NIRS, EEG and heart rate (HR) signals. From the experimental result by periodical NIRS and EEG recordings of 4 healthy subjects who participated for over 2 months, temporal changes in FAA, LIR, and HR were compared with BDI-II and STAI scores. We found a cross-correlation between the values of STAI and LIR ($r = 0.70$) with a week-long delay. Importantly, by annotating the larger changes of LIR and HR on the daily life event such as “satisfied”, “irritate” and “nervous”, these larger changes were associated with the life events, and the changes of LIR and HR were different depending on the type of life events. We concluded that the combination of LIR and HR can form a Mental-Physical scale to evaluate the degree of unbalance in mental and physical stresses from the time-series of LIR and HR.

O.02-2

Characterizing tissue oxygen kinetics during continuous real-time monitoring in healthy subjects

Scott P. Nichols[a], Monica Lozano[b], Erin Sproul[b], Dylan Li[b], Jaime Heiss[b], Oxana Pantchenko[b], and Natalie A. Wisniewski[a,b]

[a]*Pre-Clinical and Advanced Technologies, Profusa, Inc. USA*
[b]*Wearables Technology, Profusa, Inc. USA*

scott.nichols@profusa.com

Abstract: Profusa injectable phosphorescent sensors enable real-time, continuous measurement of interstitial oxygen. Previously, monitoring tissue oxygen was typically only feasible during acute applications (e.g., with percutaneous probes, liquid injectable probes) and/or during clinic visits. Fluctuations in oxygen concentration inside the body in daily life may provide insights into patient health for acute and chronic applications. The present study evaluated tissue oxygen through wireless monitoring transmitted via Bluetooth to a smart phone application (Wireless Lumee™ Oxygen Platform by Profusa). The wireless readers reported continuous oxygen concentration (every 5 seconds) in 10 healthy volunteers. Subjects had 2- 4 sensors injected subcutaneously in the arm, chest, abdomen, and/or leg. Subjects wore wireless readers for three 7-day periods, immediately post-injection, and 1- and 3-months post-injection. Subjects recorded contextual information regarding activities performed such as exercise, sleep, driving, flying on an airplane and other activities of daily life. Oxygen concentrations in different anatomical regions across subjects revealed site-to-site and subject-to-subject variability. Tissue oxygen concentration in the chest/abdomen were significantly higher than in the extremities (e.g. arm). Furthermore, a significant elevation in oxygen concentration was observed in subjects during putative sleep compared to awake. Profusa's Lumee Oxygen sensor provides new insight into tissue oxygen concentrations using a wireless non-invasive device following an initial sensor injection. Relative changes and trends in tissue oxygen may provide new insights into subject health as well as early indication of systemic or local changes in the balance of oxygen supply and demand.

I.03

Pathophysiology of microcirculation and oxygen supply in traumatic brain injury

D.E. Bragin

Department of Neurosurgery, University of New Mexico School of Medicine, USA

D.E. Bragin: dbragin@salud.unm.edu

Abstract: Traumatic brain injury (TBI) is a major cause of death and long-term disability contributing to 30% of all injury-related deaths. Over the last decades, TBI research has been focused almost exclusively on neuroprotective strategies to reduce neuronal cells loss that failed to produce any clinically approved therapy. While little can be done to reverse the direct neuronal damage caused by trauma, the vascular/microvascular alterations and dysregulation of cerebral blood flow (CBF) and oxygen supply initiated by TBI is potentially preventable. Thus, as most patients who die after TBI show evidence of ischemic brain damage, the critical role of the vasculature, cerebral circulation, oxygen supply, and their repair in TBI states is beginning to emerge. In my talk I will discuss the pathophysiology of the early post-traumatic alterations in cerebral microcirculation and in oxygen supply that have been reported to reach ischemic levels, initiating a cascade of secondary injury events and energy mediating secondary injury processes.

P.01-1

Extracellular gradients of pH direct migration of MDA-MB-231 cells

D. Yamaguchi, K. Kojima, Y. Yamaoka and **E. Takahashi**

Graduate School of Advanced Health Sciences, Saga University, Japan

eiji@cc.saga-u.ac.jp

Abstract: To determine whether gradients of extracellular pH direct migration of MDA-MB- 231 cells *in vitro*, we followed for 24 hours migrations of individual cells under the gap cover glass (GCG) reported in the previous ISOTT meetings (1, 2). We used Leibovitz's L-15 medium as the extracellular medium that does not contain potent buffer such as bicarbonate. At a cell density of 2 x 10^6 cells/ml, ~0.15 units/mm gradients of extracellular pH developed under the GCG in 3 hours. (3) In this condition, the cell preferentially migrated towards higher pH regions in the GCG. The directional migration was completely disappeared when the extracellular pH gradient was abolished by adding hepes (15 mM) in the L-15 medium. From these results, we conclude that extracellular pH gradients may determine directionality of MDA-MB-231 cell migration *in vitro*.

1. Yahara D *et al*. Directional migration of MDA-MB-231 cells under oxygen concentration gradients. Adv Exp Med Biol. 2016;923:129-134.
2. Tsuruno Y *et al*. An In vitro model for determining tumor cell migration under metabolic gradients. Adv Exp Med Biol. 2018;1072:201-205.
3. Enokida Y *et al*. Directional migration of MDA-MB-231 cells under O_2/pH gradients. Adv Exp Med Biol. 2017;977:169-174.

This work was supported by JSPS KAKENHI 17K07173.

P.01-2

Mitochondria-derived reactive oxygen species mediate enhanced basal pulmonary arterial tone following chronic hypoxia

S. Yan, J.R. Sheak, N.L. Jernigan, B.R. Walker and T.C. Resta

Vascular Physiology Group, Department of Cell Biology and Physiology, University of New Mexico Health Sciences Center, U.S.A.

Corresponding author e-mail address: syan@salud.unm.edu

Abstract: Chronic hypoxia (CH) augments pulmonary arterial tone through O_2^--dependent stimulation of RhoA, a response that may contribute to the vasoconstrictor component of pulmonary hypertension. Although mitochondria are an important source of reactive oxygen species (ROS) in pulmonary arterial smooth muscle cells (PASMCs), the role of mitochondria-derived ROS (mitoROS) in enhanced vasoconstrictor reactivity following CH is unknown. We hypothesized that CH increases mitoROS generation in PASMCs, leading to enhanced basal pulmonary arterial tone. To test our hypothesis, we measured mitoROS levels in transiently cultured PASMCs from normoxic and CH (4 wk, 0.5 atm) rats using the fluorescent indicator MitoSOX (5 μM). Basal pulmonary arterial tone was determined by videomicroscopy in isolated, pressurized small pulmonary arteries [~150 μm inner diameter (i.d.)] in the presence or absence of the nitric oxide (NO) synthase inhibitor N^{ω}-nitro-L- arginine (L-NNA; 300 μM), or after endothelial disruption to minimize the influence of endothelium-derived mitoROS. Pulmonary arterial tone was calculated as the percent difference in i.d. between Ca^{2+}-free and Ca^{2+}-containing conditions. All experiments were performed in the presence of mitochondria-targeted antioxidants, MitoQ (1 μM) or MitoTEMPO (200 μM), or their respective vehicles. We found that MitoSOX fluorescence was significantly ($P < 0.05$) greater in PASMCs from CH rats compared to normoxic controls. In addition, exposure to CH significantly increased basal pulmonary arterial tone in either the presence or absence of NO synthase inhibition, or following endothelial disruption. These responses to CH were abolished by treatment with either MitoQ or MitoTEMPO, indicating that mitoROS provide a major contribution to CH-induced increases in basal pulmonary arterial tone. In addition, we found that CH-induced basal tone was markedly augmented by L-NNA ($P < 0.05$), but not by endothelial disruption, suggesting the endothelium exerts a mitoROS-dependent vasoconstrictor influence following CH that is opposed by NO.

P.01-3

Simulation study of breast cancer lipid changes affecting membrane oxygen permeability

Qi Wang[a] and Sally C. Pias[a]

[a] *Department of Chemistry, New Mexico Institute of Mining and Technology, USA*

qi.wang@student.nmt.edu; sally.pias@nmt.edu

Abstract: Hypoxia is common in cancers of the breast, yet tumor radiotherapy relies on intracellular oxygen (O_2) to generate reactive species that trigger cell death. *De novo* lipid synthesis in tumors supports cell proliferation but also leads to unusually high levels of the 16:1 palmitoleoyl (Y) phospholipid tail, which is two carbons shorter than the 18:1 oleoyl (O) tail abundant in normal breast tissue. Here, we use atomic resolution molecular dynamics simulations to test the hypothesis that lipid bilayers rich in 16:1 Y tails will show reduced permeability because of closer tail packing in the interleaflet region. Indeed, the estimated permeability of the *de novo* lipid biosynthesis product 1-palmitoyl,2-palmitoleoyl- phosphatidylcholine (PYPC) is 17.8 ± 0.3 cm/s at 37°C, compared with the higher permeability of 23.3 ± 0.5 cm/s for 1-palmitoyl,2-oleoylphosphatidylcholine (POPC). Inclusion of cholesterol in a 1:1 ratio with phospholipid partially neutralizes the effect of chain length, giving 9.6 ± 0.3 cm/s for PYPC/cholesterol and 7.9 ± 0.2 cm/s for POPC/cholesterol. These findings indicate an interplay between lipid chain length and lateral packing density. Investigation of chain- length effects in more complex membrane models will be required to understand the influence of *de novo* lipids on cellular oxygenation.

P.01-4

Protein influence on membrane oxygen permeability

R. J. Dotson[a] and S. C. Pias[a]

[a] *Department of Chemistry, New Mexico Institute of Mining and Technology, USA*

Corresponding author e-mail address: sally.pias@nmt.edu

Abstract: Intracellular oxygen (O_2) levels are crucial to energy metabolism, as well as to the success of tumor radiotherapy and the survival of cells in engineered tissue constructs. Yet, the process of oxygen diffusion within and across tissues is only partially understood. Computer modeling has provided valuable insight into membrane-level oxygen diffusion, but transmembrane proteins have rarely been included in the models. Here, we continue previous work with protein/lipid/water systems, using atomistic molecular dynamics simulations with an updated oxygen model. Consistent with previous experimental and simulation work, we find that transmembrane proteins nonspecifically reduce the effective oxygen permeability of membranes. The magnitude of permeability reduction is roughly proportional to the size of the protein and also depends on the size of the protein-lipid interface. In particular, we note here that smaller or uncomplexed proteins have a greater relative effect on permeability than larger proteins and multisubunit complexes. These findings imply that protein complexation can modulate membrane permeability to oxygen and other solutes

P.01-5

Application to the piglet model of a systems biology model of cerebral oxygen delivery and metabolism during therapeutic hypothermia

J. Russell-Buckland[a], I. Tachtsidis[a]

[a]*Dept. Of Medical Physics and Biomedical Engineering, University College London, United Kingdom*

Corresponding author e-mail address: joshua.russell-buckland.15@ucl.ac.uk

Abstract: Hypoxic ischemic encephalopathy (HIE) is a significant cause of death before, during and after birth. Therapeutic hypothermia is one of the most common treatments and generally improves outcome, but 45-55% of injuries still result in fatalities or severe neurodevelopmental disability. Our work has focussed on developing a new systems biology model that includes temperature, as well as a Bayesian framework for analysis of models. Through this we can simulate the effects of temperature on oxygen delivery and metabolism, as well as analysing clinical and experimental data to identify mechanisms to explain differing behaviour and outcome.

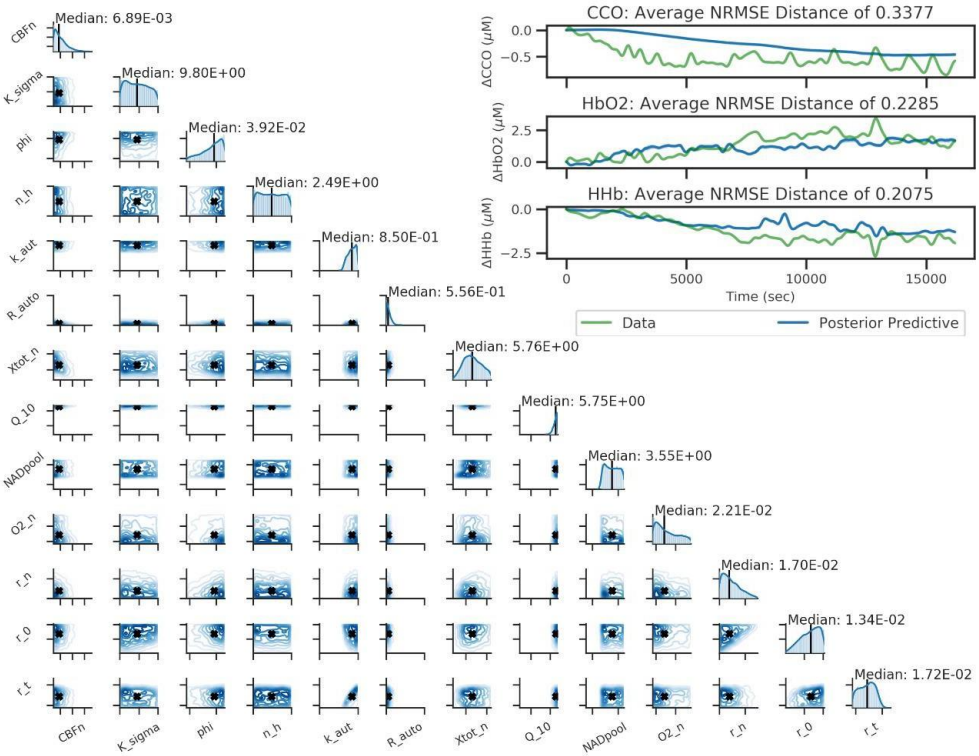

Fig 1: Model parameter posterior and posterior predictive distributions for the hypothermia model.

Presented here is an application of both the new Bayesian model analysis framework and the hypothermia model to data from two piglets showing differing responses and outcome during and following therapeutic hypothermia. We show how the new model identifies possible mechanisms for these differences and how Bayesian analysis can define distinct parameter spaces for each piglet.

P.01-6

Long-term monitoring of physical and mental health conditions using IoT monitoring system

K Sakatani [a, b], M Ishida [c], Y Nagasawa [c], S Ushioda [c], L Hu [a]

[a] *Universal Sport Health Science Laboratory, Dept of Human and Engineered Environmental Studies, Graduate School of Frontier Sciences, The University of Tokyo*
[b] *Institute for Healthcare Robotics, Future Robotics Organization, Waseda University*
[c] *Dept of Electrical and Electronics Engineering, College of Engineering Nihon University, Japan*

k.sakatani@edu.k.u-tokyo.ac.jp

Abstract: We developed the IoT-based monitoring system for long-term monitoring of systemic blood pressure (BP), heart rate (HR), and body weight (BW); this system also allowed measurements of prefrontal cortex (PFC) activity using a near-infrared spectroscopy (NIRS). In the pilot study, we observed that the IoT monitoring system allowed ordinary people (members of a fitness gym) to measure physical and mental health conditions by themselves (ISOTT2019)., which was set up in a local fitness gym (ISOTT2018) [1]. In the present study, employing the IoT monitoring system, we performed long-term monitoring of physical and mental health conditions in the fitness gym (March 1st ~December 31st 2018). We studied116 volunteers (25 males and 91 females, average age 69.0 ± 7.5 years old) recruited from the gym; mean body weight (BW) = 56.0 ± 9.2 Kg, BMI = 22.9 ± 3.1. The subjects provided written informed consents as required by the Human Subjects Committee in the gym. After instruction of use of the IoT monitoring system, the subjects were requested to monitor their physical and mental conditions by themselves when they visited the gym. We evaluated the relations between BP, HR, BW, and ages. In addition, we evaluated the left/right asymmetry of the PFC at rest and BP. We calculated the Laterality index at rest (LIR) for assessment of left/right asymmetry of PFC activity; a positive LIR (0<) indicates right dominant PFC activity, while a negative LIR (<0) indicates left dominant PFC activity [2]. We found statistically positive correlations between BW ($r = 0.243$, $p<0.01$), BMI ($r = 0.191$, $p<0.01$) and ages. Systolic BP positively correlated with ages ($r = 0.178$, $p<0.01$); however, HR negatively correlated with ages ($r = -0.164$, $p<0.01$). The BMI positively correlated with systolic ($r = 0.287$, $p<0.01$) and diastolic BP ($r = 0.309$, $p<0.01$). In addition, there were positive correlations between ages and systolic BP ($r = 0.178$, $p<0.01$), while negative correlations between ages and HR ($r = -0.164$, $p<0.01$). Finally, we observed weak but statistically significant positive correlation between LIR and systolic BP ($r = 0.065$, $p<0.01$) (Fig.1), which is consistent with the studies demonstrating that right PFC has a greater role in cerebral regulation of sympathetic effects [3].

Fig. 1 Relation between systolic BP and LIR

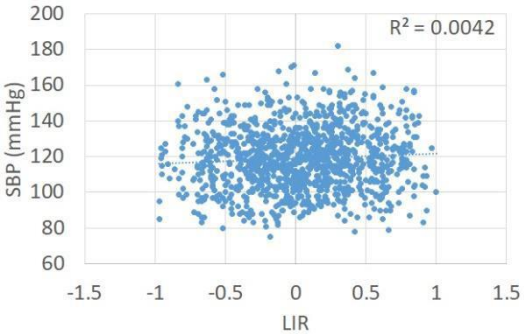

References

[1] Ishida, et al. Adv Exp Med Biol, 2019 (in press)
[2] Ishikawa, et al. J Biomed Opt. 19(2):027005, 2014
[3] Tanida, et al. Neuroscience Letters 369:69-74, 2004

P.01-7

NIRS might contribute to detect the harmful effect of adrenaline

Y. Okuma[a], K. Shinozaki[a], T. Yagi[a], T. Yin[a], T. Kiguchi[b], T. Iwami[b], J. Kim[a], and L.B. Becker[a]

[a] *Department of Emergency Med-Cardiopulmonary, Feinstein Institute for Medical Research, Northwell Health System, Manhasset, NY, USA*
[b] *Kyoto University Health Service, Kyoto, Japan*

Corresponding author e-mail address: y8u2bear4@hotmail.com

Abstract: Guidelines recommended intravenous adrenaline as a crucial pharmacologic treatment during cardiac arrest (CA) resuscitation. Recent studies revealed that adrenaline increased the likelihood of return of spontaneous circulation but also worse neurological outcomes. The specific reasons are still unclear. Recently we observed the bimodal trend of mean arterial pressure (MAP) after adrenaline injection in rodent's CA model. In this study, we evaluated the trend of oxyhemoglobin (Oxy-Hb), Deoxy-Hb, and tissue oxygenation index (TOI). Next, we evaluated the relationship between MAP and Oxy-Hb, Deoxy-Hb, and TOI. Male Sprague-Dawley rats were used. We attached the near-infrared spectroscopy (NIRS) between the nasion and upper cervical spine. Rats underwent 10-minute asphyxial CA. After CA, we performed manual cardiopulmonary resuscitation (CPR). 30 seconds after the beginning of CPR, we administrated a 20 μg/kg bolus of adrenaline. We monitored animal physiology 2 hours after resuscitation. First, we normally observed Oxy-Hb and TOI went up as MAP went up. We also observed the similar bimodal trend of MAP. Interestingly, when MAP exceeded a certain value, Oxy-Hb and TOI paradoxically went down and Deoxy-Hb went up as MAP went up. Based on this result, we compared Oxy-Hb, Deoxy-Hb, and TOI at the first MAP ≈ 100mmHg and second MAP ≈ 100mmHg. Evaluating the difference between the average of the current 20 seconds and that of the previous 20 seconds revealed that Oxy-Hb and TOI significantly went down at the second 100mmHg, while Deoxy-Hb significantly went up. Finally, comparing the MAP at which the paradoxical trend was starting firstly and secondly showed that second MAP was significantly lower than the first one.
When adrenaline increased MAP especially for the second time, the effect on cerebral blood flow might be inconsistent. We need to experiment more detail, but NIRS might contribute to detect the harmful effect of adrenaline.

P.01-8

Scalp hemodynamics over brain motor regions: A homogeneous or inhomogeneous phenomenon?

Dominik Wyser[a,b], Felix Scholkmann[b,c], Michelle Mattille[a], Olivier Lambercy[a], Roger Gassert[a], Martin Wolf[b]

[a] *Rehabilitation Engineering Lab (RELab), Department of Health Sciences and Technology, ETH Zurich, 8092 Zurich, Switzerland*

[b] *Biomedical Optics Research Laboratory (BORL), Department of Neonatology, University Hospital Zurich, University of Zurich, 8091 Zurich, Switzerland*

[c] *University of Bern, Institute of Complementary and Integrative Medicine, 3012 Bern, Switzerland*

Corresponding author: domink.wyser@hest.ethz.ch

Abstract: Functional near-infrared spectroscopy (fNIRS) measurements on the human head can be influenced by scalp hemodynamics. The understanding of scalp hemodynamics is important for the reliable application of short-channel regressions (SCR), where the scalp hemodynamics is measured with a short-separation channel (typically < 15 mm source- detector distance) and is regressed from a long-separation channel (~30 mm). As a result, more accurate estimations of cerebral hemodynamics can be realized. While studies mainly investigated the advantages of different SCR algorithms, the question of which scalp hemodynamic signal to use for the regression has only been partially investigated. Different assumptions can be found in the literature about the spatial aspects of scalp hemodynamics being homogeneous or inhomogeneous. This can lead to different results in fNIRS studies using SCR. In this work, we investigated the spatial topology of scalp hemodynamics in 5 subjects during resting-state and a hand motor execution task. Measurements were performed with a commercially available system (NIRSport, NIRx Medizinaltechnik GmbH Germany) including a novel cap design including 8 short channels of 7 mm distance. We found that (i) there is a global pattern of scalp hemodynamics (Pearson's correlation coefficient > 0.7) in two frequency ranges (i.e., hemodynamic-response and Mayer- wave frequency bands), and that (ii) there are local differences between the short-separation channels that should not be neglected. In particular, we show that the phase shifts between different head regions can lead to significant residuals after applying SCR. The understanding of the inhomogeneity of scalp hemodynamics is important to improve future SCR algorithms and will increase the sensitivity of fNIRS to cerebral hemodynamics.

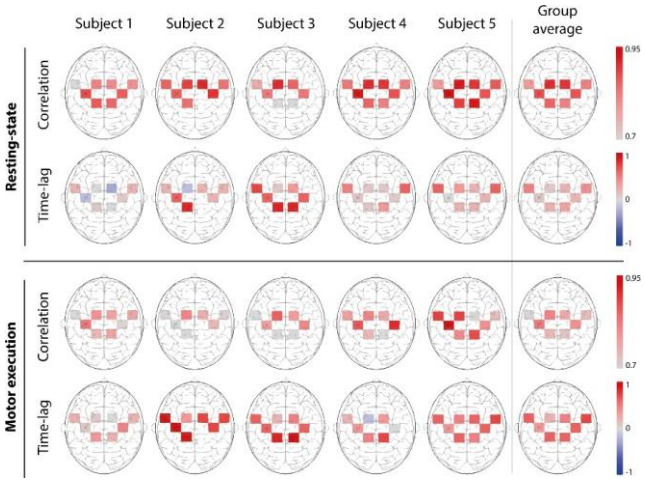

Figure 1: Hemodynamic-response frequency band analysis (0.01-0.3 Hz): Correlation and lag of 5 subjects and the group-average for resting-state and a motor execution task. The correlations are calculated between a long channel placed over the left primary motor cortex and the 8 short-separation channels. Most channels show a global behavior with Pearson's correlation coefficients > 0.7, but lower correlations and more inhomogeneous spatial patterns during motor execution tasks are observed.

P.01-9

Two consecutive invasive surgeries utilizing Zymogen Protein C (ZPC) that enhanced patient safety and reduced costs

D. F. Bruley[a], J. M. Abdallah[b], M. B. Streiff[c], S. E. Reeg[b], C. C. Hasty[b], K. C. Bruley[a], M. Duncan[b], R. Duncan[b], **E. E. Thiessen**[a], M. B. White[a] and S. B. Bruley[a]

[a] *Synthesizer,Inc., Ellicott City, MD, USA*
[b] *Vidant Medical Center, East Carolina University, Greenville, NC, USA*
[c] *Johns Hopkins Medical Institutions, Baltimore, MD, USA*

Eileen Thiessen <eileen@chemicalgraphics.com>

This case report concerns the safer surgery for a protein C deficient, hypercoagulable patient who underwent two back-to-back invasive surgeries, hip replacement and spinal stenosis correction. The patient, an eighty-four-year-old male with a history of deep vein thromboses (DVT) and pulmonary emboli (PE), was treated pre-, peri- and postoperatively with zymogen protein C (ZPC-Baxter, International) and recovered without clotting or increased bleeding. During the procedure, the patient was not administered any other anticoagulants. Since there are now at least seven independent case reports worldwide, the procedure is becoming a viable choice for patients with a high probability of clotting during and after invasive surgery. This case focuses on accomplishing safer surgery while reducing costs (two surgeries with ZPC cost for one at reduced ZPC administration) from the ZPC used. This procedure might also be useful for many medical situations where acquired protein C deficiency is a problem (e.g. sepsis, pregnancy, etc.). In addition, this approach may have greater application to medical conditions other than Protein C deficiency (elevated prothrombin, etc.), where clotting and inflammation could be an issue. Further research and case studies will have to be completed to establish the efficacy of using ZPC more broadly to increase patient safety for all surgical patients.

P.01-10

A new needle mounted optical scanner for measuring spatio-temporal distributions of tissue oxygen in cancer tumors

S. Ashkenazi[a,b], D. Cho[c], and C. W. Song[c]

[a] *Department of Biomedical Engineering, University of Minnesota, Minneapolis, Minnesota, USA*
[b] *A-Scan LLC, Minneapolis, Minnesota, USA*
[c] *Department of Therapeutic Radiology-Radiation Oncology, University of Minnesota, Minneapolis, Minnesota, USA*

Corresponding author e-mail address: ashke003@umn.edu

Abstract: A novel optical scanner for measuring tissue oxygen distribution in small animals has been developed. An optical fiber scanning mechanism is housed inside a glass capillary, protected by a stainless-steel needle. A longitudinal window along the needle allows for a direct contact between the tissue and an oxygen-sensitive layer, coated on the outer surface of the glass capillary. This configuration enables tissue oxygen measurement at any point along the needle shaft. In contrast to currently used oxygen needle probes, no movement of the needle with respect to the tissue is required. This feature allows for repeated scans while avoiding excessive tissue damage.

In this presentation, we show preliminary results from a small-scale experiment demonstrating the ability to repeatedly scan a cancer tumor in a mouse model. Results show a transient pO2 profile, following the insertion of the needle, possibly, due to oxygen redistribution by fluid motion caused by the needle insertion. Repeated scans are necessary to monitor the process of reestablishing a steady tissue oxygen distribution after the needle has been positioned. Cancer tumors scanned in this experiment show a highly hypoxic tumor core.

This newly developed tissue oxygen scanner provides a simple mean to obtain depth profiles of pO2 along a single line and to track temporal change. The fact that the needle is static with respect to the tissue while scanning enhances measurement stability and reliability.

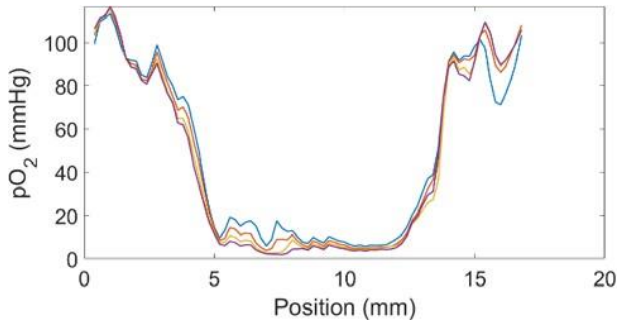

P.01-11

Transcranial photobiomodulation of clearance of beta-amyloid from the mouse brain: the effects on meningeal lymphatic drainage and blood oxygen saturation of the brain

O. Semyachkina-Glushkovskaya[a], A. Abdurashitov[a], M. Klimova[a], A. Terskov[a], I. Blokhina[a], V. Tuchin[a]

[a] *Saratov State University, Russia*

Corresponding author e-mail address: glushkovskaya@mail.ru

Abstract: In this pilot study we analyzed effects of transcranial photobiomodulation (tPBM, 1267 nm, 32 J/cm2) on clearance of beta-amyloid (Aβ) from the mouse brain. The immunohistochemical and confocal data clearly demonstrated significant reduction of deposition of Aβ plagues in mice after tPBM vs. untreated animals. The behavior tests showed that tPBM improved cognitive, memory and neurological status of mice with Alzheimer's disease (AD). The study of mechanisms of therapeutic effects of tPBM showed that tPBM increased the blood oxygen saturation (SpO2, measured by pulse oximetry) that was associated with activation of meningeal lymphatic drainage system (evaluated by optical coherence tomography with gold nanorods 98 nm as contrast agents) without any changes in the relative cerebral blood flow (rCBF, evaluated by laser contrast speckle imaging). These pioneering results open breakthrough strategies for non-pharmacological therapy of Alzheimer's disease and clearly demonstrate that tPBM might be a promising therapeutic target for preventing or delaying Alzheimer's disease based on stimulation of oxygenation of the brain tissues and activation of clearance of toxic molecules via the cerebral lymphatics.

This study was supported by grants from Russian Science Foundation 18-75-10033 (Immunohistochemical, confocal and behavior data) and 19-15-00201 (measurement of rCBF, SpO2 and lymphatic drainage).

P.01-12

Gene expression pattern of the primo vascular system is similar to that of the spleen

Yiming Shen[1], Kang-Hoon Lee[2], Je-Yoel Cho[2], Pan-Dong Ryu[1]

Departments of Veterinary Pharmacology[1] and Biochemistry[2], College of Veterinary Medicine and Research Institute for Veterinary Science, Seoul National University, Seoul 08826, Republic of Korea

pdryu@snu.ac.kr

Abstract: The primo-vascular system (PVS) is a novel putative circulatory system composed of primo-nodes and primo-vessels. Recently we observed that the morphological changes of organ surface PVS tissue are associated with erythropoiesis in the rats with heart failure, or hemolytic anemia. Here, we further investigated whether those morphological changes are consistent with the changes in gene expression. To this end, the transcriptome of the organ surface PVS tissue in normal rats was analyzed by total RNA-Seq. The gene expression pattern of the rat organ surface PVS tissue showed higher similarity to that of the spleen among those of other tissues such as the lung, kidney, liver, and colon from human, mouse, dog, and monkey. The top 100 genes expressed more than three folds in the organ surface PVS appeared associated with the bone marrow, blood, elliptocytosis, hemolytic anemia, and heme biosynthesis. We also compared the transcriptomes of the organ surface PVS from normal and anemic rats. Hemolytic anemia was induced by an intraperitoneal injection of phenylhydrazine. There were 118 genes up-regulated and 26 genes down- regulated more than two folds in the organ surface PVS tissue from the anemic rats compared to those from normal rats. The up-regulated genes were highly combined with erythroblast, bone marrow, anemia, erythroid cell, and heme biosynthesis, whereas the down-regulated genes were macrophage, blood platelet, immune system, and cytokines, and inflammatory response. The results are consistent with the previous reports showing the morphological changes associated with erythropoiesis in the organ surface PVS tissues in the rat with heart failure or hemolytic anemia. Taken together, our results from normal and anemic rats show that the PVS is similar to the spleen in the gene expression pattern and in the extramedullary erythropoiesis. The results indicate that the PVS may function as a lymphoid organ.

Acknowledgment: This study was supported by the National Research Foundation of Korea funded by the Ministry of Education (2018R1D1A1B07043448).

O.03-1

Simultaneous measurement of pH and partial pressure of oxygen in solutions using Electron Paramagnetic Resonance (EPR) spectroscopy: A feasibility study by 750 MHz EPR

A. Taguchi[a], S. DeVience[b], B. Driesschaert[b], V.V. Khramtsov[b], and **H. Hirata**[a]

[a] *Division of Bioengineering and Bioinformatics, Hokkaido University, Japan*
[b]*Department of Biochemistry and In Vivo Multifunctional Magnetic Resonance Center, West Virginia University, WV, USA*

hhirata@ist.hokudai.ac.jp

Abstract: Acidosis and low-oxygen status are hallmarks of solid tumors; thus simultaneous measurement and eventually, simultaneous mapping of extracellular pH (pHe) and the partial pressure of oxygen (pO_2) are in high demand to monitor the pathophysiological status of tumors. To develop a method of simultaneous mapping of pHe and pO_2, we conducted the feasibility test of a 750-MHz home-built continuous-wave electron paramagnetic resonance (CW-EPR) spectrometer/imager (1) with a monophosphonated trityl radical (p1TAM). This probe has multifunctional sensing capability for pO_2, pHe, and inorganic phosphate (2,3), and was synthesized according to the previous report (4). To obtain the calibration data of pO_2 and pH, the solution samples of p1TAM were prepared for various conditions (pH in the range of 6.0 to 7.5 and pO_2 in the range of 0 to 76 mmHg). The linewidth of the Lorentzian component and the fraction of two absorption peaks were obtained using spectral fitting. Since these values depend on pO_2 and pH of the solution sample, pO_2 and pH can be measured by those spectral parameters simultaneously. From the measured spectral data, the sensitivity of pO_2 was obtained to be 0.49 mG/mmHg. Also, the pH titration of the fraction of EPR peaks was obtained. Since the simultaneous measurement of pO_2 and pH is feasible with our EPR spectrometer, we plan to develop a method of three-dimensional simultaneous mapping of pO_2 and pH for tumor model animals.

Acknowledgements
This work was supported by JSPS KAKENHI grant numbers JP19H02146, JP18KK0304 and NIH grants CA194013, CA192064, EB023990.

References
(1) H. Sato-Akaba *et al*., *Anal Chem* **2009**, *81*, 7501.
(2) A. A. Bobko *et al*., *Angew Chem Int Ed* **2014**, *53*, 2735.
(3) A. A. Bobko *et al*., *Sci Rep* **2017**, *7*, 41233.
(4) I. Dhimitruka *et al*., *J Am Chem Soc* **2013**, *135*, 5904.

O.03-2

Developing quantitative optical redox imaging techniques to identify potential Alzheimer's Disease biomarkers

H. N. Xu[a], S. Gourmaud[b], A. Podsednik[a], A. Jacob[a], F. E. Jensen[b] and L. Z. Li[a]

[a] *Department of Radiology,*[b] *Department of Neurology, Perelman School of Medicine, University of Pennsylvania, USA*

Corresponding author e-mail address: hexu2@pennmedicine.upenn.edu

Abstract: Novel and effective approaches to characterizing and diagnosing Alzheimer's disease (AD) in its early stage are urgently needed. Optical redox imaging (ORI) collects intrinsic fluorescence of two important co-enzymes: reduced nicotinamide adenine dinucleotide (NADH) and oxidized flavoproteins (Fp containing flavin adenine dinucleotide) and has been widely applied to study cellular energetics and metabolism, and for disease diagnosis /prognosis. Given that the etiology of AD is unclear and metabolic changes at the molecular level may be detected prior to histological changes, we examined whether ORI of brain tissues could identify and characterize certain AD-associated metabolic changes. Fresh brain tissues of 5XFAD (an early on-set AD mouse model) and wild type (WT) littermate mice at various ages (spanning ~1-14 months) were collected. Fresh hippocampal sections maintained in glucose-spiked imaging solution were imaged by ORI *ex vivo* using a wide-field fluorescence scope. They were then metabolically perturbed sequentially by a mitochondrial uncoupler and inhibitors and imaged accordingly to obtain the redox plasticity. Snap-frozen hemispheres and hippocampi were also imaged in a 3D fashion by the Chance redox scanner. To examine brain tissues at the individual cell level using formalin-fixed tissue slides [1], fixation effects on tissue redox were evaluated with 4% paraformaldehyde (PFA). We found 1) strong redox signals in the fresh, snap-frozen, and formalin-fixed brain tissues and time- dependent redox changes of the fresh tissues; 2) differential redox plasticity between 5XFAD and WT hippocampi; 3) good alignments between the redox patterns and brain hemisphere anatomical regions with a differential redox state between 5XFAD and WT brains in the same regions; 4) differential age-associated hippocampal redox changes between 5XFAD and WT;
5) a significant increase in Fp signals and the redox ratio, Fp/(NADH+Fp), in both groups due to PFA fixation. These observations indicate a promising potential for ORI to be further developed for AD biomarkers.

[1] Xu HN, Zhao H, Chellappa K et al. (2019) Optical Redox Imaging of Fixed Unstained Muscle Slides Reveals Useful Biological Information. Molecular Imaging and Biology, 21:417- 425.

O.03-3

Online assessment of hemodynamics in suctioned volume of biological tissue by the embedded near-infrared spectroscopy sensor

Chenyang Gao[1] and Ting Li[1,*]

[1]Institute of Biomedical Engineering, Chinese Academy of Medical Sciences & Peking Union Medical College, Tianjin 300000, P. R. China

**Correspondence: liting@uestc.edu.cn*

Abstract: Cupping therapy is a promising method to cure or reduce symbol of some diseases including muscle pain/tendency/fatigue. Although the applications of cupping therapy have thousand-year history in traditional Chinese medicine and has been spread to abroad in recent years, the cupping therapy is something like a black box and the unskilled users can hardly control it due to the absence of physiological observations. Therefore, we developed a near infrared spectroscopy (NIRS) instrument with three probes to detect the blood-oxygen of skin tissue on where the cupping therapy is carried out. Each probe includes tow detection channels. One of the probes is embedded in the cup to monitor the hemodynamic parameters in the cupping site. And the other two probes are placed outside surrounding the cupping site. Using this instrument, we can observe the alternations of [HbO2], [Hb] and [tHb], as well as the heart rate calculated from the change curves of [HbO2] during cupping therapy in real time. We tested the electrical performance parameter and the ability of in-vivo detection of the NIRS monitor. For the in-vivo detection, significant hemodynamic changes occurred during cupping therapy and the results of inner cup and outside cup were opposite, indicating the redistribution of blood oxygen due to the cupping treatment. Results showed that the NIRS monitor can detect the hemodynamic changes during the cupping therapy on/surrounding the cupping site. The users can evaluate the curative effect and control the cupping process based on the hemodynamic signals.

P.02-13

Skeletal muscle deoxygenation and its relationship to aerobic capacity during early and late stages of aging

S. Takagi[a], R. Kime[b], N. Murase[b], M. Niwayama[c], S. Sakamoto[d] and T. Katsumura[b]

[a] *Faculty of Health and Sports Science, Doshisha University, Japan*
[b] *Department of Sports Medicine for Health Promotion, Tokyo Medical University, Japan*
[c] *Department of Electrical and Electronic Engineering, Shizuoka University, Japan*
[d] *Faculty of Sport Sciences, Waseda University, Japan*

shtakagi@mail.doshisha.ac.jp

Abstract: Leg blood flow is reduced during large muscle exercise in elderly, compared to young people, and the enhancement of muscle deoxygenation during submaximal exercise can generally be explained by reduced convective O_2 transport due to aging. However, the time course of aging on microcirculation and metabolism in skeletal muscle during exercise is not fully understood. The aim of this study was to investigate muscle O_2 dynamics during cycling exercise and their relationship to aerobic capacity in elderly (n=10, 73 ± 3 years), middle-aged (n=9, 50 ± 6 years), and young (n=10, 25 ± 3 years) subjects. The subjects performed ramp bicycle exercise until exhaustion. Muscle O_2 saturation (SmO_2) and relative changes from rest in oxygenated hemoglobin (Δoxy-Hb), deoxygenated hemoglobin (Δdeoxy- Hb) and total hemoglobin concentration (Δtotal-Hb) were monitored continuously at vastus lateralis muscle by near infrared spatial resolved spectroscopy, with optical correction for the effect of light scattering in the fat layer. At given absolute workloads, SmO_2 and Δoxy-Hb were significantly lower in elderly than the other groups, while Δdeoxy-Hb, Δtotal-Hb, and pulmonary O_2 uptake (VO_2) were similar among the three groups. In contrast, there were no significant differences in muscle O_2 dynamics during submaximal exercise between middle-aged and young subjects. Moreover, change in SmO_2 was significantly positively correlated with peak VO_2 in elderly, while a significant negative relationship was observed in middle-aged and young subjects. These results suggest that during submaximal exercise, muscle O_2 dynamics may be relatively preserved in early stages of aging, although muscle deoxygenation is enhanced in late stages of aging, probably due to reduced convective O_2 supply. In late stages of aging, diminished peak VO_2 is mainly caused by attenuated convective O_2 transport, rather than diffusive O_2 transport, while reduced peak VO_2 can partly be explained by lowered muscle O_2 extraction in early stages of aging.

P.02-14

Near-Infrared Spectroscopy (NIRS) of muscle oxygenation during exercise

E. M. Nemoto

Department of Neurosurgery, University of New Mexico, USA

Abstract: Introduction: Continuous noninvasive monitoring of muscle oxygenation has important clinical applications. NIRS has such potential and been used to detect deep venous thrombosis and limb perfusion and revascularization. The aim of this study is to examine the relationship between muscle oxygenation and venous saturation during exercise.

Methods: Eleven normal subjects were studied with informed consent an an IRB approved protocol. A 22 ga Intracath was inserted retrograde into the antecubital vein draining the region over which the NIRS sensor (INVOS4100, Somanetics, Corp.) was applied on the volar aspect of the forearm. A baseline rSO2 reading was obtained with simultaneous venous blood sampling with the arm held at the level of the heart. The forearm was raised above the head and a second reading was obtained with simultaneous sampling of venous blood for blood gas and oxygen saturation measurements. The subjects were asked to exercise their forearm by clenching and relaxing their fist while observing the oximeter and driving the reading to specified levels from 90 to 15% (minimum possible reading). At each level, a venous blood sample was withdrawn for measurement of blood gases and oxygen saturation (IL-Co- Oximeter). Results: Fig. A. RSO_2 (%) vs VO_2 Sat showed a two-component HbO_2 desaturation suggesting representation of venous HbO_2 desaturation and perhaps Myoglobin Oxygen (MBO_2) desaturation. Fig. B. Subtraction of the linear venous HbO_2 curve from the two-component curve suggests MbO_2 desaturation at venous hemoglobin oxygen saturation of about 10-20%. Conclusions: The kinetics of desaturation during exercise revealed two-components likely representing hemoglobin and myoglobin deoxygenation.

The data suggest that myoglobin represents approximately 40% of the NIRS signal and the balance or 60% to hemoglobin.

A

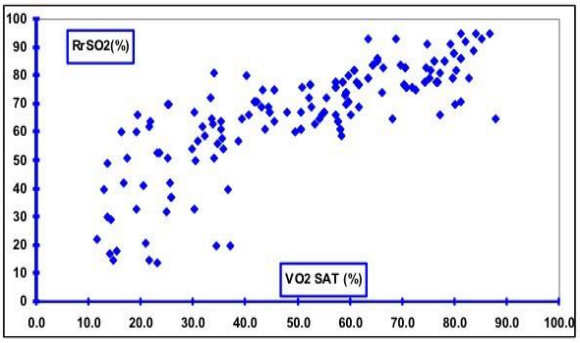

Curvilinear relationship between rSO2 and venous oxyhemoglobin saturation ($HbvO_2$) revealing two-component desaturation kinetics.

B

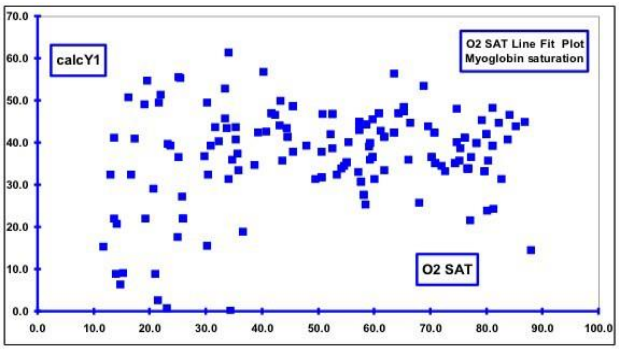

Subtraction of oxyhemoglobin from the 2-component A curve shows full saturation of myoglobin until venous hemoglobin oxygen saturation of about 40%.

P.02-15

Relationship between corticosteroid dose and muscle oxygen consumption in recipients of hematopoietic stem-cell transplantation

Shinichiro Morishita[1,2*], Tatsushi Wakasugi[3], Katsuji Kaida[4], Yusuke Itani[3], Kazuhiro Ikegame[4], Yoshihiro Fujimori[4], Kazuhisa Domen[2]

.

[1] *Institute for Human Movement and Medical Science, Niigata University of Health and Welfare Adress:1398 Shimami-cho, Kita-ku, Niigata-city, Niigata 950-3198, Japan*
[2] *Department of Physical Medicine and Rehabilitation, Hyogo College of Medicine*
[3] *Department of Rehabilitation Medicine, Hyogo College of Medicine Hospital*
[3] *Division of Hematology, Department of InternalMedicine, Hyogo College of Medicine*

Corresponding author e-mail address: morishita@nuhw.ac.jp

Abstract: *Introduction*: After hematopoietic stem-cell transplantation (HSCT), patients exhibit decreased muscle strength and muscle oxygen consumption. Furthermore, total corticosteroid dose affects the reduction in muscle strength after HSCT. However, to date, no studies have investigated the relationship between corticosteroid dose and muscle oxygen consumption and saturation in these patients. The purpose of this study was to investigate the relationship between steroid dose and deoxy-hemoglobin (ΔHHb) and muscle oxy-hemoglobin saturation (ΔSmO_2) in patients undergoing HSCT. *Methods:* This study included 17 men with hematologic disease who underwent allogeneic HSCT. We evaluated ankle dorsiflexor muscle force, ΔHHb, and ΔSmO_2 in skeletal muscles by near-infrared spectroscopy (NIRS) in patients before and after HSCT. *Results:* Peak ankle dorsiflexion, ΔHHb, and ΔSmO_2 decreased significantly after transplantation as compared to measurements taken before transplantation ($p < 0.01$). The change in peak ankle dorsiflexion from before to after HSCT was not significantly correlated with total steroid dose. However, ΔHHb and ΔSmO_2 from before to after HSCT were significantly correlated with total steroid dose ($p < 0.01$). *Conclusion*: This study showed that higher corticosteroid doses are associated with diminished skeletal muscle O_2 consumption and skeletal muscle O_2 demand relative to supply. Therefore, rehabilitation staff, nurses, and physicians should take note of these findings in patients undergoing HSCT. Moreover, physiotherapists should be carefully changing muscle oxidative metabolism on skeletal muscle when planning physical exercise in such patients.

P.02-16

Relationship between the Borg scale rating of perceived exertion and leg muscle deoxygenation during incremental exercise in healthy adults

Shinichiro Morishita[1.2*], Atsuhiro Tsubaki[1.2], Kazuki Hotta[1.2], Sho Kojima[1], Daichi Sato[2], Akihito Shirayama[2], Yuki Ito[2], and Hideaki Onishi[1,2].

1 Institute for Human Movement and Medical Science, Niigata University of Health and Welfare
2 Department of Physical Therapy, Faculty of Rehabilitation, Niigata University of Health and Welfare

Corresponding author e-mail address: morishita@nuhw.ac.jp

Abstract: Introduction: The Borg scale rating of perceived exertion is a reliable indicator, and widely used to monitor and guide exercise intensity. We aimed to evaluate the relationships between the Borg scale score and oxygenated hemoglobin (O2Hb) and deoxygenated hemoglobin (HHb) concentrations in the leg muscle as measured by near infrared spectroscopy (NIRS) during cardiopulmonary exercise testing (CPET) in healthy adult men. We also investigated the relationships between the Borg scale score and the work rate (WR), heart rate (HR), oxygen uptake (VO2) and minute ventilation (VE). Methods: Participants comprised 12 healthy men. Cardiopulmonary and NIRS parameters were assessed during each minute of CPET and at the end of the test. Results: The Borg scale score was significantly correlated with cardiopulmonary parameters including WR, HR, VO2, and VE during CPET (Rs=0.87-0.95; $p<0.05$). Furthermore, the Borg scale score was significantly correlated with NIRS parameters including O2Hb and HHb levels during CPET (Rs=-0.48, and 0.45, respectively; $p<0.05$). Discussion: The Borg scale score is significantly correlated with cardiopulmonary parameters (WR, HR, VO2, and VE), as well as with leg-muscle oxygenation parameters as assessed by NIRS, during CPET in healthy adults. The correlation coefficients obtained from NIRS parameters were lower than those of cardiopulmonary parameters. Conclusions: The Borg scale score might better reflect cardiopulmonary responses than muscle deoxygenation during exercise. These results can aid in the planning of rehabilitation programs for healthy adults.

P.02-17

Effects of exercise training on cardiac and skeletal muscle function in chronic heart failure patients

T. Watanabe, N. Murase, R. Kime, Y. Kurosawa, S. Fuse and T. Hamaoka

Department of Sports Medicine for Health Promotion, Tokyo Medical University, Tokyo, Japan

hhspj139@ybb.ne.jp

Abstract: Introduction: The primary symptom in patients with chronic heart failure (CHF) is exercise intolerance. Many previous studies have reported that reduced exercise tolerance in CHF can be explained not only by cardiac output (a central factor), but also by reduced skeletal muscle aerobic capacity (a peripheral factor). Although exercise training in CHF improved exercise tolerance, few studies have reported the effects of exercise training on each specific central and peripheral factor in CHF. The aim of this study was to investigate the central and peripheral aerobic functions in CHF, and the effects of exercise training in CHF on cardiac output and skeletal muscle deoxygenation during exercise.
Methods: This study included seven patients with CHF and eight age-matched healthy subjects. We assessed peak oxygen uptake during cardiopulmonary exercise testing (CPX), as well as peak cardiac output by noninvasive hemodynamic monitor, and muscle oxygen saturation by near-infrared spectroscopy (NIRS). The patients with CHF were trained for 12 weeks, and performed ramp cycling exercise until exhaustion before and after the exercise training.
Results: Peak oxygen uptake, peak cardiac output and change in muscle oxygen saturation from rest to peak exercise (ΔSmO2) were significantly lower in CHF than those in healthy subjects. As a result of exercise training, peak oxygen uptake in patients with CHF was improved, and additionally, positively associated with change in ΔSmO2. In contrast, there was no change in peak cardiac output.
Conclusion: Both cardiac and skeletal muscle function in patients with CHF were lower than those in healthy subjects. This suggests that exercise capacity in patients with CHF was improved by exercise training, and might be involved in the improved utilization of oxygen in skeletal muscle.

P.02-18

Reduced scattering coefficient during incremental exercise is constant without being affected by changes in muscle oxygenation or hemodynamics

T. Endo, R. Kime, T. Watanabe, N. Murase, S. Fuse, R. Tanaka, M. Kuroiwa, Y. Kurosawa and T. Hamaoka

Department of Sports Medicine for Health Promotion, Tokyo Medical University, Japan

Corresponding author e-mail address: endo-tasuki-fv@ynu.jp

Abstract: Continuous wave near-infrared spectroscopy (NIRS) based on the modified Beer-Lambert Law, a widely used NIRS calculation, assumes that the extended optical pathlength and the light losses due to scattering are constant. However, Ferreira et al. (2007) have reported that a reduced scattering coefficient (μ_s') increased due to changes in blood volume or accumulation of metabolic byproducts during exercise. Since it is suspected that greater deoxygenation and blood volume changes during exercise may induce the increase in μ_s', we examined μ_s' dynamics during exercise in subjects with various aerobic capacities, including endurance-trained athletes. Healthy young men with matched fat layer thickness (FLT) to minimize the influence of FLT on NIRS variables participated in this study (n=23; BMI, 20.8 ± 1.7 kg/m^2; mean ± SD). To investigate the relationship between whole body aerobic capacity and μ_s' dynamics during exercise, the subjects were divided into two groups: control group (Con: n=12; peak pulmonary oxygen uptake per kg of fat-free mass (VO_2/FFM), 54.2 ± 5.3 ml/min/kg) and trained group (Tr: n=11; VO_2/FFM, 69.7 ± 5.2 ml/min/kg) by median of VO_2/FFM. All subjects performed a ramp incremental cycling exercise test until exhaustion. Oxygenated, deoxygenated and total hemoglobin concentration (oxy-Hb, deoxy-Hb and total- Hb, respectively) at vastus lateralis were monitored during the test by three-wavelength (763, 801 and 836 nm) time-resolved NIRS. Similarly, μ_s' in each wavelength was monitored continuously. Throughout the test, oxy-Hb, deoxy-Hb and total-Hb were significantly higher in Tr than Con, and furthermore, the peak amplitude of total-Hb (Δtotal-Hb) was significantly greater in Tr and the peak amplitude of deoxy-Hb tended to be greater. In addition, VO_2/FFM was significantly related to Δtotal-Hb. Conversely, there were no changes in μ_s' in each wavelength during exercise. These results suggest that the great deoxygenation and blood volume changes during incremental exercise do not affect μ_s' dynamics.

P.02-19

The influence of posture on lower limb muscle oxygenation during incremental- cycle bicycle ergometer exercise

A. Tsubaki[a], T. Yuda[b], S. Fujiwara[b], W. Qin[a], S. Kojima[a], K. Hotta[a] and S. Morishita[a]

[a] *Institute for Human Movement and Medical Sciences, Niigata University of Health and Welfare, Japan*

[b] *Department of Physical Therapy, Niigata University of Health and Welfare, Japan*

Corresponding author e-mail address: tsubaki@nuhw.ac.jp

Abstract: An ergometer-based exercise in the supine position (SP) has been used in clinical settings to improve exercise tolerance. However, the effects of exercise position on the lower extremity muscle are not well understood. This study aimed to clarify the effect of body position on lower limb muscle oxygenation (O_2Hb) during cardiopulmonary exercise test (CPET). Ten healthy adult men (20.7±0.5 years old) participated in this study. After familiarization with the CPET with ramp exercise protocols, they performed the exercise (20 watts/min) for measurement of peak oxygen consumption (VO_2 peak) and aerobic threshold (VO_2 AT) in the upright (UP) and SP. The left vastus lateralis (VL) muscle O_2Hb was measured using near-infrared spectroscopy during the CPET. Pulmonary oxygen consumption (VO_2) was obtained on a breath-by-breath basis using a gas analyzer. To normalize the time, the beginning and end of the incremental exercise replaced 0% and 100%, respectively, and averaged every 10%. Two-way repeated measures analysis of variance was used to reveal each main effect (position or time) and interaction (position×time). The VO_2 peak and VO_2 AT were higher in the UP than in the SP (UP vs. SP in mL/kg/min, 37.0±1.8 vs. 31.7±0.9 and 18.9±0.9 vs. 16.1±0.7, respectively, $p<0.01$). The VO_2 increased temporally in both position and significant position×time interaction ($F_{(1,10)}=2.56$, $p<0.01$). The O_2Hb in the VL muscle significantly declined during exercise in both the UP and SP; however, O_2Hb was lower in the SP than in the UP through the exercise, with a significant position×time interaction ($F_{(1,10)}=2.60$, $p<0.01$). On the other hand, while deoxygenation in the VL muscle increased gradually in the SP and UP through the exercise, no significant position×time interaction was observed ($F_{(1,10)}=1.88$, $p>0.05$). The VO_2 and O_2Hb in the VL muscle were higher in the UP than in the SP during incremental CPET.

P.02-20

Relationship between the decrease of oxygenation during incremental exercise, partial pressure end-tidal carbon dioxide: Near-infrared spectroscopy vector analysis

S. Kojima[a,b], S. Morishita[b], K. Hotta[b], W. Qin[a,b], T. Kato[c], K. Oyama[d] and A. Tsubaki[a,b]

[a] *Graduate School of Health and Welfare, Niigata University of Health and Welfare, Japan*
[b] *Institute for Human Movement and Medical Sciences, Niigata University of Health and Welfare, Japan*
[c] *College of Engineering, Nihon University, Japan*
[d] *Department of Brain Environmental Research, KatoBrain Co., Ltd., Japan*

Corresponding author e-mail address: hpm18008@nuhw.ac.jp

Abstract: A previous study reported a decrease in cerebral oxygenated hemoglobin (O_2Hb) level immediately before maximal exercise during incremental exercise. This O_2Hb decrease is suggested to be related to cerebral blood flow (CBF) and partial pressure end-tidal carbon dioxide ($P_{ET}CO_2$). However, the levels of total hemoglobin [O_2Hb+deoxygenated hemoglobin (HHb)] which indicates cerebral blood volume (CBV), was increased. This study aimed to investigate the relationship of O_2Hb, $P_{ET}CO_2$, and the estimated value of CBV with cerebral oxygen exchange (COE) by using a vector analysis. Twenty-four healthy young men participated in this study. They performed the incremental exercise (20 W/min) after a 4-min rest and warm-up. The O_2Hb and HHb levels in the prefrontal cortex (PFC) were measured using near-infrared spectroscopy (NIRS) during incremental exercise. $P_{ET}CO_2$ was measured using an exhaled gas analyzer. O_2Hb, HHb and $P_{ET}CO_2$ were calculated as the amount of change (ΔO_2Hb, ΔHHb, and $\Delta P_{ET}CO_2$) from an average 4-min rest. Changes in CBV (ΔCBV) and COE (ΔCOE) were estimated subsequently using ratios of change in ΔO_2Hb and ΔHHb levels based on previously reported NIRS vector analysis (Kato, 2018). Moreover, the respiratory compensation point (RCP), which relates to the O_2Hb decline, was detected. The Pearson correlation coefficient was used to establish the relationships among ΔO_2Hb, $\Delta P_{ET}CO_2$, ΔCBV, and ΔCOE from the RCP at maximal exercise. ΔO_2Hb correlated significantly with ΔCBV (r = 0.85, $p < 0.01$) and ΔCOE (r = 0.93, $p < 0.01$). However, $\Delta P_{ET}CO_2$ did not correlate significantly with ΔO_2Hb (r = 0.03, $p = 0.88$) or ΔCBV (r = −0.21, $p = 0.3$). ΔO_2Hb correlated with ΔCBV and ΔCOE. However, $\Delta P_{ET}CO_2$ did not correlate with ΔO_2Hb and ΔCBV. These results suggest that the decreases in O_2Hb and CBF are difficult to explain from the change in $P_{ET}CO_2$ during incremental exercise.

References: Toshinori Kato (November 5th, 2018). Vector-Based Approach for the Detection of Initial Dips Using Functional Near-Infrared Spectroscopy, Neuroimaging - Structure, Function and Mind, Sanja Josef Golubic. IntechOpen, DOI: 10.5772/intechopen.80888.

Acknowledgments: This study was supported by a Grant-in-Aid for Scientific Research (C) from the Japan Society for the Promotion of Science (A. Tsubaki) and a Grant-in-Aid for Exploratory Research from Niigata University of Health and Welfare (A. Tsubaki).

P.02-21

Exercise-induced blood volume expansion measured by NIRS is derived from muscle tissue, not from skin

R Kime[a], T Endo[a], S Fuse[a], T Watanabe[a], M Niwayama[b], M Kuroiwa[a], R Tanaka[a], Y Kurosawa[a] and T Hamaoka

[a] *Department of Sports Medicine for Health Promotion, Tokyo Medical University, Japan*
[b]*Department of Electronic and Electrical Engineering, Shizuoka University, Japan*

Email address: kime@tokyo--med.ac.jp

Abstract: We have reported that total hemoglobin (tHb) progressively increased during cycling exercise at constant work rate, assessed using near infrared spectroscopy (NIRS). Although the increase of tHB may be caused by exercise-- induced hyperemia in muscle tissue, we cannot exclude the possibility that the tHb increase during exercise may be due to the effects of skin blood flow. Therefore, we adapted an NIRS device to monitor both skin and muscle hemodynamics simultaneously, to compare the kinetics of skin and muscle hemodynamics during cycle exercise. The purpose of this study was to determine whether the exercise-- induced hyperemia measured by NIRS is influenced by skin hemodynamics. During the first visit, the subjects performed a ramp--incremental cycling exercise test to determine peak VO2, gas exchange threshold (GET), and work rates for the constant work rate tests. On the second visit, the constant work rate cycling exercise was performed. The cycling exercise protocol consisted of 1 min of rest and 1 min of unloaded exercise, followed by 6--min bout of constant work rate exercise. The exercise work rate was estimated to require VO2 to be equal to ∼50% of the difference (Δ) between the subject's GET and peak VO2, i.e., a value of (GET + 0.50Δ), based on the initial VO2/work rate observed during the ramp exercise.
Oxygenated hemoglobin (O2--Hb), HHb, and tHb from skin and muscle tissue were measured by NIRS at the vastus lateralis muscle. Each optode distance was 0.3 cm for skin and 3 cm for muscle tissue. During the constant work rate exercise, muscle tHb showed progressive increases until the end of exercise, after an initial decrease at the start. In contrast, skin tHb gradually decreased during the former part, and gradually increased during the latter part. These results provide evidence that the increased muscle tHb during cycling exercise may is caused by exercise--induced blood volume expansion in muscle tissue, and the tHb increase measured by NIRS is not derived from skin.

P.02-22

Cerebral oxygenation is enhanced during arm cranking incremental exercise compared to cycling in healthy male adults

K. **Hashimoto**[a], K. Hotta[b], R. Kanai[a], H. Takahashi[a], S. Morishita[b], and A. Tsubaki[b]

[a] *Department of Physical Therapy, Niigata University of Health and Welfare, Niigata, Japan b Institute for Human Movement and Medical Science, Niigata University of Health and Welfare, Niigata, Japan*

Corresponding author e-mail address: kazuki-hotta@nuhw.ac.jp

Abstract: The purpose of this study was to compare cerebral oxygenation during arm cranking and cycling exercise in healthy male adults. Twelve healthy male volunteers (mean age 20.8±0.60 years) participated in exercise test. Two test protocols cranking and cycling (cranking 5 W/min, cycling 20 W/min) were performed. By using near-infrared spectroscopy, cortical oxyhemoglobin (O2Hb) was measured in the exercise-related cortical area including left and right prefrontal cortex (PFC), left and right premotor area (PMA), and supplementary motor area (SMA). Cardiovascular and respiratory responses including cardiac output (CO), end-tidal carbon dioxide partial pressure (PETCO2), pulmonary oxygen uptake (VO2) and forehead skin blood flow (SBF) were measured non-invasively and simultaneously. Data analysis was performed the incremental load start as 0%, the end point as 100%, and the average value of each index at each exercise time every 10%. The O2Hb at PFC, PMA and SMA gradually and significantly increased during cranking, but did not with cycling (Two-way ANOVA revealed a significant interaction between time x exercise type; $P < 0.05$). The O2Hb during cranking was significantly higher than cycling at high intensity (90-100% at left PFC, 60-100% at left PMA, 100% at right PMA, 80-100% at SMA; $P < 0.05$). As compared to rest, the CO and the SBF gradually increased during cranking and cycling and there was significant difference between cranking and cycling at 60-80%. The PETCO2 and VO2 were lower during cranking than cycling from warming up to end point. These results that cranking elevates cerebral oxygenation at motor-related area as compared to cycling, especially at high intensity exercise. Enhanced neural activity likely contribute to cranking exercise induced cerebral oxygenation.

Acknowledgements: This study was supported by a Grant-in-Aid for Exploratory Research from the Niigata University of Health and Welfare (A. Tsubaki).

O.04-1

Localization of deep ischemia and hemorrhage in preterm infants' head with near infrared optical tomography: A numerical case study

Jingjing Jiang, Alexander Kalyanov, Di Costanzo Mata Aldo, Scott Lindner and Martin Wolf

Biomedical Optics Research Laboratory (BORL), Department of Neonatology, University Hospital Zurich (USZ), 8091 Zurich, Switzerland

Corresponding author e-mail address: Jingjing.Jiang@usz.ch

Abstract: Preterm infants have a high incidence of brain lesions that may lead to long-term disabilities. Early diagnosis of cerebral ischemia and hemorrhage may enable protecting the brain by prevention or neuroprotective treatment. Our time-resolved near infrared optical tomography (TR NIROT) system provides images to diagnose neonatal brain injury. Our aim is to study the achievable image quality from the TR NIROT signals perturbed by noise for two common cases: ischemia and hemorrhage. We implemented simulations on a spherical model of diameter 60 mm representing a typical neonatal head where the absorption μ_a = 0.08 cm^{-1} and scattering μ'_s = 4.1 cm^{-1}. Injury– mimicking spherical inclusions of various diameters (1 ~ 10) mm were placed at depths of 10 ~ 20 mm in the ischemia case (2.5 × μ_a) and 14 ~ 30 mm for the hemorrhage case (50 × μ_a). TR data were generated from a large number of source-detector pairs, i.e. 208 detectors placed within a circle of diameter 40 mm on the surface surrounded by 18 sources (Fig. 1). Up to 5 % Gaussian noise were added in the simulations. 3D images were reconstructed with the modified Tikhonov minimization with the initial guess of a homogeneous phantom and the segmented images were evaluated by positional error and Dice similarity. The inclusions were localized correctly with low positional errors (< 1 mm) and the segmented images share a high Dice similarity with the ground truth for both the ischemia and the hemorrhage case, even for tiny inclusions of 1 mm in deep tissue. The hemorrhage case with a high contrast tolerates a substantial level of noise even though the performance drops with higher noise as expected. The large amount of data provided by our novel TR NIROT system provides rich enough information for correctly locating hemorrhage and ischemia in the neonatal brain.

.

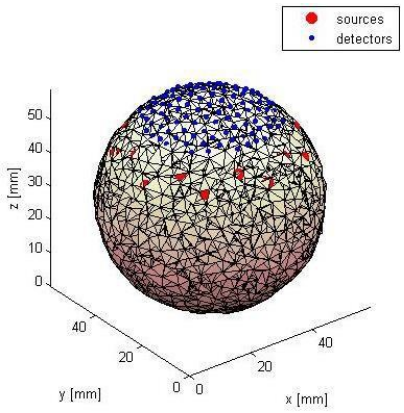

Figure 1. Geometry of neonatal head model center of the brain

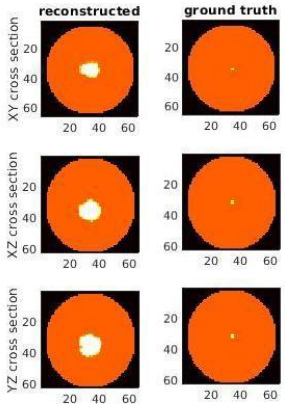

Figure 2. Image of a simulated hemorrhage at the

O.04-2

Molecular origins of ROS formation revealed by hybrid modeling of CIII-CIV supercomplexes

Jon Nguyen[1,2], Chun Kit Chan[3], Emad Tajkhorshid[3], Eugenia Mileykovskaya[4], and Abhishek Singharoy[1,2]

[1]School of Molecular Sciences, Arizona State University, USA
[2]Biodesign Center for Applied Structural Discovery, Arizona State University, USA
[3]Theoretical and Computational Biology Group Biophysics and Quantitative Biology, University of Illinois at Urbana-Champaign, USA
[4]Department of Biochemistry and Molecular Biology at McGovern Medical School, University of Texas, USA

Corresponding author e-mail address: asinghar@asu.edu

Abstract: Mitochondria, the powerhouse of the cell, is responsible for processes such as ATP production and cellular respiration. A dysfunctional mitochondrion is implicated in brain damage, cancer, and aging. The main contributing factor to the dysfunctional mitochondrion is excessive production of reactive oxygen species (ROS), which is a direct result of improper cell redox signaling. A key protein in this cell signaling process is cytochrome *c*, which serves as an electron carrier between complex III (CIII) and complex IV (CIV) in the electron transport chain (ETC) [1]. In mammals, these two complexes form a respiratory supercomplex with complex I (CI); in yeast, CIII and CIV form the supercomplex, as yeast does not possess CI. Previous work has shown that formation of these supercomplexes increase the efficiency of electron transfer, thus decreasing the amount of ROS generated [2]. In order to decrypt the mechanistic advantage of supercomplex formation within the ETC, we model the cytochrome *c*-bound CIII$(CIV)_2$ complex from *Saccharomyces cerevisiae,* combining cryo-electron microscopy, *de novo* protein folding and molecular dynamics simulations. Our key target is the unresolved acidic segment of the QCR6 subunit. It has been suggested that this hinge- like subunit promotes cytochrome *c* turnover at CIII [3]. We test how QCR6 assumes a number of conformations that is uniquely leveraged by the supercomplex to tunnel electrons between CIII and CIV, rather than losing them towards ROS formation. These conformations are absent when CIII and CIV are dispersed in the mitochondrial membrane, making the ETC more prone to energy leakage. The QCR6 domain is compared between supercomplexes from a number of organisms to study how its hinge opens and closes. Essentially, we explore a robust mechanism that is deployed to avoid ROS by chaperoning electron transport with flexible proteins of adjustable length to connect dynamically separated donor and acceptor sites.

References:
[1] Guerra-Castellano et al., PNAS, 2018.
[2] Genova et al., BBA, 2014.
[3] Smith et al.,Biochim Biophys Acta, 2012.

O.04-3

Discerning membrane steady-state oxygen flux by Monte Carlo Markov Chain Modeling

G. Angles[a] and S. C. Pias[a]

[a] *Chemistry Department, New Mexico Institute of Mining and Technology, USA*

Corresponding author e-mail address: sally.pias@nmt.edu

Abstract: Molecular oxygen (O_2) permeability coefficients for lipid bilayers have previously been estimated using both electron paramagnetic resonance (EPR) oximetry and molecular dynamics simulation data. Yet, neither technique captures the fluxes that exist physiologically. Here, the dynamic steady state is modeled using a stochastic approach built on atomic resolution molecular dynamics simulation data. A Monte Carlo Markov chain technique is used to examine membrane-level fluxes of oxygen in lipid-water systems. As in other studies, the concentration of oxygen is found to be higher inside the model membranes than in surrounding water. Sixty percent more oxygen molecules are present at steady state inside palmitoyloleoyl-phosphatidylcholine (POPC) bilayers than in POPC/cholesterol bilayers (1:1 mixing ratio). Steady-state levels of oxygen are reached in both bilayer types within the same timeframe, but depletion of oxygen from the bilayer interior occurs ~15% faster for POPC than for POPC/cholesterol. These results are consistent with prior experiments in red blood cells (RBCs) with varying membrane cholesterol content, in which additional cholesterol slowed oxygen unloading from RBCs but did not affect the oxygen uptake rate. Further work is needed to understand whether differences in RBC membrane cholesterol content would affect the delivery of oxygen to tissues.

I.04

Computer modeling of oxygen transport in cells and tissues

Sally C. Pias, Rachel J. Dotson, Gary Angles, and Qi Wang

Department of Chemistry, New Mexico Institute of Mining and Technology, USA

Corresponding author e-mail address: sally.pias@nmt.edu

Abstract: There is a surprising gap in knowledge regarding the mechanism of oxygen (O_2) diffusional delivery at the level of tissues and cells. Yet, the effectiveness of tumor radiotherapy, the success of tissue engineering, and healthy metabolism all require ample intracellular O_2. Oxygen availability within tissues depends on O_2 solubility and diffusivity in crowded aqueous fluids and structurally complex membranes. We have carried out several atomic resolution studies of oxygen diffusion using molecular dynamics simulations. Our studies, along with several lines of experimental evidence, support the "hydrophobic channeling" model of oxygen diffusion along lipid-accelerated pathways. Our work has confirmed that membrane cholesterol reduces lipid bilayer oxygen permeability and has implicated cholesterol as a key player in hydrophobic channeling. In addition, we have found that transmembrane proteins nonspecifically reduce oxygen permeability. Recently, we have developed a stochastic modeling technique built on molecular dynamics simulation data, to enable prediction of steady-state oxygen transport dynamics. Overall, our work indicates that pathways and rates of oxygen diffusional transport are altered by molecular compositional changes. Identifying physicochemical determinants of cellular oxygenation will empower researchers and clinicians to influence oxygen availability within tissue.

Acknowledgements: This work was made possible by funding from the National Institutes of Health, under grant P20GM103451, and by a gift from the Glendorn foundation.

I.05

Cherenkov excited luminescence imaging of pO2 in tumors during radiation therapy

B. W. Pogue[a,b], X. Cao[a], E. LaRochelle[a], P. Bruza[a], J. Shell[a], J. Feng[a], D. J. Gladstone[a,b,c], L. A. Jarvis[b,c] and S. A. Vinogradov[d]

[a] *Thayer School of Engineering, Dartmouth College, Hanover NH USA*
[b] *Department of Medicine, Geisel School of Medicine at Dartmouth, Hanover NH USA*
[c] *Norris Cotton Cancer Center, Lebanon NH USA*
[d] *Dept of Biochemistry & Biophysics, Perelman School of Medicine, University of Pennsylvania, Philadelphia PA USA*

Corresponding author e-mail address: brian.w.pogue@dartmouth.edu

Abstract: Radiation therapy produces substantial amounts of Cherenkov light within tissue during the dose delivery process, and this optical signal can be used as an excitation source for molecular probes. Because linac radiation is pulsed in 4 microsecond bursts, time-gated emissions can be sampled with very low background. Luminescence imaging metalloporphyrin complexes (PtG4-Oxyphor) has been shown to allow pO2 measurement in vivo with spatial resolution defined by the exciting x-ray beam scan design. By sweeping narrow radiation beamlet shapes from the linear accelerator, it is possible to detect the signals and reconstruct their origin with 100 micron spatial resolution, with demonstrations in ymph nodes and tumors. Time-gated sensing allows for quantitative imaging of the emitted luminescence lifetime of PtG4, so that pO2 distributions can be reconstructed from these surface emissions. We show pO2 histogram sampling from the tumor surface during each fraction of radiotherapy. Additional imaging of luminescent and radioluminescent molecular sensors is possible. The three key parameters that dictate sensitivity are 1) depth of tissue, 2) probe concentration, and 3) radiation dose have been analyzed for the tradeoffs in signal to noise and detectability, and the signal to background optimization has been completed in a recent paper [1]. Preliminary studies in human body phantoms illustrate the potential for this type of sensing of superficial body sites such as lymph nodes.

References, acknowledgements: [1] Pogue BW, et al, “Maps of in vivo oxygen pressure with submillimetre resolution and nanomolar sensitivity enabled by Cherenkov-excited luminescence scanned imaging.” Nature BME 2018 Apr;2(4):254-264.
This work is funded by NIH grant R01EB024498.

O.05-1

An observation on enhanced extracellular acidification induced by inhibition of the Warburg effect

L. Z. Li, J. Jiang, J. Roman, H. N. Xu, and M. Feng

Department of Radiology, Perelman School of Medicine, University of Pennsylvania, USA

Corresponding author e-mail address: linli@pennmedicine.upenn.edu

Abstract: The Warburg effect, representing high glucose metabolism and lactate production in cancer cells, has been widely regarded to cause extracellular acidification. However, we have recently observed that FX-11, an inhibitor of the Warburg effect by inhibiting lactate dehydrogenase A (LDHA) activity, caused dose-dependent increases in extracellular acidification (ECAR) and oxygen consumption rate (OCR) in MDA-MB-231 breast cancer cells as measured by the Seahorse cellular bioenergetics assay. The intracellular NADH measured by optical redox imaging (ORI) also increases with FX-11 dosage. This is consistent with the inhibition of LDH reaction, which couples pyruvate-to-lactate conversion with the NAD^+/NADH redox potential. The inhibition of LDH is also expected to increase intracellular proton concentration and decrease intracellular pH according to the reaction equation of LDH. This perspective and our observed stimulation of ECAR suggest that the Warburg effect and extracellular acidification may not be positively correlated and that inhibition of the Warburg effect may encourage extracellular acidification. More experiments are needed to confirm this observation in other breast cancer cell lines and to understand its underlying mechanism.

O.05-2

Role of MicroRNA expression for proliferation and apoptosis of tumor cells: Impact of hypoxia-related acidosis

L. Lange,T. Husing, M. Rauschner, A, Riemann, and O. Thews.

Julius-Bernstein-Institute of Physiology, University of Halle, Germany

luisa.lange@student.uni-halle.de

Abstract: Tumor microenvironment is characterized by hypoxia and acidosis. Insufficient neoangiogenesis leads to hypoxic areas within the rapidly growing tissue. To fulfill energy requirements, cells increase glycolysis but tumors also use glycolytic metabolism even with sufficient oxygen supply (Warburg effect), with increased lactic acid production and an acidic extracellular pH below 6.0. Tissue pH impacts tumor cell proliferation and apoptosis but how cell cycle progression is affected by low pH is not understood. One mechanism may be in the expression of small non-coding, regulatory RNAs, so called microRNAs. MiRNAs miR-7, miR- 183, miR-203 and miR-215 shown to be pH-regulated. We studied the impact of the miRNAs on proliferation, apoptosis and necrosis in tumor cells. AT1 prostate and Walker-256 mammary carcinoma cells were transfected with miRNAs or with the respective antagomirs and incubated at pH 7.4 and 6.6 for 24 hours. The effect on proliferation was examined with BrdU staining and cell cycle analysis. Apoptosis and necrosis were analyzed with caspase assay and LDH release. AT1 cells undergo a G0/G1 cell cycle arrest under acidic conditions whereas the cell-cycle distribution of Walker-256 cells was unaffected by low pH. Both cell lines showed a marked reduction in number of actively DNA-synthesizing cells, reduction of apoptosis and in Walker-256 an increase in cell death. Transfection of tumor cells with miR- 215, which is significantly down-regulated under acidic condition leads to a higher number of proliferating cells (BrdU-positive) with an increase in apoptosis and reduction in necrosis. Overexpression of miR-183, down-regulated in acidosis, leads to a higher number of proliferating AT1 cells with an increase in apoptosis. Hypoxia-related tumor acidosis affects the expression of small non-coding RNAs and these microRNAs can influence the proliferation, apoptosis and necrosis of tumor cells. miR-183 and miR-215 could mediate the impact of extracellular acidosis on malignant behavior of tumor cells

O.05-3

Functional impact of acidosis-regulated microRNAs on migration and invasiveness of tumor cells

T. Hüsing, L. Lange, M. Rauschner, A. Riemann and O. Thews

Julius-Bernstein-Institute of Physiology, Martin-Luther-University Halle-Wittenberg, Germany

thea.huesing@student.uni-halle.de

Abstract: Tumor tissue differs strongly from healthy tissue due to its special features in metabolism. Tumors are characterized by distinctive oxygen deficiency leading to intensified glycolytic metabolism. Furthermore, tumor cells run glycolysis although sufficient O_2 is available (Warburg-Effect). Glycolysis causes an increased proton formation, accumulating in the extracellular space leading to a pronounced acidification (down to pH 6.0 or lower). As shown in previous studies, motility and cell migration are increased in AT-1 prostate carcinoma cells after incubation at pH 6.6 and leading to a higher number of lung metastases *in vivo*. However, the signaling pathway causing these functional changes is still unknown. A possible mediator could be microRNAs, which are small non-coding RNAs, regulating gene expression on a post-transcriptional level. Previous studies brought up 4 microRNAs which seem to be regulated by acidosis (miR-7, miR-183, miR-203, miR-215). The aim of the study was therefore to analyze whether a change in the expression of these acidosis-regulated microRNAs has an impact on tumor cell migration and invasion.
Studies were performed using AT-1 rat prostate cancer cells which were incubated for 24h at pH 7.4 or pH 6.6. Additionally, the respective microRNAs were modulated by transfecting the cells either with the microRNA themselves (mimics) or with antagomirs which reduce the intracellular expression (inhibitor). The migratory capacity of these cells was measured by time-lapse microscopy over 100 min analyzing the migratory speed as well as the covered distance. For the quantification of invasiveness, a transwell-migration assay was used.
Keeping AT1 tumor cells at low pH increased the migratory capacity. The average migratory speed increased by about 50% whereas the covered distance was about 150% higher at pH 6.6 compared to pH 7.4. The expression of acidosis-regulated microRNAs also had a marked impact on the cell movement. At control pH inhibition of the miR-215 increased migratory speed strongly. Inhibition of miR-203 also increased the velocity but to a smaller extent. On the other hand, at low pH an increase of miR-203 further raised the speed and distance. Overexpression of the miR-183 at low pH reduced the covered distance. The miR-7 had practically no effect on migration. The invasiveness was markedly reduced at normal pH by an inhibition of the miR-203. At low pH the overexpression of the miR-215 had the same effect. These results clearly indicated that the extracellular pH has an impact on migration and invasiveness of tumor cells. In this mechanism pH-regulated microRNAs could play a relevant role since changes in the expression of these microRNAs (especially miR-203 and miR-215) are also able to modulate the migratory behavior.

Acknowledgments: This study was supported by the Dr. med. h.c. Erwin Braun Foundation, Basel, Switzerland, and the Deutsche Forschungsgemeinschaft (DFG) (grant TH 482/6-1).

O.05-4

Impact of acidosis-regulated MicroRNAs on the expression of their target genes in experimental tumors *in vivo*

M. Rauschner, A. Riemann, S. Reime and O. Thews

Julius-Bernstein-Institute of Physiology, Martin-Luther-University Halle-Wittenberg, Germany

mandy.rauschner@medizin.uni-halle.de

Abstract: Solid tumors are at acidic extracellular pH from hypoxia-induced glycolytic metabolism and from aerobic glycolysis (Warburg effect) affecting tumor cell proliferation, invasion or migration. Acidosis modulates the expression of different microRNAs: miR-7, miR- 183, miR-203 and miR-215 which might be mediators between tumor acidosis and malignant behavior. Three genes were identified which were regulated by acidosis and which are putative targets of the acidosis-regulated microRNAs: thioredoxin-interacting protein (Txnip), glutaminase 2 (Gls2) cAMP responsive element modulator (Crem). We investigated how the modulation of microRNAs miR-7, miR-183, miR-203 and miR-215 affects the expression of these targets in experimental tumors *in vivo* and whether they were acidosis dependent. Cells of the subline AT-1 of the R3327 prostate carcinoma and of the Walker-256 mammary carcinoma were transfected with microRNA mimics or control microRNAs, and subcutaneously implanted on the hind foot dorsum of rats. After about seven days, pronounced tumor acidosis was induced in some animals by 24 hr respiratory hypoxia (8% O_2) combined with a single injection of MIBG. MicroRNA expression mRNA and protein levels of the target genes were determined. Txnip was upregulated (>100%) in both tumor models by acidosis. MiR-203 overexpression led to an increase of Txnip in AT-1 tumors, whereas miR-7 mimic diminished Txnip expression in W256 tumors. Both effects were acidosis-independent. MiR-7 and miR- 183 overexpression showed increased Gls2 expression by acidosis. Crem expression was enhanced by miR-183 mimic under normoxic (371±47%) and acidic conditions (290±31%) in AT-1 tumors. In contrast, miR-7 overexpression induced a reduction of Crem in Walker-256 tumors. MicroRNAs and some of their targets are affected by hypoxia- relatedtumor acidosis *in vivo*. The modulation of microRNA levels by transfection with microRNA mimics affects expression of the targets in tumors. Gls2 is an interesting candidate as it is targeted by miR-183 in an acidosis-dependent manner. This gene plays an important role in mitochondrial energy metabolism and affects expression of other transcription factors influencing malignant behavior of tumors.

Acknowledgments

Deutsche Forschungsgemeinschaft DFG (grant TH 482/6-1).

I.06

The Warburg Effect: Historical dogma *vs.* current rationale

P. Vaupel[a] and G. Multhoff[b]

[a]*Department of Radiation Oncology, University Medical Center, Mainz, Germany*
[b]*Center for Translational Cancer Research, Technical University, Munich, Germany*

Corresponding author e-mail address: vaupel@uni-mainz.de

Abstract: In the early 1920s, Otto Warburg published experimental data on a substantially enhanced conversion of glucose to pyruvate (followed by lactate formation) even under adequate oxygen supply. This condition has been termed "aerobic glycolysis" (or later on "Warburg effect"). Warburg initially attributed this metabolic trait to a permanent respiratory (mitochondrial) damage and considered this a universal alteration in carcinogenesis. Although Warburg's dogma was questioned since the early 1950s, realistic causative mechanisms and a biological rationale were described only during the past 20 years. Here, we have analyzed these recent data and describe their current relevance.

Contrary to Warburg's historical interpretation, "aerobic glycolysis" not only leads to a compensatory increase in glycolytic flux in order to meet bioenergetic demands of cancer cells through a high-speed ATP production in the cytoplasma, but also represents an aggressive phenotype with biosynthetic programs required to sustain cell survival, proliferation, migration, invasion, metastasis, suppression of anti-tumor immune responses, and favoring radioresistance. The corresponding transcriptional responses are mediated primarily by (hypoxic or normoxic) activation of HIF-1α, activated PI3K/Akt/mTOR and deactivated LKB1/AMPK pathways, cMyc and mut-p53. Feedback loops exist between these signaling alterations and the hypoxic tumor microenvironment (TME) to which they contribute. Metabolic features of the "Warburg phenotype" include: (a) Considerably accelerated glycolytic flux rates (via upregulation of GLUT1 and key glycolytic enzymes, which are activated cooperatively or independently by HIF-1α and cMyc). (b) An efficient energy generation ("low yield, but high-speed ATP production"), permitting the survival of cancer
cells. (c) Backup and diversion of glycolytic intermediates feeding metabolic pathways which facilitate the biosynthesis of nucleotides, non-essential amino acids, lipids, and, therefore, the sustained synthesis of cancer biomass. This backup is caused by a low activity of PKM2, which inhibits the phosphoenolpyruvate to pyruvate conversion (1st "bottleneck") and PDK1- induced inhibition of mitochondrial pyruvate import (2nd "bottleneck") at the end of glycolysis, which shunts pyruvate away from the TCA cycle. (d) In aerobic glycolysis, pyruvate is converted to lactate by upregulated LDH-A. Large amounts of lactate are generated and exported through MCT4-transporters into the extracellular space. Lactate -*inter alia*- stimulates tumor angiogenesis, suppresses anti-tumor immunity, can act as an energy source for adjacent normoxic cancer cells and may mediate radioresistance. (e) Elevated lactate levels also contribute to the development of extracellular acidosis which strongly drives malignant progression. (e) The switch from oxidative to glycolytic metabolism in cancers is accompanied by low ROS generation and provides antioxidant moieties, thereby supporting cell survival. (f) The deactivated AMPK pathway and HIF-1α inhibit mitochondrial biogenesis and, thus cellular respiration.

In conclusion, the "Warburg effect" is part of the "selfish" metabolic reprogramming, which results from the interplay between HIF-1α-transcription, oncogene-activation, loss-of-function of suppressor genes, altered signaling pathways and the "hostile" TME. The "Warburg phenotype", therefore, constitutes a major driver of the cancer progression machinery.

O.06-1

The acidic tumor microenvironment affects epithelial-mesenchymal transition markers as well as adhesion of NCI-H358 lung cancer cells

A. Riemann, M. Rauschner, M. Gießelmann, S. Reime and O. Thews

Julius Bernstein Institute of Physiology, University of Halle-Wittenberg, Germany

Corresponding author e-mail address: anne.riemann@medizin.uni-halle.de

Abstract: Epithelial-mesenchymal transition (EMT) is a critical step in metastasis formation, the leading cause of cancer-associated death worldwide. EMT involves reprogramming of gene expression by key transcription factors including SNAIL and ZEB and signals from the cellular microenvironment, hypoxia, can modulate the process of EMT. Hypoxia is associated with a reduction of extracellular pH of the tumor microenvironment (acidosis) in the range of 6.0 to 7.0. Metabolic reprogramming independent of hypoxia (Warburg effect) can induce acidosis. Whether acidosis alone impacts the expression of EMT markers E-cadherin, N- cadherin and vimentin, as well as on adhesive properties, was studied in NCI-H358 lung cancer cells. Reducing extracellular pH (24 h, pH 6.6) decreased E-cadherin mRNA by the factor of 2, while vimentin and N-cadherin mRNA were doubled. At a protein level E-cadherin and N-cadherin were both reduced by about 50%, while vimentin was up-regulated by 40 %. E-cadherin and N-cadherin expression at the cell surface, which is the relevant parameter for cell-cell- and cell-matrix-interaction, decreased by about 25%. The reduction of cell surface protein was due to diminished protein expression and not changes in cellular localization, since localization of EMT markers in general was not affected by acidosis. Adhesion of NCI-H358 cells on a surface was measured by standard cell adhesion assays and by continuous impedance measurements using the xCELLigence RTCA DP system. Adhesion was decreased when the cells were primed in an acidic medium before measuring the cell adherence, in line with the reduced expression of cadherins at the cell surface. A possible mechanism for the regulation of EMT markers involves the action of microRNA- 203a (miR-203a). We recently reported an up-regulation of miR-7a and a down- regulation of miR-183 and miR-203a in prostate and breast tumor cells (Riemann et al. 2019). In NCI-H358 lung cancer cells miR-203a and miR-7a were regulated likewise by acidosis. Since a decrease in the level of miR-203a has been shown to induce EMT, it might be involved in the modulation of EMT marker expression by the acidic tumor microenvironment in NCI- H358 lung cancer cells.

Reference

Riemann A, Reime S, Thews O (2019) Acidic extracellular environment affects miRNA expression in tumors *in vitro* and *in vivo*. Int J Cancer 144:1609–1618.

Acknowledgements

The study was supported by the Deutsche Forschungsgemeinschaft DFG (grant TH 482/6-1).

O.06-2

Assessment of the probability of tumor control for prescribed doses based on imaging of oxygen partial pressure

A. Ureba[a,b], E. Kjellsson Lindblom[a,c] , I. Toma-Dasu[a,c], A. Dasu[b] and M. Lazzeroni[a,c]

[a] *Karolinska Institutet, Medical Radiation Physics, Department of Oncology-Pathology, Stockholm, Sweden*
[b] *Skandionkliniken, Uppsala, Sweden*
[c] *Stockholm University, Medical Radiation Physics, Department of Physics, Stockholm, Sweden*

ana.ureba@ki.se

Abstract: In radiotherapy, hypoxia is a known negative factor, occurring especially in solid malignant tumours. Nitro-imidazole-based PET tracers, due to their selective binding to hypoxic cells, could be used as surrogates to image and quantify the underlying oxygen distributions in tissues. The spatial resolution of a clinical PET image, however, is much larger than the cellular spatial scale where hypoxia occurs. A question therefore arises regarding the possibility to quantify different hypoxia levels based on PET images and prescribe a corresponding radiotherapeutic dose.

Assuming that the relation between uptake and pO_2 is known [1], a tumor oxygenation model was created consisting of two concentric spheres with different pO_2 distributions. To mimic a PET image of the simulated tumor, fundamental effects that limit spatial resolution in a PET camera were considered. The initial oxygen distribution was processed with a Gaussian 3D filter of FWHM 0.02–1.22 cm and a re-binning to increase the initial image voxel size from
0.02 to 0.2 and 0.4 cm, respectively. The prescription doses needed for overcoming tumor hypoxia and the predicted TCPs for different fractionation schedules were calculated based on the processed images. Knowing the underlying oxygenation, the actual TCP expected after the delivery of the prescription doses considering the spatial and temporal relationship between oxygenation and cell killing during the treatment was evaluated (Fig.1).

The differences between TCP predicted and TCP evaluated indicate that careful consideration must be taken on the dose prescription strategy and the selection of the number of fractions, depending on the severity of hypoxia and the clonogenic cell number.

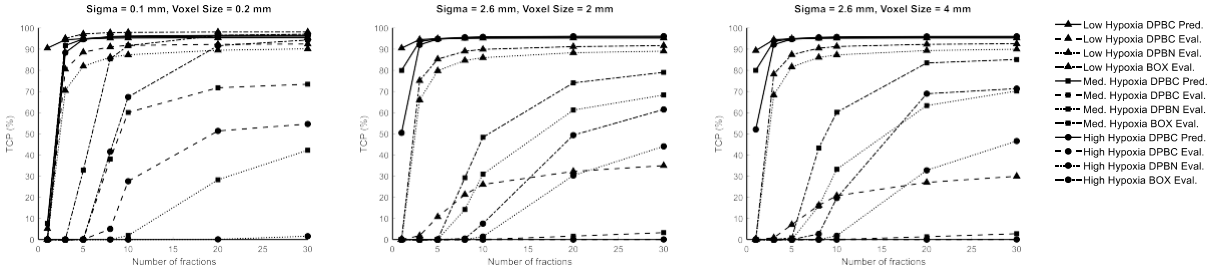

Fig.1 TCP predicted based on the image and evaluated on the original oxygenation map, considering different prescription doses strategies: contour (DPBC), numbers (DPBN) and voxel clustering using the highest dose per cluster (BOX).

References: [1] Toma-Dasu et al. *Adv Exp Med Biol* 2009; 645:267-27.

P.03-23

Oxidative stress and oxygen transport impairment in Coho Salmon (*Oncorhynchus kisutch*) exposed to urban runoff

S.I. Blair[a], C.H. Barlow[b] and J.K. McIntyre[a]

[a]*Department of Environmental and Natural Resource Sciences, Washington State University Puyallup Research and Extension Center, USA*
[b]*Department of Analytical Chemistry, Evergreen State College, USA*

Corresponding author e-mail address: stephanie.blair@wsu.edu

Abstract: Coho salmon (*Oncorhynchus kisutch*) are an ecologically, economically and culturally valuable species of Pacific Salmon (*Oncorhynchus* spp.) and are highly susceptible to diffuse contaminants present in urban stormwater. Exposure to highway runoff elicits acute mortality and behavioral symptoms in coho suggesting cardiorespiratory impairment (e.g. surfacing, gaping, loss of equilibrium) and physiological changes in blood parameters, such as a rise in hematocrit and loss of plasma electrolytes. Although the causal contaminants remain a mystery, highway runoff contains a complex mixture of organic and inorganic pollutants known to induce oxidative stres (e.g. metals and polyaromatic hydrocarbons). Juvenile coho salmon exposed to lethal concentrations of highway runoff were assessed for changes in plasma protein, total thiols and ferric reducing antioxidant power (FRAP). We found that runoff-affected coho showed increased plasma protein concentrations and antioxidant system disturbance. We also assessed changes in blood volume and vascular permeability using albumin-complexed Evans Blue dye and sodium fluorescein. We conclude that oxidative stress induced by a mixture of pollutants present in highway runoff leads to circulatory collapse as a potential mechanism of toxicity. Further studies should continue to elucidate toxic modes of action in so-called coho urban runoff syndrome, which may also help identify environmental chemicals of concern, as well as their sources.

P.03-24

Real-time tissue oxygen monitoring reveal hind limb hypoxia following REBOA treatment in a swine model

Scott P. Nichols[a], Malcom D. Prince[b], Irene A. Polykratis[b], Dylan Li[a], Natalie A. Wisniewski[a], Michael A. Dubick[b]

[a] Pre-Clinical and Advanced Technologies, Profusa, Inc. USA
[b] US Army Institute of Surgical Research, JBSA Fort Sam Houston, USA

scott.nichols@profusa.com

Abstract: Resuscitative Endovascular Balloon Occlusion of the Aorta (REBOA) is gaining popularity as an adjunctive therapy for the temporary control of bleeding from non-compressible torso wounds. For the military it has sparked much interest in endovascular approaches to hemorrhage control. However, understanding the impact of REBOA and tissue health, leading to loss of limb function, is not well understood. Profusa's subcutaneously (SC) injected microsensors make it possible to monitor tissue hypoxia in various regions of the body to assess the effects of hemorrhage and REBOA inflation.

The study evaluated tissue oxygen in four anatomical locations (neck, chest, flank, and limb). Tissue oxygenation was continuously tracked before, during, and after severe trauma, REBOA treatment and resuscitation in an uncontrolled hemorrhage liver injury swine model. Profusa oxygen sensors reported an average of 22-55% decrease in tissue oxygenation due to the hemorrhage across 14 pigs. The inflation of the REBOA balloon to stop hemorrhage resulted in an expected dramatic decrease in tissue oxygen of distal sensors to ~0 µM. After deflation of the REBOA balloon to resume blood flow, an initial hyperoxia followed by an unexpected long-term tissue-level ischemia was detected in the lower limbs. Although femoral blood pressure in the limb demonstrated reperfusion of the large vessels, the measured tissue oxygen suggests a deterioration of capillary perfusion in the limb. In contrast, tissue oxygen was not ischemic in the upper body (head region).

Continuous monitoring tissue oxygen in a porcine trauma showed dramatic differences in oxygen in the upper body versus the limb after REBOA treatment. Data suggest that a one hour REBOA balloon occlusion may have long-term repercussions on downstream capillary perfusion. Tracking tissue oxygenation in further studies with various experimental re- perfusion fluid and REBOA methodologies (e.g. partial or intermittent REBOA) may help identify optimal REBOA balloon usage by continuous tracking for hours or days after deflation of the REBOA balloon and subsequent survival studies of limb function preservation.

P.03-25

On feasibility of pulse wave velocity imaging for remote assessment of physiological functions

G.Saiko[a] and A. Douplik[b]

[a] *Swift Medical Inc, Toronto, Canada*
[b] *Dept. of Physics, Ryerson University, Toronto, Canada*

gsaiko@ryerson.ca

Abstract: Peripheral artery disease (PAD) is the "silent cardiovascular disease." In Canada, the prevalence can be estimated at 10% with an incidence of 3% for the population greater than 40 years of age. Clinical symptoms tend to present late in the course of the disease, and even in extreme cases, 50% of patients can be asymptomatic. In primary care, the ankle- brachial index (ABI) has been used as a screening tool for PAD. By way of the ABI, a primary care practitioner may be able to diagnose PAD with a high degree of specificity (up to 99%), but sensitivity can vary greatly (15-79%). Recently, the use of the brachial-ankle pulse wave velocity (baPWV) has been used as another diagnostic tool with regards to coronary artery disease (CAD). Although aortic stiffness is a larger component of the baPWV, numerous studies have shown that there is a correlation between baPWV and PAD. We have developed an approach, termed Pulse Wave Velocity imaging (PWVi), which can determine remotely pulse transit time, pulse wave velocity, perform a waveform analysis at the bedside and can be acquired within 30 seconds in any environment (e.g., operating room, bedside, patient's home). In the current pilot study, we assess the feasibility to use PWVi for remote extraction of physiological parameters. The study design was approved by REB at Ryerson University. A scientific grade RGB camera (Basler acA-2000-165uc (Basler, Germany)) was used to collect 10sec videos at 1000fps. Data were pre-processed to extract pulse transit time between various spots on the frame. The pulse wave velocity was calculated accordingly. Data were collected on two various locations (back of the left hand and back of the right hand) on 10 healthy volunteers18-60 years old. The calculated pulse wave velocity is within known physiological range: 5-10 m/s. The initial data shows feasibility using PWVi for remote extraction/monitoring physiological parameters. Further studies are required to establish the natural rate of variability between patients and stratify this variability based on a skin type (melanin concentration in the skin).

P.03-26

Mechanisms of sound-induced opening of the Blood-Brain Barrier

O. Semyachkina-Glushkovskaya[a], D. Bragin[b], O. Bragina[b], Y. Yang[c], A. Abdurashitov[a], A. Esmat[a], A. Khorovodov[a], A. Terskov[a], M. Klimova[a], I. Agranovich[a], I. Blokhina[a], V. Salmin[a,d], A. Morgun[a,d], N. Malinovskaya[a,d], E. Osipova[d], E. Boytsova[d], A. Shirokov[a,e], N. Navolokin[a,f], V. Tuchin[a,g], J. Kurths[a,h,i].

[a] Saratov State University, Russia
[b]University of New Mexico School of Medicine, United States
[c]University of New Mexico, College of Pharmacy
[d]Krasnoyarsk State Medical University named after Professor VF Voino-Yasenetsky, Russia
[e]Institute of Biochemistry and Physiology of Plants and Microorganisms, Russian Academy of Sciences, Russia
[f]Saratov State Medical University, Russia
[g]Tomsk State University, Laboratory of Biophotonics, Russia [h]Humboldt University, Physics Department, Germany [i]Potsdam Institute for Climate Impact Research, Germany

Corresponding author e-mail address: glushkovskaya@mail.ru

Abstract: We have shown that repeated loud music and sound (100 dB, duration 2 h, the sequence of 60 sec – sound; 60 sec – pause, independently on frequency) reversibly open the BBB to high and low molecular weight molecules. The time of BBB opening/closing is 1h and 4 h after sound exposure, respectively. The results of our study suggest that the BBB opens via stress-mediated effects of the loud sound. The stress responses (immediately after sound-off) were accompanied by adrenergic mechanism (rise of serum epinephrine) for increasing of relative cerebral blood flow (rCBF) and energy metabolism through elevation of the blood oxygen saturation (SpO_2) in all brain regions. However, in post-stress period (1h after sound exposure) during opening of the BBB, we observed opposite hemodynamic and metabolic changes, i.e. the level of serum epinephrine, rCBF and SpO_2 decreased. These changes were associated with dysregulation of expression of tight junction (TJ) proteins: a decrease in expression of claudin-5 and occluding and an increase in expression of ZO-1. When BBB closed (4h after sound exposure), serum level of epinephrine, TJ proteins and rCBF were over the normal levels. However, SpO_2 was significantly increased in this time that was accompanied by activation of clearance of molecules crossing the opened BBB (dextran 70 kDa) from the brain into meningeal and cervical lymphatics. These results suggest that loud music/sound opens BBB in post-stress period via mechanisms of reversible dysregulation of expression of TJ and reducing of rCBF and SpO_2. The recovery of BBB function is based on quick activation of metabolic and lymphatic processes of clearance of molecules crossing of opened BBB.

This study was supported by grants from Russian Science Foundation 17-15-01263.

P.03-27

Multimodal measurements of brain tissue metabolism and perfusion in a neonatal model of hypoxic-ischaemic injury

G. Bale[a], A. Rajaram[b,c], M. Kewin[b,c], L. Morrison[b], A. Bainbridge[d], L. Liu[b], U. Anazodo[b,c], M. Diop[b,c], K. St. Lawrence[b,c], I. Tachtsidis[a]

[a]*Medical Physics and Biomedical Engineering, University College London, London, UK*
[b]*Imaging Program, Lawson Health Research Institute, London, ON, Canada*
[c]*Department of Medical Biophysics, Western University, London, ON, Canada*
[d]*Medical Physics and Biomedical Engineering, University College Hospital, London, UK*

Corresponding author e-mail address: g.bale@ucl.ac.uk

Abstract: This is the first multimodal study of cerebral tissue metabolism and perfusion post-hypoxic-ischaemic (HI) brain injury with broadband near-infrared spectroscopy (bNIRS), diffuse correlation spectroscopy (DCS), positron emission tomography (PET) and magnetic resonance spectroscopy (MRS). In 5 piglet models of HI, we measured cerebral tissue saturation (StO2), cerebral blood flow (CBF), cerebral oxygen metabolism (CMRO2), changes in the mitochondrial oxidation state of cytochrome-c-oxidase (oxCCO), cerebral glucose metabolism (CMRglc), and tissue biochemistry (Lac+Thr/tNAA). At baseline, the parameters measured were: 64±6 % StO2, 35±11 ml/100g/min CBF, and 2.0±0.4 µmol/100g/min CMRO2. After HI the parameters measured were: 68±6% StO2, 35±6 ml/100g/min CBF, 1.3±0.1 µmol/100g/min CMRO2, 0.4±0.2 Lac+Thr/tNAA, and 9.5±2.0 CMRglc. This study demonstrates the capacity of a multimodal set up to interrogate the pathophysiology of HIE using a combination of optical methods, MRS, and PET.

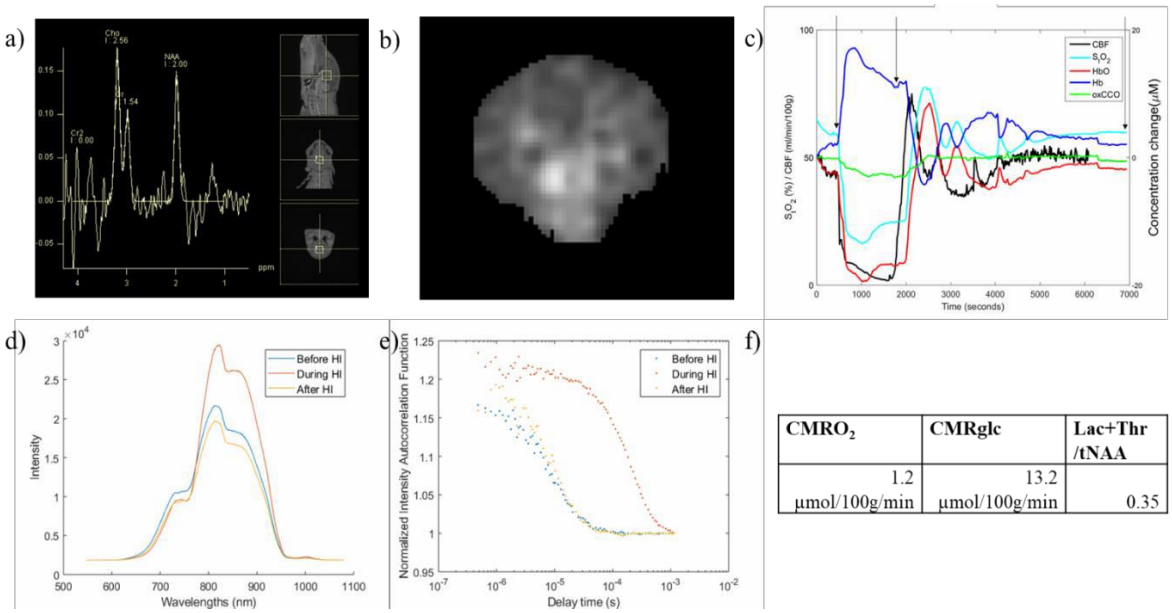

$CMRO_2$	CMRglc	Lac+Thr /tNAA
1.2 µmol/100g/min	13.2 µmol/100g/min	0.35

Figure 1: Examples of data collected from all modalities in one piglet (piglet 26): a) basal ^{1}H MRS spectra and voxel location, b) FDG PET glucose map, c) bNIRS and DCS signals during HI; arrows indicate start and end of HI, and final measurement, d) NIRS intensity spectra before, during and after HI, e) DCS normalized intensity autocorrelation functions before, during and after HI, f) results obtained from all modalities at the final measurement after HI.

P.03-28

Effects of aging, cognitive dysfunction, brain atrophy on cerebra; blood oxygenation and optical characteristics in the prefrontal cortex: A time-resolved spectroscopy study

K Sakatani [a, b], K Oyama [c], L Hu [a], Y Yamada [d]

[a] Universal Sport Health Science Laboratory, Dept of Human and Engineered Environmental Studies, Graduate School of Frontier Sciences, The University of Tokyo, [b] Institute for Healthcare Robotics, Future Robotics Organization, Waseda University, [c] Dept of Computer Science, College of Engineering, Nihon University; [d] Center for Neuroscience and Biomedical Engineering, The University of Electro-Communications, Japan

k.sakatani@edu.k.u-tokyo.ac.jp

Abstract: Time-resolved near infrared spectroscopy (TRS), which employs light sources of laser diodes emitting picosecond light pulses and a time-resolved detector with a picosecond time-resolution, can measure hemodynamic conditions at rest due to its capability of acquiring baseline hemoglobin (Hb) concentrations quantitatively. By employing TRS in our previous study, we measured the Hb concentrations and the optical pathlengths (OPLs) in various brain regions of healthy adults [1]. However, the effects of aging and brain atrophy associated with cognitive decline are not yet clear. In the present study, by employing TRS, we focused on measuring the Hb concentrations and OPLs at rest in the prefrontal cortex (PFC) of patients under rehabilitation, and investigated the relationship between the TRS parameters and cognitive functions assessed by the mini mental state examination (MMSE). In addition, we investigated the relationship between the TRS parameters and the brain atrophy assessed by MRI.

We studied 202 subjects (87 males, 115 females; age 73.4 ± 13.0 years (mean ± SD) who were receiving rehabilitation; 68.8% of the subjects suffered from cerebrovascular diseases including 79 cases of cerebral infarction, 41 cases of cerebral haemorrhage, 21 cases of subarachnoid haemorrhage. In addition, 94.6% of the subjects suffered from at least one life- style diseases. Employing TRS (TRS-20, Hamamatsu Photonics, Japan), we measured Hb concentrations and OPLs at rest in the PFC, and evaluated the relationship between the TRS parameters and cognitive function assessed by Mini-Mental State Examination (MMSE). In addition, 55 subjects underwent an MRI study on a 1.5T Vision Plus imager (Siemens, Germany).We analyzed the morphological changes of the brain using the voxel-based specific regional analysis system for Alzheimer's disease (VSRAD) [2]. Then, we evaluated the relationship between the TRS parameters and the brain atrophy assessed by MRI.

We found positive correlations between MMSE scores and oxygen saturation (SO_2), oxy-Hb in the PFC, suggesting that the greater the degree of PFC activity, the higher the cognitive function. In addition, we found the negative correlation between the subject's age and SO_2 and oxy-Hb in the PFC, suggesting that the older the subject, the lower the PFC activity at rest. Moreover, the OPLs in the right PFC negatively correlated with degree of brain atrophy evaluated by MRI, indicating that the shorter the OPL, greater degree of brain atrophy.

TRS allowed us to evaluate the relation between the cerebral blood oxygenation (CBO) in the PFC at rest and cognitive function.

References: [1] Murayama et al. Adv Exp Med Biol. 2017;977:269-276. [2] Matsuda H. Aging Dis. 2013;4: 29-37.

P.03-29

Disruption of Cross Frequency Coupling (CFC) by Cortical Spreading Depression (CSD)

T. Zhang and E. M. Nemoto

Department of Neurosurgery, University of New Mexico, USA

Abstract: Introduction: Cortical Spreading Depression (CSD) temporarily suppresses the connection of underlying neurons to the rest of the brain including deep subcortical regions which occurs by cross frequency coupling (CFC) high amplitude delta waves (0.5-4Hz) which are gradually reconnected after the CSD. Our aim was to determine the effect of *repetitive CSD* on the suppression and restoration of CFC. Methods: Rats anesthetized with urethane 1.5 g/kg, i.p., were intubated and mechanically ventilated on 30% O_2/70%N_2.Arterial blood gases, pH and temperature were monitored. Arterial blood pressure was monitored. Ag/AgCl ball bi-polar electrodes inserted over the parietal cortex and connected to high input impedance bioamplifiers with the left ear as a reference. Before application of cortical electrical stimulation to elicit CSD, background brain activities were recorded to establish the baseline CFC. A stimulating electrode at 1.5 mA, 10 Hz, 2 sec duration was used to electrically induce CSD. We selected lower delta waves at 0.1~2 Hz as a predictor in the General Linear Model (GLM) procedure. The phases are wrapped to – □. to □. We then studied the phase of this low frequency band cross coupled to 4 physiological neuronal activity frequency bands i.e., /(5~7 Hz), 0 (8~12 Hz), 1 (13~30 Hz) and 2 (30~80 Hz).
Results: CFC changes with repetitive CSD recording is illustrated (Fig). The higher frequency EEG spikes ride on a slow wave at 2 Hz. Four CFC, namely, Theta, Alpha, Beta and Gamma, are plotted under repetitive CSD. All four CFC are progressively suppressed decreasing to very low coupling (r=0.3) after the CSD from r>1 before CSD. Conclusions: Complete suppression of CFC was not achieved but we noted that CFC were decreasing before arrival of the CSD even while the ECoG appears unchanged suggesting that the local neurons are not yet affected but CFC is already decreasing.

Figure

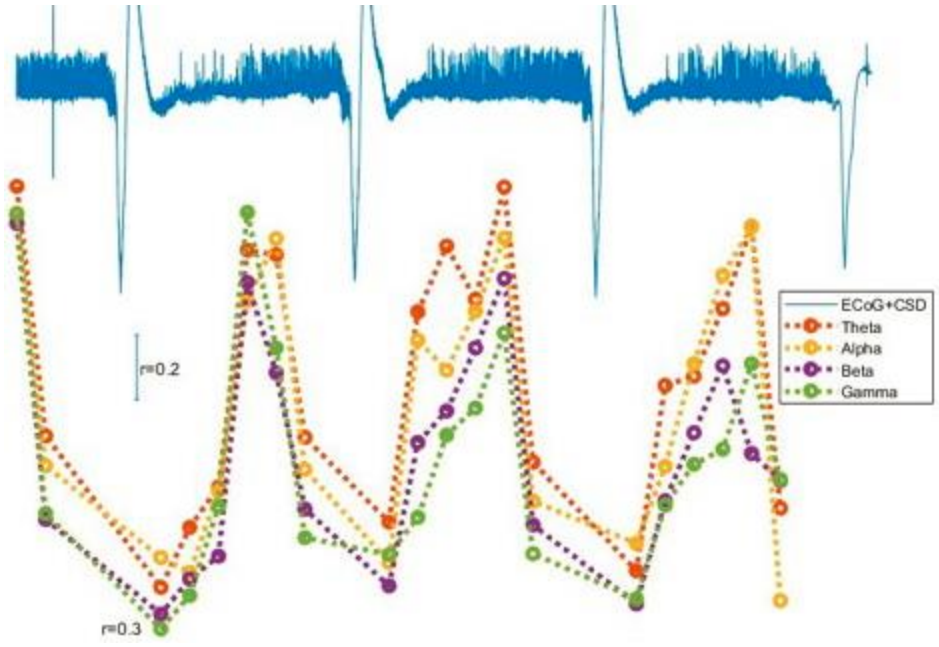

P.03-30

Effects of long-term blue-colored light exposure on frontal and occipital cerebral hemodynamics: A subgroup analysis of fNIRS data

Hamoon Zohdi[1], Felix Scholkmann[1,2], and Ursula Wolf[1]

[1] *University of Bern, Institute of Complementary and Integrative Medicine, Bern, Switzerland*
[2] *University Hospital Zurich, University of Zurich, Biomedical Optics Research Laboratory, Department of Neonatology, Zurich, Switzerland*

Corresponding author e-mail address: *hamoon.zohdi@ikim.unibe.ch*

Abstract: Background: In the modern society, we are increasingly exposed to numerous sources of blue-colored light including digital screens from electronic devices (e.g., TVs, computers, laptops, smartphones, tablets), as well as light from fluorescent and LED lamps. In contrast to its wide range of applications, the effects of blue-colored light on the human physiology are not completely understood. Aim: We investigated the impacts of long-term blue- colored light exposure (CLE) on frontal and occipital human cerebral hemodynamics using functional near-infrared spectroscopy (fNIRS). Materials and Methods: 32 healthy right-handed subjects (20 female, 12 male, age: 23.8 ± 2.2, range 20-28 years) were exposed to blue LED light (wavelength: 450 nm; illuminance: 120 lux at eye level) for 15 minutes. Before (baseline, 8 min) and after (recovery, 20 min) the CLE, subjects were in darkness. We measured the concentration changes of oxyhemoglobin ([O_2Hb]) and deoxyhemoglobin ([HHb]) bilaterally over the prefrontal cortex (PFC) and visual cortex (VC) by fNIRS during the experiment. Signals from the left and right PFC and VC were averaged to obtain signals for the whole PFC and VC, respectively. In order to analyze the changes of [O_2Hb] and [HHb] for each subject, the signals were normalized with respect to the last 5 minutes of the baseline period. Subjects were then classified into different groups based on their hemodynamic response pattern of [O_2Hb] at the PFC and VC during CLE. Results: On the group level (32 subjects), we found an increase in [O_2Hb] and a decrease in [HHb] at both cortices during CLE. Evoked changes of [O_2Hb] were higher at the VC compared to the PFC ($p < 0.001$; effect size (Cohen's d): $d = 1.03$), while [HHb] changes at the PFC were more prominent than that of the VC ($p < 0.001$; $d = 1.15$). Eight different hemodynamic response patterns were detected (Table 1), while an increase of [O_2Hb] in both cortices was the most common pattern (8 out of 32 cases, 25%) during CLE.
Discussion and Conclusion: Our study showed that the hemodynamic changes at the PFC and VC during a CLE with blue light (i) were generally higher in the VC compared to the PFC, (i) vary depending on the subject, and (ii) can be classified into 8 groups. Taking the intersubject- variability of cerebral hemodynamic responses into account is important for fNIRS studies, especially when non-classical paradigms are investigated.

	PFC	VCNumber of Subjects within the group
Group 1	↑	↑8 (5 female, 3 male); 63% female, 37% male
Group 2	↑	↓6 (4 female, 2 male); 67% female, 33% male
Group 3	↓	↑5 (1 female, 4 male); 20% female, 80% male
Group 4	↓	–4 (4 female); 100% female
Group 5	–	↑3 (1 female, 2 male); 33% female, 67% male
Group 6	↑	–2 (2 female); 100% female
Group 7	↓	↓2 (2 female); 100% female
Group 8	–	–2 (1 female, 1 male); 50% female, 50% male

Table 1: Classification of hemodynamic response of [O_2Hb] patterns (decrease ↓, increase ↑ , and inconclusive **–**) at the PFC and VC during CLE.

P.03-31

Cerebral blood flow changes in the prefrontal cortex induced by standing up measured by NIRS -Comparison between healthy adults and post-stroke patients-

M. Moriya[a, b] and K. Sakatani[C]

[a] *Department of Physical Therapy, Faculty of Health Care and Medical Sports, Teikyo Heisei University, Japan*
[b] *Cellular and Integrative Neuroscience, Jikei University Graduate School of Medicine, Japan*
[c] *Universal Sport Health Science Laboratory, Department of Human and Engineered Environmental Studies, Graduate School of Frontier Sciences, The University of Tokyo, Japan*

k.sakatani@edu.k.u-tokyo.ac.jp

Abstract: The ability to maintain a nearly constant cerebral blood flow regardless of changes in cerebral perfusion pressure is known as autoregulation. Autoregulation is likely to break after a stroke, resulting in unstable cerebral blood flow and cerebral perfusion pressure. The pathophysiology of autoregulation in stroke patients is still unknown. Therefore, in this study, we measured cerebral blood flow changes in the prefrontal area with postural changes using near-infrared spectroscopy (NIRS), and examined autonomic nervous control function and cerebral circulation control mechanism. In addition, the laterality index at rest (LIR) of the prefrontal activity at rest was calculated as follows [1]:

$$LIR=\frac{\Sigma t\{(\Delta oxyRt-\Delta oxyRmin)-(\Delta oxyLt-\Delta oxyLmin)\}}{\Sigma t\{(\Delta oxyRt-\Delta oxyRmin)+(\Delta oxyL-\Delta oxyLmin)\}}$$

LIR>0 indicates right dominant activity, while LIR<0 indicates left dominant activity. Previous studies demonstrated that LIR>0 is associated with sympathetic activity while LIR<0 is associated with para sympathetic activity [2]. We investigated the relationship between LIR and oxy-Hb changes induced by standing up. First, we confirmed normal circulatory responses in healthy adults. Postural changes from sitting to standing significantly reduced oxy-Hb ($p = 0.01$), HR significantly increased ($p = 0.01$), L / H tended to increase ($p = 0.15$), CCV (HF) It showed a significant decrease ($p = 0.04$). Healthy adults often show LIR <0 (rest activity at the left), while stroke patients show LIR> 0 (rest activity at the right) significantly more ($\chi 2$ (1) = 7.721, $p = 0.005$). Interestingly, in stroke patients with LIR> 0, oxy-Hb increased with standing, suggesting that cerebral blood flow changes to paradoxical.

There was a positive correlation between LIR and oxy- Hb in stroke patients ($r = 0.64$, $p = 0.02$) (Fig. 1). In addition, six of the stroke patients had orthostatic hypotension and LIR> 0. These results suggest that the post-stroke patients associated with right PFC dominant activity at rest shows a paradoxical increase of oxy-Hb (i.e., rCBF) in the PFC, which might be caused by an increase of sympathetic activity.

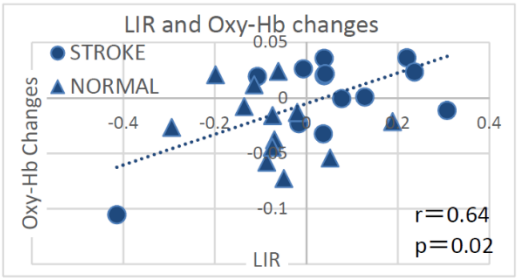

Fig. 1 Correlation between LIR and oxy-Hb

References

[1] Ishikawa W, et al. J Biomed Opt. 2014 Feb;19 (2):027005.
[2] Tanida M, et al. Brain Res. 2007 Dec 12;1184:210-6.

P.03-32

Parasympathetic nervous activity associated with dis-coordination between physical acceleration and heartrate variability in patients with sleep apnea

K. Taniguchi[a,b,d], A Shimouchi[b,c], N. Jinno[b], N Okumura[b] and A. Seiyama[a]

[a] *Human Health Sciences, Graduate School of Medicine, Kyoto University, Japan*
[b] *College of Life and Health Science, Chubu University, Japan*
[c] *National Cerebral and Cardiovascular Research Center, Japan*
[d] *Department of Bioscience, Nagahama Institute of Bio-Science and Technology, Japan*

Corresponding author e-mail address: ashimouc@isc.chubu.ac.jp

Abstract: Sleep apnea syndrome (SAS) often accompanies alterations of heart rate variability (HRV). The severities of SAS are sometimes evaluated by the oxygen desaturation index (ODI), i.e., the frequencies of 3% or more decreases in oxygen saturation in one hour during night sleep. We studied whether or not autonomic nervous systems be associated with coordination between HRV and physical acceleration (PA) during the free-moving in patients with SAS. Among 33 older women aged 60 and more, 19 subjects had high 3%ODI (>5). Their HRV and PA were simultaneously obtained every minute for 24 hours. Their ODI were analyzed during night sleep. The ratio of low/high frequency (LF/HF) and high frequency in normalized units (HFnu) were used as HRV indices. We defined %Lag0 as the % frequency of the lag=0 min between HRV and PA in 1 h. Low levels of %Lag0 considerably indicated dis-coordination between HRV and PA. Nineteen patients were divided into high %Lag0 between LF/HF or HFnu and PA before sleep (n = 9: as group A) and those with low %Lag0 (n = 10: as group B). In group B with high %ODI and low %Lag0, HFnu was significantly increased than that of group A with high %ODI and high %Lag0 in 1 h after wake-up ($p < 0.05$), although there were no significantly differences in HFnu during 1 h before and after falling asleep and wake-up in the morning. Significant differences were not observed in the HFnu in low ODI group or total 33 subjects. These results suggested that close associations of high ODI and dis-coordination between HRV and PA could be caused by higher activities of parasympathetic nervous system after wake-up.

References: Taniguchi K, Shimouchi A, Seki J, Jinno N, Shirai M, Seiyama A. Factors affecting coordination between heart rate variability and physical acceleration in daily lives of free- moving adults. Adv Biomed Eng. 2015; 4:35-41.

P.03-33

The changes in brain oxygenation during tACS at consequences of TBI: a near-infrared spectroscopy study

A. Trofimov[a], M. Dobrzeniecki[a], D. Martynov[b], A. Dubrovin[a], A. Zorkova[a], A. Sheludyakov[a] and D. Bragin [c]

[a]Department of Neurosurgery, Privolzhsky Research Medical University, Russia [b]Nizhny Novgorod State Technical University named after R.E. Alekseev, Russia [c]Department of Neurosurgery, University of New Mexico School of Medicine, USA

xtro7@mail.ru

Abstract: Traumatic brain injury (TBI) triggers a sequence of dynamic and long-term pathological responses, making TBI a risk factor for neurodegenerative and other pathological conditions such as posttraumatic encephalopathy (PTE). The aim was to evaluate the changes in brain oxygenation, assessed by near-infrared spectroscopy (NIRS), during transcranial alternating current stimulation (tACS) in patients with PTE. A cohort of nineteen patients with PTE (4 women and 15 men, aged 32.7 ± 11.4 years) was used in a study. Patients were treated by 10-Hz in-phase tACS applied for 30 minutes to the medial frontal cortex and right lateral prefrontal cortex at 21 days after TBI. The tATS devise was designed and manufactured at Nizhny Novgorod State Technical University. Regional cerebral tissue oxygen saturation ($SctO_2$) in the frontal lobes was measured simultaneously and bilaterally by cerebral oximeter Foresight 2030 (Casmed, Branford, USA). $SctO_2$ values were compared before stimulation, by the 15th minute and at the end of the tACS. Statistical analysis of all results was performed using Mann-Whitney U- criterion. Significance was preset to $P < 0.05$. In all patients, the stimulation was accompanied by an improvement in clinical status (neurological symptoms decrease and general condition relief). No complications were identified. Before the stimulation, $SctO_2$ values were not different between hemispheres ($p>0.05$). After 15 minutes of tACS, a significant ($p <0.05$) decrease in regional $SctO_2$ on the in-phase side was observed. However, at the end of the stimulation (30 minutes), the hemispheric differences in cerebral oxygen saturation became statistically insignificant again ($p >0.05$). Despite the improvement in clinical status in patients with PTE, tACS causes a significant ($p <0.05$) decrease in regional $SctO_2$ due to a tissue reaction to neuronal activation. Probably the restoration of the cerebral oxygen status at the end of stimulation reflects the neurovascular coupling. Further research is required.

P.03-34

Cerebral capillary dilation and constriction in the somatosensory cortex of awake mouse: *in vivo* two-photon microscopic studies

Hiroki Suzuki[a], Takuma Sugashi[a], Hiroshi Takeda[a], Hiroyuki Takuwa[b], Iwao Kanno[b], Ji Bin[b], Naruhiko Sahara[b], Makoto Higuchi[b], Kazuto Masamoto[b,c]

[a] *Graduate School of Informatics and Engineering, Tokyo, Japan*
[b]*Department of Functional Brain Imaging Research, National Institute of Radiological Sciences, 4-9-1 Anagawa, Inage, Chiba 263-8555, Japan*
[c] *Center for Neuroscience and Biomedical engineering,University of Electro-Communications, 1-5-1 Chofugaoka, Chofu, Tokyo 182-8585, Japan*

Corresponding author e-mail address: suzuki@nvu.mi.uec.ac.jp

Abstract: Cerebral capillary responds to changes in neural activity to maintain regional balances between energy demand and supply. However, its quantitative aspects of the capillary dilation and their contribution to increases in oxygen supply to tissue remain incompletely understood. In the present study, we experimentally determined three dimensional (3D) changes in capillary morphometry during evoked neural activity in the somatosensory cortex of the awaken mice. Two-photon microscope images of the microvessels captured in the somatosensory cortex of transgenic mice (Cre-CaMKII/GCaMP3, N=6) were analyzed with custom written Matlab software. The animals expressed fluorescence calcium indicator GCaMP3 in the cortical neurons, while blood plasma was fluorescently labeled with intraperitoneal injection of sulforhodamine 101. The contralateral side of whiskers was mechanically simulated with variable frequencies (1-8 Hz), while evoked neurons and capillaries (< 8 μm in diameter) were simultaneously imaged over depths of 50- 320 μm from the cortical surface. For each stimulation 20 trials were repeated with a random order of the different frequency stimulation including resting (no stimulation) trials. For each volume images, 3,000-7,000 measurement points were extracted along a center line of the capillary by a 3D thinning method. We found that 84% of the capillary locations showed no detectable changes in capillary diameter during functional activation trials, whereas other locations showed dilation (9%) or constriction (7%). These capillary locations had different diameters at rest (without stimulation trials); a mean of 5.0 μm, 4.6 μm, and 5.4 μm at unchanged, dilation, and constriction points, respectively. Detailed spatial analysis showed that a portion of the single capillaries reacts to the stimulation and a location of the capillary constriction tends to be present near the branching points of the capillaries. The morphometric analysis of the cerebral capillary responses *in vivo* could be useful for better understanding the realistic oxygen dynamics in the functioning brains.

Acknowledgements: This study was partly supported by JSPS KAKENHI (JP201710551 to TS and 19K07795 to KM).

O.07-1

Potential biomarker for triple negative breast cancer invasiveness by optical redox imaging

Min Feng[a,b], He N. Xu[a,b,*], Jinxia Jiang[a,b], and Lin Z. Li[a,b,*]

[a] *Department of Radiology,* [b] *Britton Chance Laboratory of Redox Imaging, Johnson Research Foundation, Perelman School of Medicine, University of Pennsylvania, Philadelphia, PA 19104, USA*

**Corresponding author e-mail addresses: linli@pennmedicine.upenn.edu, hexu2@pennmedicine.upenn.edu*

Abstract: Cancer invasion to neighboring tissues is a significant event in cancer progression to metastases. Predicting tumor invasive/metastatic potential remains a challenge in cancer research and clinical diagnosis. Optical redox imaging (ORI) is based on detecting the endogenous fluorescence signals of reduced nicotinamide adenine dinucleotide (NADH) and oxidized flavin adenine dinucleotide (FAD). Previously, we found that ORI can discriminate between cancer and normal tissues specimens from clinical breast cancer patients and can differentiate the relative invasiveness of melanoma and breast tumor. In this study, we aimed to identify ORI biomarkers for differentiating the invasive potentials of four triple-negative breast cancer cell lines (TNBC). Using a fluorescence microscope, we acquired NADH and FAD fluorescent signals from TNBC lines in culture: MDA-MB-231, MDA-MB-436, HCC1806 and MDA-MB-468. We found that: 1) the redox ratio, FAD/(NADH+FAD) differentiated the four TNBC lines ($p< 0.001$); 2) the transwell invasion assay showed a significant difference of invasive potential between MDA-MB-231 and the other three TNBC lines ($p < 0.001$); 3) there was a positive logarithmic correlation between the redox ratio and the invasive potential ($R^2=0.87$, $p=0.07$), where the most invasive MDA-MB-231 has the highest redox ratio, and the least invasive MDA-MB-468 has the lowest redox ratio. These results suggest that the redox ratio can potentially be used for TNBC prognosis as a biomarker for invasiveness.

O.07-2

Optical redox imaging differentiates triple-negative breast cancer subtypes

J. Jiang, M. Feng, A. Jacob, L. Z. Li, and H. N. Xu

Department of Radiology, Perelman School of Medicine, University of Pennsylvania, USA

Corresponding author e-mail address: hexu2@pennmedicine.upenn.edu

Abstract: Triple-negative breast cancer (TNBC) is a highly diverse group of cancers with limited treatment options, responsible for about 15% of all breast cancers. TNBC cells differ from each other in many ways such as gene expression, metabolic activity, tumorigenicity, invasiveness, etc. Recently, many research and clinical efforts have focused on metabolic targets for therapy. Metabolic characterization and classification of TNBC cell lines can facilitate the assessment of therapeutic effects and assist in metabolic drug development. Herein, we used optical redox imaging (ORI) techniques to characterize TNBC subtypes metabolically. We performed ORI of TNBC cell lines MDA-MB-231, MDA-MB-436, MDA-MB- 468, and HCC1806, and found that these cell lines had differing redox statuses (NADH, flavin adenine dinucleotide (FAD), and redox ratio). We then metabolically perturbed the cells with mitochondrial inhibitors and an uncoupler and performed ORI accordingly. As expected, we observed that these TNBC cell lines had similar response patterns to the metabolic perturbations. However, they exhibited differing redox plasticity. These results suggest that subtypes of TNBC cells are different metabolically and that ORI can serve as a sensitive technique for the metabolic profiling of TNBC cells.

O.07-3

An implantable microChip for clinical EPR oximetry

Maciej M. Kmiec, Dan Tse, Jesse M. Mast and Periannan Kuppusamy

Geisel School of Medicine, Dartmouth College, Lebanon, NH 03756, USA

Presenting author e-mail address: Kmiec@Dartmouth.edu

Abstract: EPR oximetry has been established as a viable method for measuring tissue oxygen level (partial pressure of oxygen, pO_2) in animal models; however, it has not yet been established for measurement in humans. EPR oximetry requires oxygen-sensing paramagnetic probe (molecular or particulate) to be placed at the site/organ of measurement, which may pose logistical and safety concerns, including possible invasiveness of the probe- placement procedure, lack of temporal stability and sensitivity of the probe for long-term (repeated) measurements, and possible toxicity of the probe in the short and long-term.

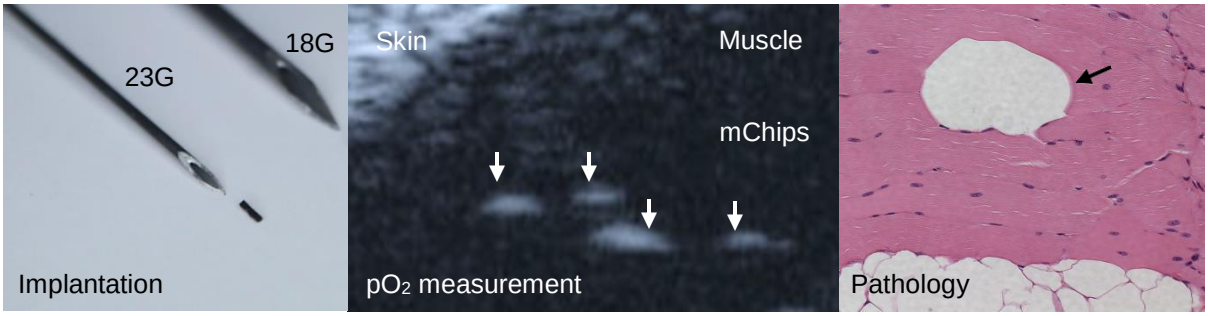

Previously, we have developed an implantable oxygen-sensing probe, called OxyChip, which we have successfully established for oximetry in pre-clinical animal models (*Hou et al. Biomed Microdevices 20; 29, 2018*). Currently, the OxyChip is being evaluated in a limited clinical trial in cancer patients. A major limitation of the OxyChip is that it is a large implant (1.4 mm^3 0.6x5.0 mm) and hence not suitable for measuring oxygen heterogeneity that may be present in solid tumors, chronic wounds, etc. Here, we describe the development of a substantially smaller version of OxyChip (0.07 mm^3 0.3x1.0 mm), called microChip, which can be placed in the tissue of interest using a 23G syringe-needle, that is routinely used in the clinic with minimal invasiveness. Using *in vitro* and *in vivo* models, we have shown that the microchip provides adequate EPR sensitivity, stability, and biocompatibility and enables robust, repeated, and simultaneous measurement from multiple implants (without magnetic field gradients) providing mean and median pO_2 estimates in the implanted region. The microChips will be particularly useful for those applications that require repeated measurement of mean/median pO_2 in superficial tissues and malignancies.

Acknowledgements: The study was supported by National Institutes of Health grants R01 EB004031, and P01 CA190193

O.07-4

Oxyhemoglobin might evaluate the quality of chest compression

Y. Okuma[a], K. Shinozaki[a], T. Yagi[a], T. Yin[a], T. Kiguchi[b], T. Iwami[b], J. Kim[a], and L.B. Becker[a]

[a] *Department of Emergency Med-Cardiopulmonary, Feinstein Institute for Medical Research, Northwell Health System, Manhasset, NY, USA*
[b] *Kyoto University Health Service, Kyoto, Japan*

Corresponding author e-mail address: y8u2bear4@hotmail.com

Abstract: The real-time evaluation of chest compression during cardiopulmonary resuscitation is important. Previous studies suggested us arterial pressure (AP) and end- tidal carbon dioxide (EtCO2) as the indicators. Other studies showed us cerebral oxygen levels played important roles in indicator for return of spontaneous circulation. Recently we developed three characteristic chest compressions for rodents. As a pilot study, we compared with oxyhemoglobin (Oxy-Hb), Deoxy-Hb, and tissue oxygenation index (TOI). After this comparison, we evaluated chest compressions. We used Male Sprague-Dawley rats. We attached the near-infrared spectroscopy (NIRS) between nasion and upper cervical spine. Rats underwent 10-minute asphyxial cardiac arrest (CA). After CA, we performed 3 types of chest compression every 30 seconds and continued for up to 4 and a half minutes. We considered mean AP (MAP) and EtCO2 as reliable. Concerning the correlation, only Oxy-Hb showed the significant coefficient to both (MAP: r=0.218, p<.0001) (EtCO2; r=0.2294, p<.0001), followed by Deoxy-Hb (MAP: r=-0.4193, p<.0001) (EtCO2; r=0.0584, p=.302), and TOI (MAP: r=-0.3125, p<.0001) (EtCO2; r=0.0239, p=.673). Next, our original
chest compressions revealed that only Oxy-Hb could detect these characters significantly, while MAP, EtCO2, Deoxy-Hb, and TOI couldn't (n=5). Finally, we performed the same chest compression, adjusting MAP below 20mmHg for first 20 seconds and MAP over 20mmHg for latter 20 seconds, and evaluated the difference between the average of the current 20 seconds and that of the previous 20 seconds (n=6). This revealed that Oxy-Hb (0.45±0.65 vs 2.24±1.30 mmol/L, p<.05) and TOI (0.13±1.00 vs 5.27±4.53 %, p<.05)
significantly went up during MAP ≥20mmHg, while Deoxy-Hb (0.31±1.31 vs -1.39±0.95 mmol/L, p=.063) went down during MAP ≥20mmHg. We considered especially Oxy-Hb had the potential to evaluate the quality of chest compression.

P.04-35

Physical stress attenuates cognitive inhibition: An fNIRS examination

Lei Ma[a], Kui Xu[b], Xiaoyan Shen[a], Jinhong Ding[c]

[a] *School of Information Science and Technology, Nantong University, Nantong 226007, Jiangsu Province, China*
[b] *School of medicine, Case Western Reserve University, Cleveland 44106, Ohio USA*
[a] *School of education science, Case Western Reserve University, Nantong 226007, Jiangsu Province, China*

Corresponding author e-mail address: lxm410@case.edu

Abstract: The aim of the study was to assess the hemodynamics in the prefrontal cortex (PFC) and salivary α-amylase response during acute Physical stress. Acute stress was induced using the cold pressor task(CPT). Subjects were 49 healthy graduate students who took a 10 minutes stress test(stress). To assess the hemodynamics in the prefrontal cortex (PFC) during acute stress induction using functional near infrared spectroscopy (fNIRS) and salivary α- amylase levels, the participants provided four salivary samples (before the stress test, at the end of each test and 5 minutes after the third sample). It was verified that individual's salivary α-amylase secretion was changed under CPT and functional oxyHb signals fluctuated with greater amplitude than systemic components for participants in the stress group relative to those in the control group. It was concluded that acute stress exposure attenuated cognitive inhibition and higher levels of oxyHb in the Left PFC following stress exposure.

P.04-36

Drag reducing polymer addition to colloid resuscitation fluid enhances cerebral microcirculation and tissue oxygenation after traumatic brain injury complicated by hemorrhagic shock

D.E. Bragin[a], O.A. Bragina[a], L. Berliba[b], M.V. Kameneva[b] and E.M. Nemoto[a]

[a] *Department of Neurosurgery, University of New Mexico School of Medicine, USA*
[b] *McGowan Institute for Regenerative Medicine, University of Pittsburgh, USA*

D.E. Bragin: dbragin@salud.unm.edu

Abstract: Hemorrhagic shock (HS) is a severe complication for traumatic brain injury (TBI) that doubles mortality due to severe microvascular cerebral blood flow (mvCBF) and oxygen delivery reduction as a result of hypotension. Volume expansion with resuscitation fluids (RF) for HS does not improve microvascular CBF (mvCBF). We showed that the addition of drag reducing polymers (DRP) to the crystalloid RF (lactated Ringer) significantly improves mvCBF, oxygen supply and neuronal survival in rats suffering TBI+HS. Here, we compared the effects of colloid RF (Hetastarch) with DRP (HES-DRP) and without (HES).
Methods: TBI was induced in rats by fluid percussion (1.5 ATA, 50 ms) and followed by controlled hemorrhage to a mean arterial pressure (MAP) =40 mmHg. HES-DRP or HES was infused to MAP =60 mmHg for one hour (pre-hospital), followed by blood re-infusion to a MAP=70 mmHg (hospital). In vivo 2-photon microscopy was used to monitor cerebral microvascular blood flow, tissue hypoxia (NADH) and neuronal necrosis (i.v. propidium iodide) for 5 hours before and after TBI/HS, followed by DiI vascular painting during perfusion-fixation. Temperatures, MAP, blood gases and electrolytes were monitored. Statistical analyses were done using GraphPad Prism by Student's t-test or Kolmogorov-Smirnov test where appropriate. *Results:* TBI/HS compromised mvCBF leading to capillary microthrombosis and tissue hypoxia. HES-DRP better than HES improved mvCBF and tissue oxygenation ($p<0.05$). The number of dead neurons in the HES-DRP was significantly less than in the HES group: 76.1±8.9 vs. 178.5±10.3 per 0.075 mm^3 ($P<0.05$). Post-mortem whole-brain visualization of DiI painted vessels revealed multiple microthromboses in both hemispheres that were 33 2% less in HES-DRP vs. HES group ($p < 0.05$).
Conclusions: Resuscitation after TBI/HS using HES-DRP effectively restores mCBF, reduces hypoxia, microthrombosis and neuronal necrosis compared to volume expansion with HES. HES-DRP requires an infusion of a smaller volume to improve tissue perfusion and oxygen delivery which reduces brain edema formation due to hypervolemia. Colloid-based RF with DRP is more neuroprotective than crystalloid RF.
Support: DOD DM160142.

P.04-37

Magnetoresistance properties of several RBCs combined with magnetic nano-particles and magnetic beads passing channel above the GMR-SV device

Jong-Gu Choi, Byeong-Uk Kang, and **Sang-Suk Lee**

[a] *Department of Oriental Biomedical Engineering, College of Health Sciences, Sangji University, 83 Sangjidaegil, Wonju, Gangwon-do 26339, Republic of Korea*

Corresponding author e-mail address: (sslee@sangji.ac.kr)

Abstract: Magnetic nano-particles (MNPs) and magnetic beads (MBs) were distinguished from each other and mixed with red blood cells (RBCs) and physiological saline solution (PBS). The MNPs had a diameter of 460 nm in which the carboxyl group (-COOH) was attached to the core Fe, and the MBs had an average diameter of about 1 μm with the -Si-OH group in the core Fe_3O_4. Four different types of RBCs were found to be located at the center and edge with common circle or elliptical round membranes due to the bonding arrangement of the MNPs and MBs with dipole moments. We observe the appearance of the cluster flow in the shape of a swirling cluster using a permanent magnet on a large amount of MNPs and MBs combined with RBCs contained in PBS. After 0.5 cc solutions of MNPs and MBs were immersed in 2.5 cc of PBS, the resistance values increased by 30 min at intervals of 2 min with the influence of external magnetic field. A dual-type giant magnetoresistance-spin valve (GMR-SV) multilayers of glass/Ta/NiFe/CoFe/Cu/CoFe/IrMn/CoFe/Cu/CoFe/NiFe/Ta or glass/NiO/NiFe/Cu/NiFe/NiO/Ta were prepared by ion beam deposition or rf- and dc- magnetron sputtering. Especially, the bottom exchange coupling field (H_{ex}) and coercivity (H_c), the top H_{ex} and H_c, magnetoresistance (MR) ratio, and magnetic sensitivity (MS) of the as- grown antiferromagnetic IrMn based GMR-SV sample were 480 G and 120 G, 240 G and 60 G, 6.3%, and 2.3%/G, respectively. The single- or multi-turn coils and a valley channel of thickness of 10 μm and width of 8 μm as a biosensor with GMR-SV device of 2 μmx18 μm were patterned by using a lithography process and an electron cyclotron resonance (ECR) Ar- ion milling system. The MR ratio and the MS of the patterned GMR-SV device were 3%-5% and 0.8 %/G-1.2 %/G, respectively. The differentially detected output signals of the common and elliptical RBC membranes were distributed the region of 1 μV - 30 μV. From this study, it is demonstrated that a GMR-SV biosensor can be used to analyze the molecular binding of the hemoglobin chain structure, depending on the oxidation concentration of RBCs combined with MNPs and MBs.

Acknowledgments: This work was supported by the NRF funded by the Korea government (Ministry of Education) with the Grant No. of NRF-2016R1D1A1B03936289.

P.04-38

Prox-1 and Hif1-a genes expression of primo vessel in rabbit's lymphatic vessel

Jun-Young Shin[a], Jong-Gu Choi[a], Sungchul Shin[b], Sujung Yeo[c] and Sang-Suk Lee[a]

[a] Department of Oriental Biomedical Engineering, College of Health Sciences, Sangji University, 83 Sangjidaegil, Wonju, Gangwon-do 26339, Republic of Korea
[b] Department of Animal Biotechnology, College of Life Sciences, Sangji University, Wonju, Republic of Korea
[c] Department of Meridian and Acupuncture, College of Korean Medicine, Sangji University, Wonju, Republic of Korea

Corresponding author e-mail address: sslee@sangji.ac.kr

Abstract: The primo vascular system (PVS) consisted of primo vessels (PVs) is one important circulatory vascular systems aimed at maintaining homeostasis and assisting in the recovery of the body by stimulating a state of control as body reacts when exposed to disease. To investigate whether the primo vasculature can successfully isolated from lymphatic vessels (LVs), can extract stable RNA with tiny primo vessels, and the candidate genes are enriched in primo vasculature in rabbit's LV under lipopolysaccharide (LPS) and acupuncture electric stimulation (AES), we investigated two marker genes (Prox-1 and Hif1-a) expression of both isolated PVs and composite LVs containing PVs (LVs+PVs) by RNA-sequencing (Seq) and quantitative reverse transcriptase polymerase chain reaction (qRT-PCR) analysis. The prospero homeobox protein 1 (Prox-1) gene is required for the development of the murine lymphatic system as the classic markers for lymphatic endothelial cells (LECs). The hypoxia inducible factor 1 alpha subunit (Hif1-a) gene is correlated with a protein of vascular endothelial growth factor C (VEGF-C) expression and lymphangiogenesis in breast cancer. RNA-Seq on the passed 10 samples on RNA-QC for three experimental groups with PVs, LVs, and LVs + LVs proceeded to the library construction stage automatically and analyzed differentially expressed genes (DEGs). From the real-time qRT-PCR analysis data, we found the marker Prox-1 gene was enriched in an isolated PVs compared to LVs. On other hand, Hif1-a gene was decreased in an isolated PVs compared to LVs. Based on mRNA transcriptional data stressed under LPS treatment and relieved by AES, Prox-1 and Hif1-a were increased and decreased in PVs compared LVs+PVs after LPS and AES treatments, respectively. This finding indicates that high and low levels of Prox-1 and Hif1-a may be involved in the function of PVs and that pathophysiological and physiological conditions could progress into inflamed lymphatic endothelial cells expanding the PV within the LV.

Acknowledgments: This work was supported by the National Research Foundation of Korea (NRF) funded by the Korea government (Ministry of Science and ICT) under Grant No. 2016R1E1A2A01953467.

P.04-39

Sympathetic activity mediates extra-medullary erythropoiesis in the primo vascular system of heart failure rats

Yiming Shen and Pan-Dong Ryu

Departments of Veterinary Pharmacology, College of Veterinary Medicine and Research Institute for Veterinary Science, Seoul National University, Seoul 08826, Republic of Korea

pdryu@snu.ac.kr

Abstract: The primo-vascular system (PVS) is a newly identified vascular tissue composed of primo-nodes (PN) and primo-vessels. Recently we reported that in the heart failure (HF), or hemolytic anemia rats there are similar morphological changes of organ surface (os) PVS associated with extra-medullary erythropoiesis. Exercise training (ExT) is known to induce beneficial effects on HF patients by normalizing the elevated sympathetic tone. However, little is known about whether ExT could also inhibit such HF-induced-morphological changes in the PVS. In this study, we examined 1) the effects of ExT on the morphology of the PVS in the HF rats, and 2) the effects of 6-hydroxydopamine (6-OHDA), a chemical sympathectomy agent on the morphological changes in the PVS of rats with phenylhydrazine-induced hemolytic anemia. HF rats were prepared by ligating the left descending coronary artery. In HF rats, we observed an increase in the size of the PNs ($p<0.01$), the number of the osPVS tissue samples per rat ($p<0.05$), the proportion of osPVS tissue samples with red chromophore ($p<0.001$), and the number of RBCs ($p<0.001$) in PN. ExT ameliorated these HF-induced changes in osPVS except the number of samples per rat. Blocking sympathetic activity with 6-OHDA dramatically reduced the number of samples per rat in normal rats. The treatment of 6-OHDA normalized the enlarged PN size ($p<0.05$) and the elevated proportion of the tissues with red chromophore ($p<0.001$) in the rats with hemolytic anemia. Taken together, the results indicate that the inhibition by ExT or removal by 6-OHDA of sympathetic tone block the erythropoietic morphological changes of the osPVS tissue in the HF and anemia rats, respectively. The results indicate that the sympathetic regulation may play important roles in regulation of the morphology and function of the osPVS in the normal and disease states.

Acknowledgment: This study was supported by the National Research Foundation of Korea funded by the Ministry of Education (2018R1D1A1B07043448).

P.04-40

Changes of prefrontal cortex and premotor area oxygenation laterality during 20 min of moderate-intensity cycling exercise

A. Tsubaki[a], S. Morishita[a], K. Hotta[a]. Y. Tokunaga[a], W. Qin[a], S.Kojima[a], and H. Onishi[a]

[a] *Institute for Human Movement and Medical Sciences, Niigata University of Health and Welfare, Japan*

Corresponding author e-mail address: tsubaki@nuhw.ac.jp

Abstract: A recent study showed that a single moderate-intensity exercise increases cortical oxyhemoglobin (O_2Hb), as measured by near-infrared spectrometry (NIRS). However, changes in O_2Hb laterality throughout exercise remain unknown. We evaluated O_2Hb laterality changes of the prefrontal cortex (PFC) and premotor area (PMA) over 20 min of moderate-intensity cycling. Twelve healthy volunteers (nine women) participated. After a 3- min rest, a 20-min exercise was performed at 50% VO_2peak workload. Right (R-) and left (L-) PFC and PMA O_2Hb levels were measured using multi-channel NIRS. O_2Hb levels for each area were expressed as changes from mean rest phase values and were averaged every 5 min over the exercise period. Laterality index (LI) was calculated using the formula (left region O_2Hb – right region O_2Hb)/ (left region O_2Hb + right region O_2Hb) every 5 min. A positive LI indicated that the O_2Hb increase was larger in the left than in the right region; negative LI indicated the opposite. To compare LIs, one-way analysis of variance was used. Statistical significance was set at $p < 0.05$. O_2Hb levels increased during the first 10 min and were maintained over the latter half of the exercise period. LI of PFC showed significant changes at each period (-0.40 ± 0.21, -0.03 ± 0.12, 0.14 ± 0.15, and 0.16 ± 0.10; 1st, 2nd, 3rd, and 4th 5-min period, respectively, $p < 0.05$). However, no significant changes were observed for PMA LI between any of the periods (-0.07 ± 0.09, 0.23 ± 0.08, 0.17 ± 0.12, and 0.19 ± 0.09 for the 1st, 2nd, 3rd, and 4th 5-min period, respectively, $p = 0.12$). PFC laterality changed over the 20-min moderate-intensity cycling exercise. L-PFC-dominant O_2Hb increases were observed in the latter half of the exercise. L-PFC plays an important role in executive functions and verbal working memory; these might increase after 10 min of a 20-min exercise.

Acknowledgements:
This study was supported by a Grant-in-Aid for Scientific Research (C) from the Japan Society for the Promotion of Science and a Grant-in-Aid for Exploratory Research from Niigata University of Health and Welfare.

P.04-41

Effects of 20-minute intensive exercise on subjects with different working memory bases

W. Qin[a]* , S. Kojima[a], S. Morishita[a], K. Hotta[a], A. Tsubaki[a]

a *Institute for Human Movement and Medical Sciences, Niigata University of Health and Welfare, Japan*

**Corresponding author e-mail: hwd19005@nuhw.ac.jp*

Abstract: Continuous moderate-intensity aerobic exercise improves cognitive function. Some studies have shown that there are individual differences in the extent of these exercise-associated improvements. The aim of this study was to assess the effects of different durations of exercise on cognitive function. Twelve healthy adult males (average age, 22.2 ± 1.5 years) participated in this study. After 4-minutes of rest and warm-up, a 20-minute exercise regime was initiated at a workload corresponding to 50% of the maximum oxygen consumption. A 2-back test was performed thrice pre-exercise and post- exercise and the reaction time and accuracy rate were recorded. Near-infrared spectroscopy was used to monitor the concentration of oxygenated hemoglobin (02 Hb) in the left (L-PFC) and right prefrontal cortex (R-PFC). Based on the reaction time before the exercise, the subjects were divided into a fast group (FG) and a slow group (SG). The changes in the reaction time before and after the 20-minute exercise were compared and the relationship between the change in the reaction time and the time required for the 02 Hb peak to reach its maximum was also determined. The reaction time of the FG decreased from 1.87 s to 1.68 s ($p = 0.71$), while that of the SG decreased from 3. 08 s to 1.84 s ($p < 0.01$). The time to reach the 02 Hb peak was significantly correlated to the FG (time): 16.17 ± 3.34 min; $r = -0.84$; $p < 0.05$). However, no relationship was observed between the time needed to reach the 02 Hb peak and the SG (18.83 ± 1.07 min; $r = -0.16$; $p = 0.75$). A 20-minute moderate-intensity exercise can improve the working memory of the SG. For those with a good working memory, the earlier the 02 Hb peak is reached, the greater the improvement in the working memory.

Acknowledgement

Scientific Research from the Japan Society for the Promotion of Science (A. Tsubaki), Exploratory Research from Niigata University of Health and Welfare (A. Tsubaki).

P.04-42

Supine cycling exercise enhances cerebral oxygenation of motor-related areas in healthy male volunteers

D. Sato[a], S. Morishita[b], K. Hotta[b], Y. Ito[a], A. Shirayama[a], S Kojima[b], W Qin[b] and A. Tsubaki[b]

[a] *Department of Physical Therapy, Niigata University of Health and Welfare, Japan.*
[b] *Institute for Human Movement and Medical Sciences, Niigata University of Health and Welfare, Japan*

Corresponding author e-mail address: kazuki-hotta@nuhw.ac.jp

Abstract: Cerebral oxygenated hemoglobin (O_2Hb) in motor-related areas increases during a single bout of acute exercise. The purpose of this study was to compare O_2Hb levels at motor-related areas during recumbent vs. supine cycling exercise. Eleven healthy volunteers (20.8 years old) performed a 30-min of cycling exercise (50% peak VO_2) with two position including supine and recumbent position. Near-infrared spectroscopy (NIRS) was used to measure the exercise-induced O_2Hb changes in the right (R-PFC) and left pre-frontal cortices (L-PFC), supplementary motor area (SMA), and primary motor cortex (M1). Skin blood flow (SBF), mean blood pressure (MBP), cardiac output (CO) and end expiratory carbon dioxide partial pressure ($P_{ET}CO_2$) were measured simultaneously. Data analysis was the average value after 10 minutes of exercise start. In R-PMA, L-PMA and SMA, the O_2Hb obtained during supine cycling exercise was significantly higher than that during recumbent cycling exercise (0.031 ± 0.01 vs 0.693 ± 0.01, 0.027 ± 0.01 vs 0.085 ± 0.013, 0.041 ± 0.011 vs 0.076 ± 0.008 mM·cm, recumbent vs supine position; R-PMA, L-PMA, SMA; $p < 0.05$, respectively). The SBF, MBP, CO and $P_{ET}CO_2$ during exercise were not different between recumbent and supine. The difference between the increase amount of O2HB in recumbent and supine position is, the increase in O2HB at R-PMA, L-PMA and SMA is not a change due to respiratory and circulatory dynamics, but is considered to be a result that reflects neural activity in the cerebral cortex. These results suggest that supine cycling exercise enhances exercise-induced cerebral oxygenation in the PMA and SMA in healthy male volunteers.

Acknowledgments: This study was supported by a Grant-in-Aid for Exploratory Research from the Niigata University of Health and Welfare (A. Tsubaki).

I.07

Biologic valdation of spin lattice relaxation based 3D patterns of tumor hypoxia: Clinical importance in preclinical models

Inna Gertsenshteyn[a,b], Matthew C. Maggio[a,b], Martyna Krzykawska-Serda[a,b], Eugene D. Barth[a,b], Richard C Miller[a,b], Charles A Pelizzari[a,b], Subramanian V. Sundramoorthy[a,b], Bulent Aydogan[a], Ralph R Weichselbaum[a], Victor M Tormyshev[c,d], Boris Epel[a,b], **Howard J Halpern[a,b]**

[a] *University of Chicago, Department of Radiation and Cellular Oncology, Chicago, IL 60637*
[b] *Center for EPR Imaging In Vivo Physiology, University of Chicago, Chicago, 60637*
[c] *Novosibirsk Institute for Organic Chemistry, Akadem Gorodok, Novosibirsk, RU, 630090*
[d] *Novosibirsk State University, Department of Chemistry, Novosibirsk, RU, 630090*

Corresponding author e-mail address: h-halpern@uchicago.edu

Abstract: Problem: Pulsed Spin Lattice Relaxation (SLR) EPR pO_2 images minimize self (spin probe)-relaxation making them nearly absolute molecular oxygen images. To validate these images, we tested relevance randomizing localized boost doses of radiation to well oxygenated (sensitive) or poorly oxygenated (nominally resistant, hypoxic) tumor portions. Simple 3D hypoxic tumor surface to volume ratio (SVR) was tested for significance in two mouse tumor types.

Methods: A sarcoma (FSa) and a carcinoma (MCa4) were grown in gastrocnemii of C3H mice. Registration of multiple images used embedded fiducial tubes in soft dental mold. T2 MRI determined often disconnected tumor surfaces. EPR pO_2 images used SLR rates from the pO_2 sensor $OX63d_{24}$ trityl infused IV via tail vein. A whole tumor dose sufficient to cure 15% of tumors was delivered with an XRAD225Cx isocentric animal CT/radiator. EPR pO_2, MRI, and CT images allowed selection of all hypoxic regions in the tumor, $pO_2 \leq 10$ torr. Plastic radiation blocks loaded with tungsten were made using 3D printers for opposing radiation boosts of 13 Gy randomizing to treat all hypoxia plus margin or well oxygenated tumor regions of equal volume. Tumors were followed sufficiently to determine clonogenic control. Significance of temporal control differences used Kaplan-Meier (K-M) analysis of the EPR pO_2 defined hypoxic or well oxygenated tumor regions.

Results: Significant doubling in local tumor control from hypoxic boosts relative well oxygenated tumor boosts was seen in both tumor types (FSa: p=0.04, MCa4: p=0.012). Surface to volume ratios of hypoxic regions lower than median in sarcomas was significantly better than higher SVR (p=0.003), but was not significantly different in carcinomas.

Conclusion: EPR provides the first significant pO_2 images based improvement in mammalian tumors with radiation. It argues effectiveness of dose painting in human cancer treatment. 3D characteristics demonstrate differences between tumor types.

I.08

"Oxygen Level in a Tissue" What do we really mean when we report this? – Part 3

H. M. Swartz[a,b], P. Vaupel[c], and A.B. Flood[a]

[a]*Geisel School of Medicine at Dartmouth, Dept. of Radiology*
[b]*Geisel School of Medicine at Dartmouth, Dept. of Medicine, USA*
[c]*Department. of Radiation Oncology, University Medical Center, Mainz, Germany*

Harold.Swartz@Dartmouth.edu

Abstract: The seemingly straightforward statement that the oxygen (O_2) level in a tissue is a particular value (e.g., "the O_2 level in this tumor was 4 mmHg") in fact does not provide very useful information in many situations because of the many variables that are implicitly involved in making such a measurement (e.g., what volume out of the total tissue volume is being sensed by the measurement technique; oxygen levels even in a given tissue vary over space and time and in the presence of pathology). In a continuation of the analysis discussed last year (1,2), here we consider the meaning of oxygen measurements in two specific pathologies, cancer and peripheral vascular disease, with a focus on what kinds of measurements may be especially useful clinically under particular conditions and for particular purposes.

Tumors: Cancer is the poster child for illustrating the limitations on meaning in reporting absolute values of oxygen, because of the well-known heterogeneity of oxygen levels within a tumor at any given time (spatial variation) and its variation over time (short term in response to adjacent microenvironment and long term in response to therapy or growth). The clinically most useful parameters that could be of high clinical value to formulate effective modifications of therapy and monitor their effectiveness are (a) changes in the oxygen levels (especially in response to interventions aimed at changing oxygen levels) and (b) indications of areas that have both viable cells and are highly hypoxic. Such information could be used to enhance therapy significantly. The desired information is not likely to be obtainable by reporting measurements of absolute oxygen level that ignore both spatial and time variations and the heterogeneity within the volume that is sensed by the technique.

Peripheral Vascular Diseases (PVD): The pathophysiological consequence of having PVD is the presence of low oxygen levels in skin, connective tissue and skeletal muscle in the limbs. The key to successful long-term treatment is to enhance those oxygen levels, so the O_2 parameter of most value clinically is changes related to interventions. There are two principal types of PVD: pathology in larger arteries and diabetic vascular disease involving the microcirculation. These quite different pathophysiological conditions therefore have different clinical needs for measurements of oxygen levels. For primary arterial disease (PAD) the impact is on relatively large regions and the clinical needs are especially to determine the point at which the circulation is critically compromised. For PVD due to diabetes mellitus there also is a clinical need to determine the overall status of the tissues at risk and, especially, the impact of therapeutic interventions aimed at modifying progression.

References:

1. Swartz HM, Vaupel P, Williams BB, Schaner PE, Gallez B, Schreiber W, Ali A, Flood AB. (2019) 'Oxygen level in a tissue' - What do available measurements really report? Adv Exp Med Biol *(In Press)*

2. Flood AB, Schaner PE, Vaupel P, Williams BB, Gallez B, Chen EY, Ali A, Liu T, Lawson VH, Schreiber W, Swartz HM. (2019) Clinical and statistical considerations when assessing oxygen levels in tumors: Illustrative results from clinical EPR oximetry studies. Adv Exp Med Biol *(In Press)*

I.09

Monitoring with near-infrared spectroscopy brain oxygenation and beyond

I. Tachtsidis[a]

[a] *Department of Medical Physics and Biomedical Engineering, University College London, UK*

Corresponding author e-mail address: i.tachtsidis@ucl.ac.uk

Abstract: Near-Infrared Spectroscopy (or NIRS) is an optical technique that uses near-infrared (NIR) light that can penetrate deep into the tissue. NIR light is transmitted to the head, non-invasively most often with the use of fibre optics. The collected, reflected NIR light from as deep as the cortex of the brain has been attenuated due to absorption of the oxygen dependent chromophore in the blood, the hemoglobin. NIRS most often measures the reflected NIR attenuation at a couple of wavelengths, to quantify the concentration of the oxygenated and deoxygenated hemoglobin ([HbO_2], [HHb]) and provide information about the brain oxygen levels. Of particular interest are the changes in brain oxygenation due to neuronal activity as they can provide us with an indirect measurement of brain function. This can be measured with functional NIRS or fNIRS. For several years now we have been developing technology that extend fNIRS instrumentation by allowing measuring hundreds of NIR wavelengths instead of just two. The technique is called broadband near-infrared spectroscopy (or bNIRS). The bNIRS system measures changes in light attenuation, reflected back from the head, over 308 near-infrared (NIR) wavelengths (610nm to 918nm). This allow us to quantify the changes in brain tissue [HbO_2], [HHb] and the concentration changes in the oxidation state of cerebral cytochrome-c-oxidase ([oxCCO]).

Our current state-of-the-art bNIRS instrument have the capacity to monitor in real time non-invasively brain oxygenation, hemodynamics and mitochondrial function. In my talk I will discuss how we have been using this technology both in our preclinical and clinical investigations in perinatal hypoxic-ischemia. In particular, I will introduce our clinical study in newborns with Hypoxic-Ischemic (HI) injury undergoing therapeutic hypothermia treatment. In 24 neonates, 54 episodes of spontaneous decreases in peripheral oxygen saturation (desaturations) were recorded between 6 and 81 h after birth. A total of 54 arterial desaturation events were recorded in 24 neonates (8 unfavorable and 16 favorable outcomes after HI, as determined by magnetic resonance spectroscopy derived lactate/N-acetyl-aspartate (MRS-measured Lac/NAA)). All desaturation events were recorded over postnatal days 1–4 during hypothermia: the first event was recorded 6 h after birth, and the last event was at 81 h. We observed differences in the cerebral metabolic responses to these episodes that were related to the predicted outcome of the injury, as determined by subsequent MRS-measured Lac/NAA. We demonstrated that a strong relationship between cerebral metabolism (broadband NIRS-measured cytochrome-c-oxidase (CCO)) and cerebral oxygenation was associated with unfavorable outcome; this is likely to be due to a lower cerebral metabolic rate and mitochondrial dysfunction in severe encephalopathy. In addition, uniquely we have obtained these results using a non-invasive bedside technique, broadband NIRS, in the first 4 days of life.

O.08-1

Assessment of cerebral blood oxygenation by NIRS during asphyxia cardiac arrest and resuscitation in rats

T. Yagi[a], K. Shinozaki[a], Y. Okuma[a], T. Yin[a], M. Nishikimi[a], T. Kiguchi[b], T. Iwami[b], L. B. Becker[a]

[a] *Feinstein Institute for Medical Research, Northwell Health System, Manhasset, NY, USA b Kyoto University Health Service, Kyoto, Japan*

Corresponding author e-mail address: tsuyagi-circ@umin.ac.jp

Abstract: Clinical investigators have focused on the real-time evaluation of cerebral blood oxygenation (CBO) by near-infrared spectroscopy (NIRS) during cardiopulmonary resuscitation (CPR). A previous study showed that an abrupt increase of Oxy-hemoglobin (Hb) concentration and tissue oxygenation index (TOI) was associated with the timing of return of spontaneous circulation (ROSC)[1)]. However, it is not clear how TOI decreases in cardiac arrest (CA) and increases by resuscitation. Therefore, this study aimed to assess CBO with asphyxia CA and its association with CPR to ROSC in rats. Male Sprague-Dawley rats were used. We attached NIRS (NIRO-200NX, Hamamatsu Photonics, Japan) from nasion to upper cervical spine in rats. 10-minute asphyxia was given to induce CA. After CA, mechanical ventilation was restarted, and manual CPR was performed. We examined the mean arterial pressure (MAP), end-tidal carbon dioxide (ETCO2), and Oxy/Deoxy-Hb and TOI. Out of 12 rats, 9 obtained sustained ROSC. After the induction of asphyxia, TOI rapidly dropped, and as subsequent CPR was undergoing, Oxy-Hb, Deoxy-Hb, and TOI increased in synchrony with chest compressions. And then, an abrupt increase in MAP, ETCO2, and TOI observed at the time of ROSC. Recent CPR guidelines suggest a use of ETCO2 during CPR since its abrupt increase is a reasonable indicator of ROSC. However, the guidelines recommended that ETCO2 should not be used in isolation and should not be used in nonintubated patients. NIRS represents easy-to-use technology for noninvasive and can be used in nonintubated patients. TOI can be an alternative of ETCO2, and in addition, it has the potential to serve as monitoring CBO during CPR and subsequently in post-ROSC care.

References; Yagi T, et al. Detection of ROSC in Patients with Cardiac Arrest During Chest Compression Using NIRS: A Pilot Study. Adv Exp Med Biol. 2016;876:151-7.

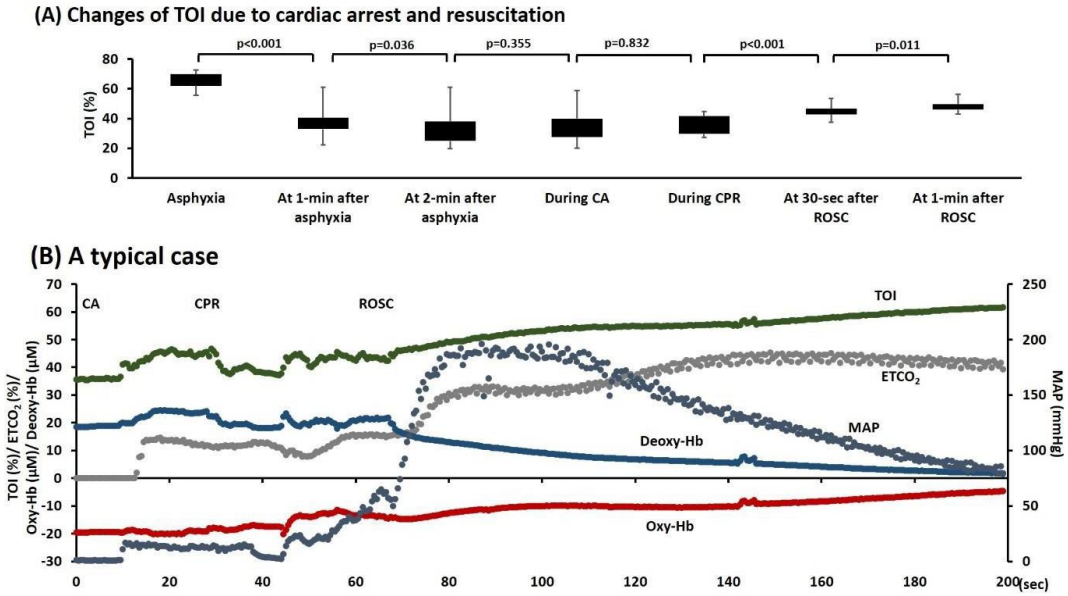

O.08-2

Effects of 3-day and 21-day hypoxic conditioning on recovery following cerebral ischemia in rats

T.R. Darlington, J. C. LaManna and K. Xu

Department of Physiology and Biophysics, Case Western Reserve University, Cleveland, Ohio, USA

Corresponding author e-mail address: kxx@case.edu

Abstract: We have previously reported that in a rat model of chronic hypoxia, HIF-1α and its target genes have significantly accumulated by three days of exposure whereas no significant increase in capillary density has occurred; there is a significant increase in capillary density at twenty-one days of chronic hypoxic exposure. In this study we hypothesize that by utilizing three days and twenty-one days of hypoxic preconditioning, we would distinguish between the relative neuroprotective contributions of the accumulation of HIF-1α and its target genes, and angiogenic adaptation in a rat middle cerebral artery occlusion (MCAO) model. Rats were randomly assigned to either hypoxic precondition groups (3-day and 21-day hypoxia) or normoxic control group. Hypoxic animals were kept in a hypobaric chamber at a constant pressure of 0.5 atmosphere (380 mmHg, equivalent to 10% normobaric oxygen at sea level) for either 3 or 21 days. Normoxic controls were housed in the same room next to the hypobaric chamber. Erythropoietin (EPO) was measured at 3 and 21 days of hypoxia using Western blotting analysis. Infarct volumes were measured following 24 hours of permanent MCAO. We found that EPO is upregulated at 3 days of hypoxia and returns to baseline by 21 days of hypoxia. The infarct volumes following were significantly reduced with 3-day hypoxic preconditioning when compared to normoxic controls (%, 31.8 ± 5, n = 9 vs. 50.1 ± 10.9, n = 7). No significant differences in infarct volume were seen between the normoxic controls and 21- day hypoxic preconditioned rats. We have shown that 3-day hypoxic preconditioning, but 21-day hypoxic preconditioning provides significant neuroprotection against focal ischemia in rats, support a larger role for the accumulations of HIF-1α and upregulation of its target genes in the neuroprotection against focal ischemia.

O.08-3

Triple-Stroke-Therapy to eliminate acute ischemic stroke as an unmet medical need

Carleton J.C. Hsia[a] and Sean I. Savitz[b]

[a] *AntiRadical Therapeutics LLC, Sioux Falls, South Dakota, USA*
[b] *Institute for Stroke and Cerebrovascular Disease, Houston, Texas, USA*

Corresponding author e-mail address: cjchsia@yahoo.com

Abstract: The golden age of stroke therapy has defined the accomplishments and limits of thrombolytic and thrombectomy for acute ischemic stroke (AIS) (1-3). However, a third pretreatment therapy is needed to further expand the therapeutic window of thrombolytic therapy within 3 hours and thrombectomy within 6-24 hours. We have developed this third stroke therapy using superoxide dismutase (SOD) mimetic as the pretreatment for thrombolysis and thrombectomy to create a triple-stroke-therapy (TST) for AIS.

The SOD-mimetic therapy has been shown to protect viable neuron and reduce lesion volume in hemorrhagic traumatic brain injury (4-5). The SOD-mimetic has been shown to protect the penumbra and reduce infarct volume in AIS (6). Therefore, SOD-mimetic treatment represents a paradigm change in stroke therapy. The SOD-mimetic is safe for use in the treatment of hemorrhagic stroke and AIS without time consuming neuroimaging. Our data provide confidence that it is feasible to initiate the SOD-mimetic treatment within 25 minutes of patient arrival to a stroke center and could even be given at a community hospital or in an ambulance before thrombolysis or thrombectomy.

The TST would greatly improve the efficacy and treatment of AIS patient population for shortening the ischemic time and provide better reperfusion. The SOD-mimetic drug is seeking fast track FDA NDA breakthrough therapy designation approval within 3-5 years as an orphan indication for treatable complete large-vessel-occlusion (CLVO) AIS patients, which is well below 100,000 patients in the US. The SOD-mimetic drug has patent protections until 2038 and beyond (7,8).

We are seeking venture capital and corporate partnerships to bring TST to stroke centers within 3-5 years with the ultimate goal of removing AIS from the list of unmet medical needs in the US and worldwide.

Acknowledgments: SOD-mimetic has been funded in part by SBIR grants from DoD (W81XWH-17-C-0223) and NINDS/NIH (U44 NS 070324) as well as South Dakota State Governor's Office of Economic Development to CJCH. CJCH is the sole proprietor of AntiRadical Therapeutics. SIS has no conflict of interest.

References:

1. Saver JL et. al. JAMA. 2016;316(12):1279-1289.
2. Savitz SI, et.al. Stroke. 2017 Dec;48(12):3413-3419
3. Fisher M. and Xiong Y., 2018 Stroke Vol:4 Issue:4 Pages 153-159
4. Shellington DK et.al. Crit Care Med. 2011 Mar; 39(3):494-505.
5. Koehler RC. et.al. Fed Exp Biol. 2019 Abstract number 6052
6. Cao S. et.al. 2017 J Am Heart Assoc. 2017;6:e006505. Doi: 10.1161/ JAHA.117.006505.
7. Jen Chang Hsia and Li Ma, 2010, US Patent No. 8273857 B2,
8. Jen Chang Hsia US App Number: US15/360,264; Filed: 2016-11-23 Pending; PCT filing# EP 168869267

O.08-4

Quantitative volumetric analysis and time scope tracking of cerebral microvascular networks imaged with *in vivo* two-photon microscopy

T. Sugashi[a], T. Niizawa[a], H. Suzuki[a], and K. Masamoto[a,b]

[a] *Department of Mechanical Engineering and Intelligent Systems Graduate School of Informatics and Engineering, Tokyo, Japan*
[b] *Center for Neuroscience and Biomedical Imaging, University of Electro- Communications, Tokyo, Japan*

sugashi@nvu.mi.uec.ac.jp, oshou.0131@gmai.com

Abstract: Dynamic changes in cerebral microvasculature have been actively studied *in vivo* in recent years, such as for adaptation to chronic hypoxia [1]. However it is still difficult to quantitatively estimate volumetric changes in enormous capillaries existing in association with neural and glial demand, and thus underlying mechanisms in balancing oxygen demand and supply remain unclear. In this study, we aimed to quantitatively determine and track transformational changes in cerebral microvascular networks during chronic hypoxia in the mouse cortex. The experiment was conducted with C57BL/6 mice in which the cortical microvessels were fluorescently labeled with sulforhodamine 101 and repeatedly imaged with two-photon microscopy. The image was captured over depths of 700 μm from the cortical surface with a step size of 2.5 to 5.0 μm and in-plane resolution of 0.45 μm/pixels. A phantom model mixed with fluorescent beads and latex beads was used to estimate point spread functions of the two-photon microscopy in the scattering tissue. The image captured was then reconstructed to 3D volume matrix on MatLab-R2018b software. The vascular region was automatically segmented along a central axis of the vessels and vessel diameter and length was measured in each segment. Each segment data were then manually checked and tracked over different days of the measurements based on developed graphical user interface. As a definition of the capillary, vessel diameter less than 8 μm at the first imaging date was selected. We observed that a median value of 5.8 μm (n=1,914 segments) of the capillaries at the first day (just before hypoxia induction) became 8.5 μm (n=942 segments) during 3-week hypoxia adaptation. And deeper tissue showed higher changes in diameters (average 1.44 times at the surface n=96 vs. average 1.57 times at 200 μm n=67, $p < 0.05$), which indicate layer dependences of the hypoxia adaptation. These preliminary results showed that the proposed methods may allow for large-scale simulation of tissue oxygen balances in the realistic microvascular networks of the brains.

Reference: [1] K. Yoshihara et al., Adv Exp Med Biol 765, 357-363, 2013.

Acknowledgements: This study was partly supported by JSPS KAKENHI (JP201710551 to TS and 19K07795 to KM).

O.09-1

Altered behavioral performance in the neuron-specific HIF-1 and HIF-2 deficient mice following chronic hypoxic exposure

Lei Ma[a], J. Sebastian Garcia-Medina[b], Geisa Ortet[b], J. C. LaManna[b] and K. Xu[b]

[a] *School of Electronic Information Science and Technology, Nantong University, Nantong 226007, Jiangsu Province, China*
[b] *Department of Physiology and Biophysics, Case Western Reserve University, Cleveland, Ohio, USA*

Corresponding author e-mail address: kxx@case.edu

Abstract: Hypoxia-inducible factors (HIFs) are transcriptional regulators that mediate mice for HIF-1 and HIF-2. The objective of this study was to investigate the effect of neuronal deletion of HIF-1 and HIF-2 on hypoxic adaptation by using the neuron-specific knockout (KO) mice. Wild-type (WT) and KO mice were used. Hypoxic mice were kept in a hypobaric chamber at a pressure of 300 torr (0.4 ATM, which was equivalent to 8% oxygen sea level) for 3 weeks. The littermate, normoxic control mice were housed in the same room next to the chamber to match ambient conditions. Body weights were monitored throughout the 3-week course. Cognitive function was measured using a Y-maze test; motor functions were measured using the Rotarod test and the grip strength test. The hematocrit increased significantly at the end of 3-week hypoxic exposure in both WT and KO mice. In Y-maze test, the alternation rate (indicative of sustained cognition) trended lower in the KO mice compared to the WT controls following hypoxia (%, 45.1± 17.9, n = 6 vs. 53.8 ± 11.5, n = 8). In the Rotarod test, the latency (seconds) in the KO mice were significantly lower compared to the WT controls (50.4 ± 5.0 vs. 77.1 ± 5.7, n = 6 each before hypoxia and 66.4 ± 3.4, n = 6 vs. 107.4 ± 15.4 after hypoxia, respectively). The grip strength in the KO mice were similar compared to the WT controls before hypoxia, but the strength of KO mice was significantly higher compared to the WT controls after hypoxic exposure. Our data suggested that deficiency of neuronal HIF-1 and HIF-2 may results in changes in behavioral performance and other adaptative responses to hypoxia.

O.09-2

Online noninvasive assessment of human brain death by near-infrared spectroscopy with protocol at varied fraction of inspired O_2

Ting Li[a,], Jiangbo Pu[a], Chenyang Gao[a], Xiping Yang[b] and Mingliang Zhao[b]

[a]*Institute of Biomedical Engineering, Chinese Academy of Medical Sciences & Peking Union Medical College, Tianjin 300192, P. R. China*

[b]*Department of Neurosurgery, Characteristic medical center of the Chinese People's Armed Police Force and Pingjin Hospital, Tianjin 300162, P. R. China*

Correspondence: liting@bme.cams.cn

Abstract: Brain death is an irreversible loss of all brain functions and the assessment is crucial for organ supply for transplantation. The noninvasive, sensitive, universally available, and timely ancillary method to assess brain death has not been established. Here we attempted to explore a noninvasive and straightforward way in brain death online assessment. Eighteen brain-dead patients and twenty healthy subjects were measured by functional near- infrared spectroscopy (fNIRS), with a multiple-phase protocol at varied fraction of inspired O2 (FIO2). the dysfunction or even the lack of function in blood oxygen metabolism responding to inspired O2 in brain death population was clearly observed in monitored cerebral hemodynamics, with comparison to the control group. We found that the concentration changes ratios of oxy-hemoglobin to deoxy-hemoglobin (Δ[HbO2]/Δ[Hb]) in the cerebral cortex of brain-dead patients were significantly higher than those of healthy subjects. And the Δ[HbO2]/Δ[Hb] in low-to-high FIO2 phase was most sensitive to distinguish brain- dead patients from healthy subjects, with a recommended threshold ranged in 1.40~1.50. The innovative incorporation of NIRS and a varied FIO2 protocol was shown to a be noninvasive, and reliable way in assessing brain death. This successful attempt of NIRS application is help for fast and accurate evaluation of brain death, promptly offering quality-assured donor organs, and indicate us a protocol aided way to expand the use of NIRS.

O.09-3

Microvascular shunts in the pathogenesis of cerebral ischemia of cerebral small vessel disease to leukoaraiosis, MS, SLE, MCI, VaD, AD White Matter Hyperintensities

E. Nemoto[a], D. Bragin[a], and M. Kameneva[b]

[a] *Department of Neurosurgery, University of New Mexico, Albuquerque, NM 87131*
[b]*McGowan Institute for Regenerative Medicine, University of Pittsburgh, Pittsburgh,* PA 15219

Enemoto@salud.unm.edu

Abstract: We first demonstrated cerebral microvascular shunts (MVS) at high intracranial pressure (ICP)[1,2] reflecting non-nutritive shunt-flow, resulting in a loss of cerebral blood flow (CBF) autoregulation, tissue ischemia, hypoxia, edema, and metabolic depression by shunting non-nutritive blood flow around injured tissue and releasing neither nutrients or oxygen to tissue. The origin of these MVS may vary in different disease states such as MS, SLE, MCI, VaD and AD but the underlying pathogenesis is the same; cerebral ischemia and MVS flow in white matter hyperintensities (WMH). Normal white matter flow is 1/3 that of gray matter flow and as in arterial watershed zones, suffers ischemia when CBF falls. In an NIH funded study evaluating hemodynamic compromise to predict a second stroke in patients with unilateral carotid occlusion, we made the incidental observation that WMH were all at different degrees of ischemic stress as characterized by the cerebrovascular reserve (CVR), Oxygen extraction fraction (OEF) and OEF response (OEFR) to an acetazolamide cerebrovascular challenge (Fig) [3]. The degree of WMH ischemic stress rather than volume of WMH may better correlate with psychological and motor symptomatology. The commonality of cerebral ischemia in all of these cerebrovascular diseases may be treated by drag reducing polymers (DRP) such as high molecular weight (HMW) 4500kDa polyethylene oxide to reverse or reduce the severity of cerebral ischemia by increasing shear rate in microvessels. HMW DRP has proven effective in animal models of stroke [4] and traumatic brain injury [5] acting by hemmorheologic reduction of turbulent and promotion of laminar flow increasing vascular wall shear stress and through the glycocalyx restores capillary endothelial integrity and nitric oxide production|. The effectiveness of HMW DRP has been shown in ischemic myocardium and in hemorrhagic shock. The effectiveness of DRP in clinical cerebral ischemia has yet to be shown.

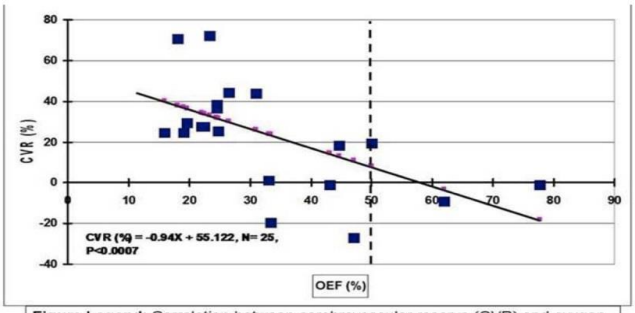

Figure Legend: Correlation between cerebrovascular reserve (CVR) and oxygen extraction fraction (OEF) in white matter hyperintensities reflecting decreasing CVR with increasing ischemic stress.

References

1. Bragin DE, Bush RC, Müller W, et al. J Neurotrauma. 2011 May;28(5):775-85.
2. Nemoto EM, Bragin D, Stippler M, et al. Acta Neurochir Suppl. 2013;118:205-9.
3. Nemoto EM, Presented at the 13th International Conference on Quantification of Brain Function with PET, 1-4. Apr.2017, Berlin, Germany.
4. Bragin DE, Peng Z, Bragina O, et al. Adv Exp Med Biol. 2016;923:239-244.
5. Bragin DE, Kameneva MV, Bragina OA, et al. J Cereb Blood Flow Metab. 2017 Mar;37(3):762- 775.

O.09-4

Effects of normobaric and hyperbaric hyperoxia on cerebral blood flow and oxygenation in traumatic brain injury

D.N. Atochin[a], N.A. Gavrisheva[b] and I.T. Demchenko[c]

aCardiovascular Research Center, Massachusetts General Hospital, Harvard Medical School, Charlestown, USA, bPavlov Medical University, Saint Petersburg, Russia, cInstitute of Evolutionary Physiology and Biochemistry Russian Academy of Sciences, Saint Petersburg, Russia

Corresponding author e-mail address: atochin@cvrc.mgh.harvard.edu

Abstract: Under physiological conditions, hyperoxia increases oxygen tension in the brain tissue but reduces cerebral blood flow by O2-induced vasoconstriction. We report the first quantitative evaluation of these opposing effects of normobaric and hyperbaric hyperoxia on cerebral oxygenation of injured brain (modified Marmarou's traumatic brain model). We assessed the contribution of inspired O2 (PiO2) and regional cerebral blood flow (rCBF) to brain PO2 in intact and injured rats breathing 100% oxygen at 1-3 atmospheres absolute (ATA). Brain PO2 and rCBF were measured in the cortex, hippocampus and striatum using collocated nafion coated platinum electrodes. Cerebral blood flow was computed from H2 clearance curves and PO2 from electrodes calibrated before and after insertion. Arterial PCO2 was controlled, and body temperature, blood pressure and ECG were monitored. Basal rCBF values in intact rats were 0.68-0.97 ml/g/min and brain PO2 17-37 mmHg. Scatter plots of rCBF versus PO2 were nonlinear ($R^2<0.75$) for intact rats breathing room air or O2 at 1 ATA but nearly linear ($R^2=0.88–0.95$) for 2 and 3 ATA. In rats with closed traumatic head, rCBF and PO2 decreased by 56-87% and 47-79% respectively. Vascular responses to oxygen at 1- 3 ATA were impaired. When rCBF was <0.22 ml/g/min, only breathing O2 at 3 ATA increased significantly brain PO2. In contrast, oxygenation of injured brain increased at 1-3 ATA when basal rCBF was > 24 ml/g/min. Oxygenation of injured brain is equally affected by inspired oxygen pressure and rCBF. Results also point out that patterns of tissue PO2 response are greatly affected by local alterations in CBF at PiO2 > 1 ATA, and that brain PO2 directly tracks CBF when hemoglobin is fully saturated. If brain PO2 needs to be raised to the appropriate level, this will be best achieved by combining hyperbaric oxygen with agents that increase cerebral blood flow.

O.09-5

Environmental enrichment improved cognitive performance in mice under normoxia and hypoxia

Sahej Bindra[a], J. C. LaManna[b] and **K. Xu[b]**

[a] *Hathaway Brown High School, Shaker Heights, Ohio, USA*

[b] *Department of Physiology and Biophysics, Case Western Reserve University, Cleveland, Ohio, USA*

Corresponding author e-mail address: (kxx@case.edu)

Abstract: The mammalian brain modulates its microvascular network to accommodate tissue energy demand in a process referred to as angioplasticity. There is an aging effect on cognitive function and adaptive responses to hypoxia. Hypoxia-induced angiogenesis is delayed in the aging mouse brain. Additionally, it has been shown that enrichment provides an environment that fosters increased physical activity and sensory stimulation for mice as compared to standard housing; this stimulation increases neuronal activity and consequently brain oxygen demand. In this study, we investigated the effect of environmental enrichment on cognitive performance in young mice (2-4 months old; n=18). We also investigated the effect of hypoxia in both young (2-4 months old; n=6) and aged mice (17-21 months old; n=5). Mice were placed in a non-enriched or an enriched environment for 4 weeks under normoxia followed by 3 weeks of hypobaric hypoxia (~0.4 atm, equivalent to 8% normobaric oxygen at sea level). Cognitive function was evaluated using Y-maze and novel object recognition tests in the enriched or non-enriched mice under normoxic or hypoxic conditions. The young mice showed a significantly higher alternation rate (%, 63 ± 7 vs. 48 ± 10, n = 8 and 10, respectively) in the Y-Maze test as compared to the old mice. Under normoxia, the enriched mice sahowed an improved alternation rate (%, 63 ± 10, n = 10) in Y-Maze test and a higher novel object exploration rate (%, 68 ± 10 vs. 52 ± 10) in the novel object recognition test compared to the non-enriched controls. Similar results were observed following hypoxic exposure: the enriched mice exhibited higher alternation rates and novel exploration rates as opposed to the non-enriched controls. Our data suggests that environmental enrichment improved the cognitive performance in the young and aged mice under normoxic and hypoxic conditions.

I.10

The whole picture: Why a holistic view of brain and body is desirable in fNIRS

U. Wolf[a] and F. Scholkmann[a,b]

[a] *University of Bern, Institute of Complementary and Integrative Medicine, 3010 Bern, Switzerland*
[b] *Biomedical Optics Research Laboratory, Department of Neonatology, University Hospital Zurich, University of Zurich, 8091 Zurich, Switzerland*

Corresponding author e-mail address: Ursula.Wolf@ikim.unibe.ch

Abstract: Systemic physiology augmented functional near-infrared spectroscopy (SPA-fNIRS) is a novel method combining state of the art optical neuroimaging using functional near- infrared spectroscopy (fNIRS) with the measurement of systemic physiological activity [1]. The method gives a more complete picture of the brain and body activity during resting-state or during task/stimulus-evoked experimental paradigms. Through our research we demonstrated that the full potential of fNIRS is realized when systemic physiological activity (e.g. blood pressure, heart rate, respiration rate, skin conductance, end-tidal CO_2 concentration) is measured simultaneously by employing SPA-fNIRS. The rationale for SPA-fNIRS is two-fold: (i) SPA-fNIRS enables to adequately interpret and more deeply understand the fNIRS signals measured at the head since they contain components originating from neurovascular coupling as well as from other (systemic) sources. (ii) SPA-fNIRS enables to study the embodied brain by linking brain with the physiological state of the entire body. This creates novel insights into the complex interplay between the brain and the body – a topic also of high importance for future human neuroscience.

References

[1] Scholkmann, F., Hafner, T., Metz, A.J., Wolf, M. & Wolf, U. (2017). Effect of short-term colored-light exposure on cerebral hemodynamics and oxygenation, and systemic physiological activity. Neurophotonics, 4 (4), 045005

O.10-1

The effect of not removing the glossy white cover on adhesive INVOS neonatal sensors on measured values in the blood-lipid phantom

M. L. Hansen[a,#], D. Ostojic[b,#], S. Kleiser[b], G. Greisen[a] and M. Wolf[b]

[a] *Department of Neonatology, Rigshospitalet, University of Copenhagen, Denmark*
[b] *Biomedical Optics Research Laboratory (BORL), Department of Neonatology, University Hospital Zurich, University of Zurich, Switzerland*
[#] *joint first authorship*

Corresponding author e-mail address: mathias.safeboosc@gmail.com

Abstract: The randomised clinical trial, SafeBoosC III, evaluates the effect of treatment guided by cerebral tissue oximetry monitoring in extremely preterm infants. Treatment should be considered, when cerebral tissue oxygenation drops below a predefined hypoxic threshold, which differs between sensors. To generate results of generic value, all commercially available cerebral tissue oximeters approved for clinical use in newborn infants may be used in the trial. Most companies produce sensors with an adhesive surface on the patient-contacting side, to make attachment to the skin easier. However, since the skin of preterm infants is particularly fragile, some neonatologists keep the cover on the adhesive sensors, to avoid the risk of skin injury when removing the sensor. Spatially resolved spectroscopy depends on the assumption of a semi-infinite medium, i.e. loss of photons reaching the surface of the tissue. This assumption may be compromised by a reflecting sensor surface between the light source and detectors. To evaluate the effect of not removing the cover, on an adhesive sensor when measuring cerebral tissue oxygenation, we performed multiple deoxygenations in a liquid phantom and compared an INVOS neonatal sensor (Medtronics), with and one without the cover, to a reference oximeter (OxiplexTS, ISS). Relationship between the INVOS neonatal sensor and OxiplexTS was linear ($R^2 = 0.999$) in both cases (with and without cover). Sensitivity to oxygenation changes only differed slightly for the INVOS neonatal sensor, dependent on whether the cover was kept on the sensor (a= 1.133 and b=7.067) or not (a=1.103 and b=11.992) (figure 1). Furthermore, the hypoxic SafeBoosC III threshold differed as well (60.3% with cover and 63.83% without cover). Based on these findings, we suggest that it is feasible to keep on the cover, on the INVOS neonatal sensor. However, clinicians must be aware that the hypoxic threshold will differ.

Figure 1 – NIRS neonatal sensor with and without cover on patient-contacting surface versus Oxiplex ISS as a reference.

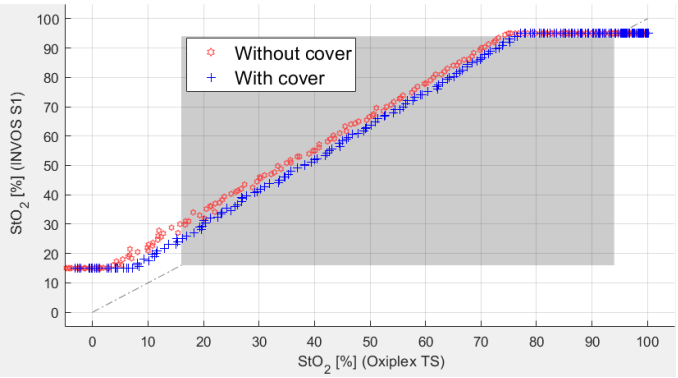

O.10-2

Influence of melanin-like absorption on near-infrared spectroscopy (NIRS) oximetry

Helene Isler[a,*], Daniel Ostojic[a], Felix Scholkmann[a], Tanja Karen[a], Martin Wolf[a], and Stefan Kleiser[a]

[a] *Biomedical Optics Research Laboratory (BORL), Neonatology Department, University Hospital Zurich, University of Zurich, Zurich, Switzerland*

Corresponding author e-mail address: martin.wolf@usz.ch

Abstract: Since Jöbsis demonstrated the possibility to monitor cerebral oxygenation with near infrared spectroscopy (NIRS) in 1977, many NIRS devices have been built and approved for clinical tissue oxygen saturation (StO_2) measurement. NIRS devices consider mainly the absorption spectra of hemoglobin, which is the most prominent absorber in the near-infrared range in tissue. Other absorbers may be present and some devices correct for it (e.g. water). However, the strong absorber melanin is often not accounted for since it is expected to have little influence if evenly distributed below the sensor. The aim was to investigate what happens if the melanin is distributed unevenly below the sensor, e.g. in form of birthmarks or hair. To this end, we investigated the effect of an asymmetrical placement of a melanin-mimicking foil on the calculation of StO_2. Three continuous wave oximeters (FORE-SIGHT ELITE, NIRO- 200NX and INVOS 5100C) with their infant sensors were placed on a liquid optical phantom mimicking the optical properties of a neonate's head. A frequency domain device (OxiplexTS) provided the reference StO_2 while the oxygenation inside the phantom was changed. We performed four runs: During run 1 and 4, no foil was applied. In run 2 and 3 the foil mimicking melanin covered the inner, respectively outer detector. As shown in Fig. 1, asymmetric light absorption by melanin mimicking foils caused substantially different StO_2 readings. Consequently, we advise to avoid intrusion of hair or the presence of birthmarks underneath the NIRS sensor to assess StO_2.

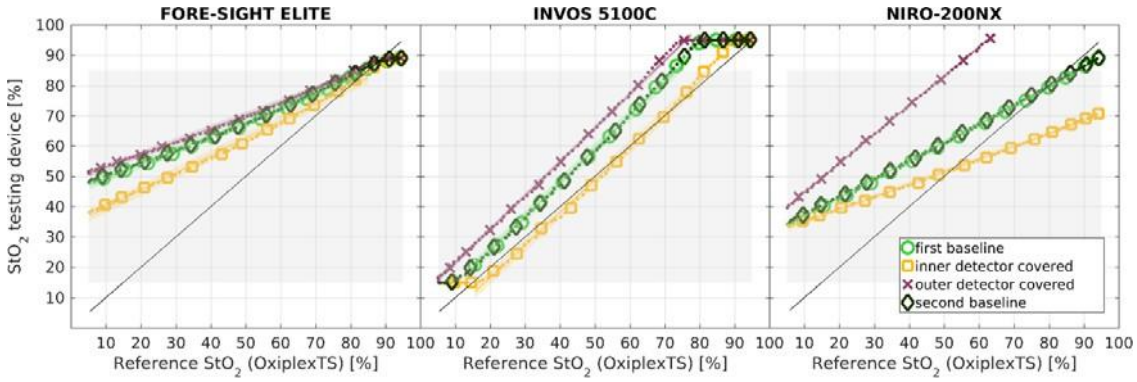

Figure 1. Scatter plots from all measurements performed within the melanin experiment. The two baseline measurements without foil at the beginning and end of the experiment show excellent agreement and the high reproducibility of the phantom. A foil mimicking melanin below the inner or outer detector influenced the StO_2 values substantially.

O.11-1

In-phantom validation of time-resolved near-infrared optical tomograph pioneer for imaging brain hypoxia and hemorrhage

A. Kalyanov[a], J. Jiang[a], S. Lindner[ab], A. Di Costanzo Mata[a], C. Zhang[c], E. Charbon[bc], M. Wolf[a]

[a]*Biomedical Optics Research Laboratory (BORL), Dept. of Neonatology, University of Zurich*
[b]*Advanced Quantum Architecture (AQUA) laboratory, School of Engineering, EPFL Lausanne*
[c]*Applied Quantum Architectures, Delft University of Technology, Delft, Netherlands.*

Corresponding author e-mail alexander.kalyanov@usz.ch

Abstract: The neonatal brain is a vulnerable organ and lesions due to hemorrhage and/or ischemia occur frequently in preterm neonates. Happening early in life, they often lead to long- term disabilities. Despite improved survival rate (~80%), up to 25% of extremely preterms develop cerebral palsy or a low IQ, and a significant cognitive delay is present in ~12% by school age[1, 2]. Even though neuroprotective therapies are existing, there is no tool available to detect ischemia or hypoxia. To address this problem, we have recently designed and built the new time-resolved near-infrared optical tomography (TR NIROT) system – Pioneer[3]. It aims at imaging the brain of preterm neonates with a high spatial resolution and at detecting hypoxia and bleeding (Fig. 1a).
Pioneer is based on a time-of-flight camera with 1024 of pixels. Each pixels comprises a single-photon avalanche diode (SPAD) with 116ps time resolution and an unprecedented sensitivity of 12% at 800nm wavelength. This camera chip was specifically designed for NIROT by BORL and AQUA[4]. Together with a super continuum laser as a light source, the system enables multispectral tomography of tissue with high spatial resolution. Thus, detection of multiple chromophores, such as oxy- and deoxyhemoglobin, fat, water, etc. is possible.
Here we present the results of a phantom study of the system performance. We used two silicone phantoms to mimic risky situations for brain lesions: hemorrhage and hypoxia, which are characterized by different optical properties and location. Employing Pioneer, we were able to reconstruct both position and properties of these inhomogeneities correctly (fig. 1b.). Therefore, we conclude that Pioneer is an effective tool for imaging the neonatal brain and detecting events such as hemorrhage and hypoxia. If these situations are detected early, brain lesions can be treated early or even prevented and we hope this will reduce the incidence of long-term disability.

a)

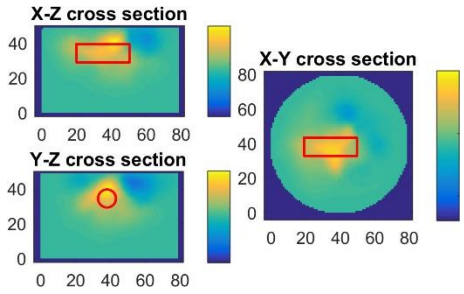

b)

Fig. 1. a) Pioneer sensor on a dummy baby head inside a NICU cot; b) reconstruction of cylinder inclusion inside a silicone phantom, with red contour marking its correct location.

1. Fischer, N., et al., Arch Dis Child Fetal Neonatal Ed, 2009. **94**(6): p. F407-13.
2. Hutchinson, E.A., et al., Pediatrics, 2013. **131**(4): p. e1053-61.
3. Kalyanov, A., et al. in *Optical Tomography and Spectroscopy*. 2018. Optical Society of America.
4. Lindner, S., et al. in *Int. Image Sensor Workshop*. 2017.

O.11-2

Phantom-based testing for evaluation of confounding factors in NIRS tissue oximetry

A. Afshari[a], P. Ghassemi[a], M. Halprin[a], J. Lin[a], **J Wang[a]*** , G. Mendoza[a], S. Weininger[a], and J. Pfefer[a]

[a] *Center for Devices and Radiological Health, U.S. Food and Drug Administration, 10903 New Hampshire Avenue, Silver Spring, Maryland USA 20993*

**Corresponding author email address: Jianting.wang@fda.hhs.gov*

Abstract: Clinical cerebral oximetry based on near-infrared spectroscopy has emerged as an increasingly popular technology for non-invasive monitoring of patients during cardiac surgery. However, it also remains controversial due to inconsistent clinical results reported in the literature. This may be due, in part, to inherent shortcomings of the human subject validation studies, including the lack of a gold standard reference, variance in human tissue properties, and ethical restrictions on oxygen saturation ranges, especially in pediatric and neonatal subjects. Tissue-simulating phantoms do not have these limitations and thus may provide complementary information on device performance and enable well-controlled testing for patient-specific confounding factors such as superficial tissue layer thickness and epidermal melanin content. We focus on development of a novel, solid, modular phantom approach based on a 3D-printed cerebrovascular module (CVM) and silicone-based superficial layers. The phantom was developed and rigorously characterized to mimic the optical properties and layered structure of the neonatal/pediatric head. Our CVM prototype includes 148 linear channels of 0.75 mm diameter each. Superficial layers were designed to represent scalp/skull and cerebrospinal fluid regions. A novel epidermis-simulating material was developed and used to mold 0.1-mm-thick layers simulating low, medium and high-melanin-content skin. The final measurement procedure involved injecting bovine blood samples at well-validated saturation levels into the CVM and performing measurements with neonatal and pediatric probes from two commercial cerebral oximeters. Results from Oximeter #1 showed a high degree of precision, whereas accuracy degraded with thicker extracerebral tissue layers and changes in pigmentation, especially for low saturation samples. Results from Oximeter #2 showed poor precision, yet greater robustness to variations in extracerebral layers and skin pigmentation. Overall, good consistency of our results with prior clinical and phantom studies was found, indicating the promise of a modular channel-array phantom approach for evaluating cerebral oximeters.

O.11-3

Time-resolved NIROT 'Pioneer' system for imaging the oxygenation of the preterm brain: 'Pioneer' probe design optimization

A. Di Costanzo-Mata[a], J. Jiang[a], S. Lindner[a, b], E. Charbon[b, c], M. Wolf[a] and A. Kalyanov[a]

[a] *Biomedical Optics Research Laboratory, Dept. of Neonatology, Univ. of Zurich, Switzerland.*
[b] *Advanced Quantum Architecture Laboratory, School of Engineering, EPFL, Switzerland.*
[c] *Applied Quantum Architectures, Delft University of Technology, Delft, Netherlands.*

Corresponding author e-mail address: aldo.dicostanzomata@usz.ch

Abstract: In preterm infants there is a risk of life-lasting impairments due to hemorrhagic/ischemic lesions. Our time-resolved (TR) near-infrared optical tomography (NIROT) system 'Pioneer' will detect both disorders with high spatial resolution. Successfully tested on phantoms, 'Pioneer' entered the phase of improvements and enhancements. The current probe (A-probe) was adapted from an opto-acoustics instrument. A new probe (B- probe) optimized for TR measurements is required. Our **aim** is to determine the optimal arrangement of light sources in the B-probe in order to increase the sensitivity and the resolution of Pioneer, and to improve the ability of the system to detect both ischemia and hemorrhage.

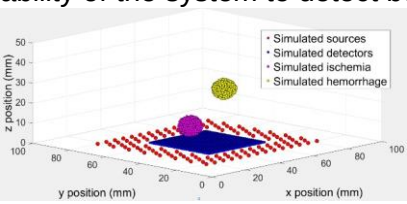

Fig.1. Simulated phantom exemplification

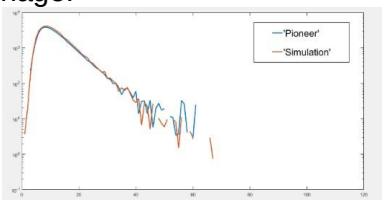

Fig.2. 'Pioneer' and 'NIRFAST' signals

a)

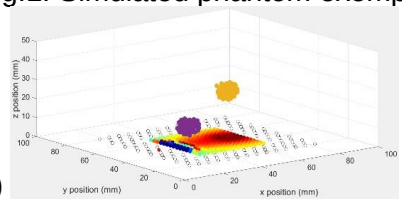

b)

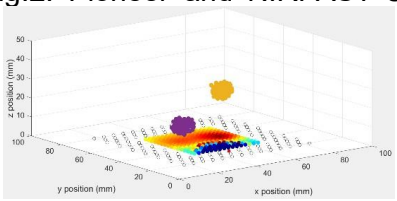

Fig.3. Late-photons contrast signal on the FOV for a TR simulation of two inclusions at 10*mm* and 25*mm* depth resembling Fig.1 phantom. a) Source at the inclusions axis. b) Source at the axis in-between the inclusions.

Method: We simulated TR-NIROT signals in NIRFAST. We used 32x32 detector array, with ~1.1*mm* distance between the detectors. Light sources were arranged around the field-of-view (FoV). We performed forward simulations of light propagation though 'homogeneous-tissue' (HT) (μ_s = 8.0 cm^{-1} , μ_a = 0.05 cm^{-1}) and compare it with a 'Pioneer' real-phantom measurement as a validation step. Next, we simulated light propagation through 'inhomogeneous-tissue' (IT) by adding ischemia (μ_a = 0.125 cm^{-1}) or hemorrhage (μ_a = 2.5 cm^{-1}) to HT as a spherical inclusion of 5*mm* radius at different locations (Fig.1) and identified the source location that provides the highest contrast on the FoV: max(sum(|$I_{HT} - I_{IT}$|)). The A-probe, with 11 sources ~23*mm* away from the FoV center, was simulated and endorsed with a real-phantom measured with 'Pioneer' (Fig.2).

Results: Sources located closer to the FoV generate greater contrast for late photons (Fig.3).

Conclusion: This study suggests the B-probe sources to be closer to the FoV. The higher signal-to-noise ratio is expected to lead to a higher image quality.

O.11-4

Treatment options for high-risk hyperperfusion patients after carotid artery stenting

Y Okuma[a,b], N. Hirotsune[b], Y. Kegoya[b], Y. Sotome[b], Y. Matsuda[b], Y. Sato[b], T. Tanabe[b], K. Muraoka[b], Shigeki Nishino[b]

[a] Department of Emergency Med-Cardiopulmonary, Feinstein Institute for Medical Research, Northwell Health System, Manhasset, NY, USA
[b] Department of Neurological Surgery, Hiroshima City Hiroshima Citizens Hospital, Hiroshima, Japan.

Corresponding author e-mail address: y8u2bear4@hotmail.com

Abstract: We recognized cerebral hyperperfusion syndrome (CHS) as rare but fatal perioperative complications after surgical correction of the carotid stenosis. Generally, in carotid artery stenting (CAS), preoperative edaravone administration, intraoperative general anesthesia, nerve monitoring, staged angioplasty (SAP), postoperative sedation helped us most part. But a certain proportion of CHS still exists after CAS. Recently, we actively introduced the outlet gate technique (OGT) in high-risk patients, deflating the embolic balloon protection step by step based on the value of Near-infrared spectroscopy (NIRS). Between June 2017 and May 2018, consecutive 44 patients with high-grade carotid stenosis underwent CAS or SAP. For 5 cases of them, mechanical thrombectomy was also carried out continuously, hence were excluded. Next, we investigated the ipsilateral/contralateral ratio of NIRS values in the OGT group at the point of 1: Pre, 2: embolic protection device (EPD) on, 3: EPD off, 4: OGT, 5: Post. 20 OGT group lesions (average age 77.3 years old) and 19 conventional group lesions (average age 76.7 years old) were evaluated. Including high-risk cases increased edaravone administration and general anesthesia significantly in the OGT. It was also true that the stepwise releasing prolonged the operative time significantly in the OGT. Even though the patient's state of OGT group, we have observed no increasing complications yet. Concerning the ipsilateral/contralateral ratio, except between 4 and 5, there were significant differences between almost every point. The ipsilateral/contralateral ratio showed that intracranial perfusion seemed so unstable during CAS and OGT could lead the perfusion stable soon. The OGT which stepwise reperfusion with reference to the NIRS had a potential of a new option to prevent immediate CHS, being relatively safe and applicable.

I.11

The interstitium and lymphatics - role in fluid volume and blood pressure regulation

H. Wiig

Department of Biomedicine, University of Bergen, Norway

Corresponding author e-mail address: helge.wiig@uib.no

Abstract: The interstitium describes the fluid, proteins, solutes, and the extracellular matrix (ECM) that comprise the cellular microenvironment in tissues. Its alterations are fundamental to changes in cell function in inflammation, pathogenesis, and cancer. Interstitial fluid (IF) is created by transcapillary filtration and cleared by lymphatic vessels. In the lecture I will discuss analysis methods to access IF, which enables quantification of the cellular microenvironment; such methods have demonstrated, for example, that there can be dramatic gradients from tissue to plasma during inflammation. I will also discuss new data indicating that the interstitium plays a role in salt and water metabolism, and that tissue-specific regulatory mechanisms are operative regulating the release and storage of Na^+ from a kidney- independent reservoir. Moreover, immune cells from the mononuclear phagocyte system not only function as local on-site sensors of interstitial electrolyte concentration, but also, together with lymphatics, act as systemic regulators of body fluid volume and blood pressure. These recent studies have established the interstitium-/extracellular matrix of the skin, its inherent interstitial fluid and the lymphatic vasculature forming a vessel network in the interstitium as new targets in blood pressure control. Aspects of the interstitium in relation to Na^+ balance and hypertension will be discussed. I will try to integrate the biophysical and biological aspects of the interstitium, and the transport of interstitial and lymph fluid in tissue physiology and pathophysiology.

Acknowledgements. Financial support from the Research Council of Norway (project number 222278 and 262079) is gratefully acknowledged.

O.12-1

Effect of prolonged pressure on sacral tissues hemodynamics assessed by diffuse optical imaging: A pilot study

B. Day[a] and L. Pollonini[a,b]

[a] *Department of Engineering Technology, University of Houston, USA*
[b] *Department of Electrical and Computer Engineering, University of Houston, USA*

Corresponding author e-mail address: lpollonini@uh.edu

Abstract: Pressure ulcers (PUs) are wounds resulting from prolonged pressure on the skin and underlying tissues over bony prominences (e.g., lower back, heels, shoulders) in bed-bound patients and wheelchair users. Clinical standard of care requires visual skin inspection and repositioning every two hours as minimizing pressure is considered the most effective preventative method, yet such strategies are often applied inadequately and do not effectively prevent PUs from becoming penetrating wounds.

Recent studies attribute PU development to cell deformation, inflammation and ischemic damage, which cumulatively propagate from the micro-scale (death of few cells) to the macro-scale (tissue necrosis) within hours. Although the nature of the PU pathogenesis is complex and multi-factorial, measuring tissue alterations in real-time may elucidate the origination mechanism and ultimately allow detecting PUs at their earliest stage.

In this pilot study, we evaluated the ability of diffuse optical imaging (DOI) to assess hemodynamic changes resulting from prolonged pressure on the sacral tissues in five healthy volunteers laying immobile in a supine position for two hours. A thin, body-conforming optical imaging probe encompassing 256 optodes arranged in a regularly spaced grid over a 16x16 cm area was used to construct volumetric images representing changes of oxyhemoglobin (□HbO) and deoxyhemoglobin (□HbR) concentration from a zeroed baseline. After two hours of body-weight pressure, all hemodynamic images were significantly different from baseline. We also found that hemodynamic patterns across subjects exhibited common spatial features (structural similarity index for □HbO: 0.6 ± 0.10, □HbR: 0.48 ± 0.11), whereas hemoglobin species within the same subject were significantly less similar (□HbO vs. □HbR: 0.36 ± 0.26, p = 0.037, Figure 1). These preliminary results indicate that prolonged pressure causes distinctive hemodynamic patterns that can be effectively investigated with DOI, and that monitoring functional changes frequently over time holds potential for clarifying the development mechanisms of PUs.

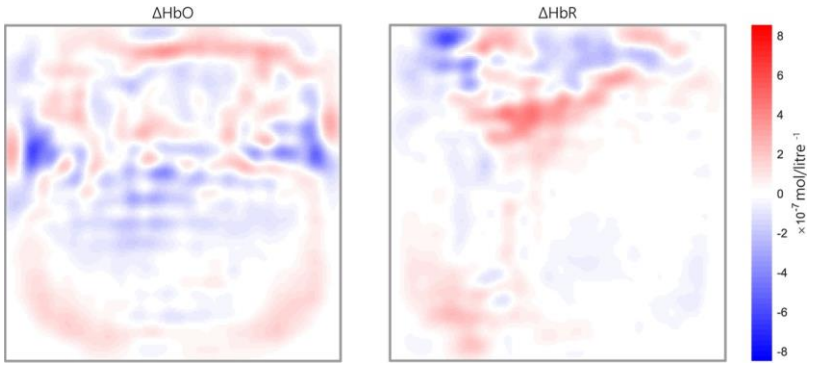

Figure 1: Hemodynamic patterns for □HbO (left) and □HbR (right) at a 10mm depth on a selected subject after two hours of body-weight pressure.

O.12-2

Gelatin-based phantoms for oximetry imaging in the presence of edema

G.Saiko[a], and A. Douplik[b]

[a] *Swift Medical Inc, Toronto, Canada*
[b] *Dept. of Physics, Ryerson University, Toronto, Canada*

gsaiko@ryerson.ca

Abstract: Oxygen supply to tissues can be seriously impacted during wound healing. Edema (accumulation of fluids in interstitial space) can increase the distance between capillaries, thus decreasing oxygen supply to cells. To elucidate the impact of edema on oxygen transport to tissues, we have developed a water-responsive skin model. The model is based on a mechanical gelatin-based human skin model [1] with adaptations to mimic optical parameters of the skin.
Methods: A 2mm thick layer of a 10 wt% solution of gelatin (type A, bloom no 300, Sigma Aldrich) in distilled water (prepared by continuous stirring at 60 °C for 2 h) was left to dry for 24 h at room temperature. The resulting structure was then placed in 1 wt% solution of glutaraldehyde (Sigma Aldrich) in Dulbecco's PBS buffer (DPBS, GIBCO) for 24 h at room temperature under continuous gentle stirring (130 rpm) to crosslink the gelatin. The crosslinked phantoms were rinsed with distilled water and slowly dried by wrapping in paper towels and squeezing between two boards with the use of a 4 kg weight, to minimize ripples caused by drying-related contraction. The paper towels were changed every day, and phantoms were considered to be dry upon mass stabilization (approximately 6 days).
To mimic the optical properties of the skin scatterers (TiO_2 (Sigma Aldrich, USA) or Intralipid (Sigma Aldrich, USA)) were added to the gelatin solution. The scatterer concentrations were based on weight percentage of TiO_2 or volume percentage of Intralipid to match the scattering properties (μ_s') of the epithelium.
To emulate various hydration levels in the skin, the water in the range of 0–300 µl/cm^2 was spread over samples. Electronic scales measured weight before and after spreading. The water content was independently measured using skin impedance technique. Optical properties of phantoms were measured using a spectrometer (Shimadzu, UV3600).
Results: Initial results show that the developed model mimics the optical scattering properties of the skin in a wide range of scatterer concentrations.
Discussion: A new water-responsive optical tissue model has been developed. The skin model with Intralipids as scatterer provides more realistic results in comparison with TiO_2 – based phantoms.

References:

[1] A. Dąbrowska, G.M. Rotaru, F. Spano, Ch. Affolter, G. Fortunato, S. Lehmann, S. Derler, N.D. Spencer, R.M. Rossi, A water-responsive, gelatine-based human skin model, Tribology Int, 113, 316-322 (2017)

I.12

Progress in characterizing structure and function of primo vascular system

Pan-Dong Ryu

Departments of Veterinary Pharmacology, College of Veterinary Medicine and Research Institute for Veterinary Science, Seoul National University, Seoul 08826, Republic of Korea

pdryu@snu.ac.kr

Abstract: The primo-vascular system (PVS), re-discovered in the early 2000s, is a putative circulatory system composed of primo-nodes (PN) and primo-vessels (PV). Recently, Hemacolor staining method is newly introduced in visualization and identification of the PVS tissue and micro CT imaging was successively introduced for a 3D scanning of the PVS tissue. Last several years, there has been a significant progress in understanding the structure and function of the PVS. The progress can be summarized as follows: 1) The PV (~250 □m) is composed of 3~4 unitary PVs that contains multiple micro-vessels (3.5 x 2.5 □m) and few sinuses (~10 mm). 2) The PN (1.3 x 0.73 micro-m) is not covered by any capsule structure, and it contains 3~4 PVs and larger sinuses. 3) Both PN and unitary PV are covered by a layer of mesothelial cells. 4) The size and color of the PVS tissue are dynamically changed by diseases (heart failure and anemia), lipopolysaccharide, exercise training and sympathetic tone. 5) The cytological features and gene expression patterns of the organ surface PVS indicate that the PVS is similar to the spleen, one of the lymphoid organs. 6) The PVS is rich with myeloid cells such as immature WBC-like cells, mast cells, and RBCs. 7) Gross structural plan of the PVS resembles that of peripheral nerves and the internal structure of PN is distinctively different from the lymph node or the spleen. Taken together, the PVS may be considered as a lymphoid organ, but its basic structural plan is quite different from any of the known lymphoid organs. Further studies are needed to elucidate the unique physiological functions of the PVS including its role in the erythropoiesis and tissue oxygen supply.

Acknowledgment: This study was supported by the National Research Foundation of Korea funded by the Ministry of Education (2018R1D1A1B07043448).

O.13-1

VIR-HBOC: A novel highly polymerized oxygen carrier

K.D. Vandegriff[a], B.K. Song[b], W.H. Nugent[b], J. Tucker[a], and W.R. Light[a]

[a] VirTech Bio, Inc., Natick MA, USA
[b]Song Biotechnologies, Baltimore MD, USA

Corresponding author e-mail address: rick.light@virtechbio.com

Abstract: VirTech Bio is developing a human hemoglobin-based oxygen carrier (HBOC), VIR-HBOC, as a large polymeric hemoglobin (Hb) solution. Design goals of VIR-HBOC are to maintain O_2 delivery to restore O_2 debt, minimize fluid shifts, and maintain cardiovascular function and microcirculatory flow. VIR-HBOC properties include: 1) high O_2 carrying capacity ([Hb]=11g/dL), 2) large Hb polymer size (Mw□1MDa), and 3) solution properties (colloidal osmotic pressure and viscosity) that mimic those of pRBCs. VIR-HBOC has a p50□35 mmHg and MetHb<10%. It is room-temperature stable and packaged in ready-to-use infusion bags. In a non-survivable rat hemorrhagic shock (HS) model, evaluation of either Lactated Ringers solution (LRS, control) or VIR-HBOC resuscitation parameters were measured. The model is 60% loss of total blood volume [T_{BV}], followed by 10% T_{BV} bolus resuscitation. Animals were observed for up to 72h. At 60 min from point of initiation of blood loss, VIR-HBOC restored mean arterial pressure (MAP) nearer to baseline, without hypertension, compared to LRS; blood lactate rose higher with LRS (150 ± 18 mg/dL) vs VIR-HBOC (117 ± 13 mg/dL). Survival at 72h increased from 0% for LRS to 25% for VIR-HBOC. These implications point to MAP maintenance (direct cardiovascular effects) and Lactate (O_2 debt) as critical physiologic outcomes for survival from severe HS, such that VIR-HBOC demonstrated resuscitation benefits in this model.[1] Decades of research have been carried out with previous HBOCs, but there have been limiting complications, such as MAP hypertension, vasoconstriction, and non- reversible O_2 debt. Our studies remain directed to VIR-HBOC as a novel highly polymerized oxygen carrier aimed at restoring O_2 debt, preventing volume overload, maintaining microvascular O_2 flow, and increasing survival time during HS.

[1] W. Richard Light, et al. 72-Hour Survival in a Rat Hemorrhagic Shock model with VIR- HBOC versus Crystalloid. Abstract, MHSRS 2019.
Acknowledgement: DoD Contract W81XWH-16-R-SOC1

O.13-2

Oxygen homeostasis and red blood cell transfusion quality

Hugang Hou[1], Jin Hyen Baek[2], Hao Zhang[3], Francine Wood[2], Yamei Gao[3], Ann Barry Flood[1], Harold M. Swartz[1] and **Paul W. Buehler[2]**

[1] Department of Radiology, Geisel School of Medicine at Dartmouth College, Hanover, New Hampshire, USA
[2] Laboratory of Biochemistry and Vascular Biology, Division of Blood Components and Devices, Center of Biologics Evaluation and Research (CBER), FDA, Silver Spring, Maryland, USA
[3] Department of Chemistry, Dartmouth College, Hanover, New Hampshire, USA
[4] Division of Viral Products, Center of Biologics Evaluation and Research (CBER), FDA, Silver Spring, Maryland, USA

Corresponding author e-mail address: Paul W. Buehler (paul.buehler@fda.hhs.gov)

Abstract: The goal of red blood cell (RBC) transfusion is to improve tissue oxygenation. RBC oxygen (O_2) parameters may be impacted in vitro and translate to impaired O_2 delivery and homeostasis. Storage, preservation strategies, pathogen reduction and erythrocyte derivation techniques can unintentionally impair RBC function. This collective work represents a proof-of-concept focused on the systematic evaluation of O_2 homeostasis that is readily adaptable to understanding the quality of transfused RBCs. Donor rat RBCs were leukocyte reduced and persevered at 4ºC (1-7-14 days). RBC morphology, O_2 equilibrium, p50 and Hill numbers from O_2 binding and dissociation curves were evaluated in vitro. Recipient rats were bled and maintained at a mean arterial pressure (MAP) of 30-40 mmHg and hind limb muscle (biceps femoris) pO_2 at 25-50% of baseline. Muscle pO_2 was monitored continuously using EPR oximetry over the course of experiments to assess RBC preparations at stages of blood loss and restoration. In a complementary guinea pig model, molecular markers including hypoxia inducible factors (HIFs) and erythropoietin (EPO) regulation were also evaluated as an assessment of oxygen homeostatic mechanisms occurring before and after transfusion. RBC morphology, O_2 equilibrium and p50 values of intra-erythrocyte hemoglobin were significantly altered by refrigerator storage for both 7 and 14 days. Transfusion of 7 and 14-day RBCs demonstrated an equivalently impaired ability to restore hind limb muscle pO_2, consistent with in vitro observations and transfusion with albumin. 1-day refrigerated RBCs demonstrated normal morphology, in vitro oxygenation and in vivo restoration of tissue pO_2. Guinea pig renal tissue HIFs and serum EPO demonstrated significant post-transfusion changes and may provide a collective estimate of oxygen status when combined with direct measurements of tissue pO_2. The systematic evaluation of O_2 homeostasis represents an effective approach to defining the quality of RBC transfusions.

O.13-3

Skeletal muscle stretching prolongs time constant of reactive hyperemia detected by a multi-channel near-infrared spectroscopy in healthy male volunteers

K. Hotta[a], S. Kojima[a], S. Morishita[a], A. Tsubaki[a]

[a] *Institute for Human Movement and Medical Sciences, Niigata University of Health and Welfare, Japan*

Corresponding author e-mail address: kazuki-hotta@nuhw.ac.jp

Abstract: Muscle contraction increases red blood cell (RBC) velocity in rat skeletal muscle capillary. By contrast, RBC velocity decreases during muscle stretching. In human, there is no plausible method of measuring skeletal muscle capillary blood flow. Temporal occlusion of femoral artery with cuff inflation induces calf muscle deoxygenation detected by a near- infrared spectroscopy (NIRS). After cuff release, oxygenated hemoglobin (O_2Hb) increases and exceeds the baseline level (post-occlusive reactive hyperemia). We hypothesized that reaction time of post-occlusive reactive hyperemia could reflect RBC blood flow in skeletal muscle capillary. To test our hypothesis, post-occlusive reactive hyperemia of skeletal muscle was evaluated in eight healthy male volunteers (23.8±1.7 years old) with stretched and non-stretched (neutral) position. Five-minute of right upper thigh occlusion was performed by cuff inflation (above 200 mmHg) followed by cuff release. Right gastrocnemius muscle was stretched by passively keeping maximal ankle dorsiflexed position. The O_2Hb was recorded at proximal, distal, surface and deep areas of gastrocnemius medial head with a multi-channel NIRS until 5-min after cuff release. Curve fitting was performed on the O_2Hb data using a one-component model: $O_2Hb = O_2Hb_{baseline} + (O_2Hb_{peak} - O_2Hb_{baseline})x(1 - exp^{-K*time})$ where $O_2Hb_{baseline}$ and O_2Hb_{peak} are O_2Hb at the beginning of hyperemic response and maximal value of O_2Hb during hyperemic response, K is the rate constant. Time constant (tau) was calculated as reciprocal of the K. The tau measured with neutral position was not different between proximal, distal, surface and deep areas of gastrocnemius (6.7-14.4 sec); however, the tau was significantly prolonged by 146-876% with stretched position as compared with neutral position ($P<0.0001$). Muscle stretching prolonged the time constant, which likely suggesting that post-occlusive hyperemia detected by NIRS reflects human skeletal muscle capillary blood flow.

O.13-4

Effect of blood flow on hemoglobin and myoglobin oxygenation in contracting muscle using near infrared spectroscopy

B. Koirala[a], G. M. Saidel[b], A. Hernández[c], L. B. Gladden[d] and N. Lai[a,b]

[a] *Department of Electrical and Computer Engineering and Institute of Biomedical Engineering, Old Dominion University*
[b] *Department of Biomedical Engineering, Case Western Reserve University, Cleveland, Ohio*
[c] *Office of Research and Economic Development, University of California, Merced, Merced, California*
[d] *Department of Kinesiology, Auburn University, Auburn, Alabama*

Corresponding author e-mail address: nlai@odu.edu

Abstract: Insufficient oxygen delivery to, and uptake by skeletal muscle can produce significant mobility limitations for patients with chronic diseases. Near-Infrared Spectroscopy (NIRS) can be used to non-invasively quantify the balance between skeletal muscle O_2 delivery and consumption during contraction. However, a debate exists on whether the oxygenated or deoxygenated NIRS signal should be used to assess muscle O_2 changes. This issue is related to the fact that the contributions of hemoglobin (Hb) and myoglobin (Mb) cannot be distinguished. This conundrum can be resolved by quantitative analysis of experimental data with a previously developed mechanistic mathematical model. In this study, our model provides computer simulations of dynamic responses of the oxygenated (HbO_2, MbO_2) and deoxygenated (HHb, HMb) Hb and Mb contributions to the NIRS signal components ($HbMbO_2$, HHbMb). Simulations of skeletal muscle oxygen uptake and NIRS kinetics correspond closely to published experimental data (J Appl Physiol. 108(5):1169-76, 2010). These demonstrate the validity of the model, which can be used to predict quantitatively the effect of blood flow kinetics on the vascular and muscle oxygenation kinetics. Model simulations of skeletal muscle oxygen uptake and oxygenation kinetics with different blood flows indicate that: 1) faster O_2 delivery is responsible for slower muscle oxygenation kinetics; 2) Hb and Mb contributions to the oxygenated NIRS signal are similar (40-60%), but Hb and Mb contributions to the deoxygenated NIRS signal are significantly different, 80% and 20% respectively. The effect of slow blood flow kinetics on oxygenated Hb and Mb kinetics is minimal while the effect on the deoxygenated Hb and Mb kinetics produce significant overshoots and undershoots caused by the transient imbalance between O_2 delivery and uptake rates.

Presenting Author Index

(V)

(W)

(X)

(Y)

(Z)

In Memory of Laraine Visser-Isles

January 13, 1943 – April 17, 2019

To all my loved ones,
I thought it might be nice if – later on – in your own time and in a place that you like, you might want to celebrate (my) life.
You could do this alone, or with someone else that we shared good times with…
With love as always
Laraine "Larry" Visser-Isles